Markets for Ancillary Services in the Presence of Stochastic Resources

Final Project Report

M-31

Power Systems Engineering Research Center

Empowering Minds to Engineer
the Future Electric Energy System

Markets for Ancillary Services in the Presence of Stochastic Resources

Final Project Report

Project Team

Kory W. Hedman, Project Leader
Arizona State University

Muhong Zhang
Arizona State University

Marija Ilic
Carnegie Mellon University

Graduate Students:

Joshua Lyon, Fengyu Wang, Chao Li
Arizona State University

Jose Fernando Prada
Carnegie Mellon University

PSERC
Publication 16-06

September 2016

For information about this project, contact

Kory W. Hedman
Arizona State University
School of Electrical, Computer, and Energy Engineering
P.O. BOX 875706
Tempe, AZ 85287-5706
Phone: 480 965-1276
Fax: 480 965-0745
Email: kory.hedman@asu.edu

Power Systems Engineering Research Center

The Power Systems Engineering Research Center (PSERC) is a multi-university Center conducting research on challenges facing the electric power industry and educating the next generation of power engineers. More information about PSERC can be found at the Center's website: http://www.pserc.org.

For additional information, contact:

Power Systems Engineering Research Center
Arizona State University
527 Engineering Research Center
Tempe, Arizona 85287-5706
Phone: 480-965-1643
Fax: 480-965-0745

Notice Concerning Copyright Material

Acknowledgements

The work described in this report was sponsored by the Power Systems Engineering Research Center (PSERC). We express our appreciation for the support provided by PSERC's industrial members and by the National Science Foundation under grant NSF EEC 9908690 received under the Industry / University Cooperative Research Center program. The work described in this report was also sponsored by the National Science Foundation under grant NSF CMMI 1333646.

The authors thank industry collaborators including Yonghong Chen (MISO); Bahman Daryanian (GE); Thomas Edmunds (LLNL); Evangelos Farantatos (EPRI); Feng Gao (ABB/Ventyx); William Henson (ISONE); Marissa Hummon, (NREL); Nikhil Kumar (GE; Liang Min (LLNL); Nivad Navid (PG&E); Jim Price (CAISO) Xing Wang (ALSTOM Grid); Feng Zhao (ISONE); Aidan Tuohy (EPRI); Eamonn Lannoye (EPRI); Andy Tillery (Southern Co).

Executive Summary

This project focuses on the challenge of managing added variability and uncertainty due to stochastic resources, resources (e.g., wind, solar, demand response products) that are not fully dispatchable or controllable like conventional generators. Market models that are inherently imprecise at capturing uncertainty and voltage limitations lead to market prices (for ancillary services) that do not accurately reflect the value provided by market participants. Ancillary services products that are procured by an ISO may not be deliverable as existing market models do not adequately capture post-contingency (or post-event) congestion. For example, MISO conducts a procedure known as *reserve disqualification* following its day-ahead market; the process disqualifies units that were scheduled to provide reserve after further analysis identifies that congestion or a lack of voltage support inhibits the delivery of the procured reserve.

While many efforts have and are being made to address this challenge, one barrier to adoption is the challenge to modify existing market models and settlement policies in such a way that is transparent and achieves stakeholder approval. Therefore, the primary objective of this work is to enhance existing market software to better predict reserve deliverability issues. More importantly, the goal is to demonstrate that enhancements to market software leads to prices that reward market participants that provide higher quality ancillary services and are more dependable. The results show that the change in compensation is aligned with the likelihood that the market participant's procured reserve is, indeed, deliverable (without violating network limitations) when needed.

The report is broken into two volumes, with three parts to volume 1 and one part to volume 2. Each part is summarized in the following subsections.

Volume 1 Summary, Parts 1-3:

Volume 1 consists of the work conducted by Arizona State University. This project leveraged the prior work conducted by Dr. Kory Hedman under the PSERC Future Grid Initiative, which ended in August 2013. Volume 1 of this project report is focused on enhancing the modeling of ancillary services requirements within existing market based security constrained unit commitment and security constrained economic dispatch tools. Volume 1 also focuses on analyzing the market implications of these adjustments. Ongoing and future efforts are now focused on leveraging this work within a project funded by the DOE Advanced Research Projects Agency – Energy (ARPAE) Network Optimized Distributed Energy Systems (NODES) program. With the assistance of industry partners, the goal is to develop a prototype tool that can run alongside energy management systems and provide guidance to operators in real-time on the adjustment of needed ancillary service products.

Part I: Market Implications and Pricing of Dynamic Reserve Policies for Systems with Renewables

Static reserve policies are used within security-constrained unit commitment (SCUC) and security constrained economic dispatch (SCED) to ensure reliability. A common policy is that ten-minute reserve must exceed the largest contingency. However, this condition does not guarantee reliability because voltage and thermal limits can hinder reserve deliverability. Many operators use zonal reserve markets to ensure reserves are dispersed across the grid. Such zonal models attempt to anticipate transmission bottlenecks, which is a difficult task due to uncertainty. This report examines the market implications of dynamic reserve policies used to mitigate uncertainty from renewable resources and contingencies. We study the market implications of policies recently proposed in the literature, such as hourly zones within day-ahead SCUC and an algorithm that formally disqualifies reserves that are expected to be undeliverable. A locational reserve pricing scheme is also proposed in connection with scenario-based reserve disqualification. Analysis on the RTS-96 test case shows that dynamic zones and reserve disqualification, along with the proposed compensation scheme, help direct reserve payments toward resources that more effectively respond to contingencies.

Part II: A Statistical Evaluation of Dynamic Reserve Policies with Consideration of Stochastic Resources

In order to reduce greenhouse gas emissions, more non-dispatchable or semi-dispatchable renewable resources are being integrated into the grid. Due to the uncertainty and variability of renewable generation, additional operating reserve may be required to ensure reliability. System reliability must be maintained by not only acquiring a sufficient quantity of reserve but also ensuring the reserve is deliverable, i.e., transmission bottlenecks must not restrict the deliverability of reserve. Existing deterministic reserve requirements locate reserve blindly inside reserve zones. Additional uneconomic adjustments, such as reserve disqualification, are necessary if the solution is unreliable due to undeliverability of reserve caused by congestion. However, such uneconomic adjustments may lead to inefficient dispatch solutions and they distort market price signals. An hourly reserve zone determination method is proposed in this report to distribute the reserve across the system efficiently and to reduce the use of uneconomic adjustments such that market efficiency and system reliability are improved. The hourly reserve zone determination method is tested on the Reliability Test System 1996 (RTS-96) with consideration of wind and load uncertainties. The market results, as well as confidence intervals after reserve disqualifications, are compared between the proposed hourly reserve zone and existing seasonal reserve zone procedures.

Part III: Market Implications of Security Requirements

Regional transmission organizations and independent system operators include different types of security requirements to ensure system security. In this report, a set of security constraints to withstand single-generator-failure contingencies are presented and the

market implications are studied. A new component of locational marginal prices, a marginal security component, which is a weighted shadow price of the security constraints, is proposed to better represent energy prices. A simple 3-bus system example is given to illustrate clearly the advantages of the new pricing scheme. The results are confirmed on a 73-bus system test case.

Volume 1 Project Papers and Publications:

[1] J. Lyon, F. Wang, K. W. Hedman, and M. Zhang, "Market implications and pricing of dynamic reserve policies for systems with renewables," *IEEE Transactions on Power Systems*, vol. 30, no. 3, pp. 1593-1602, May 2015.

[2] F. Wang and K. W. Hedman, "A statistical evaluation of dynamic reserve policies with consideration of stochastic resources," working paper.

[3] C. Li, K. W. Hedman, and M. Zhang, "Market implications of security requirements," *IET Generation, Transmission, and Distribution*, under review.

[4] J. Lyon, M. Zhang, and K. W. Hedman, "Capacity response sets for security constrained unit commitment with wind uncertainty," *Electric Power Systems Research*, vol. 136, pp. 21-30, Jul. 2016.

[5] F. Wang and K. W. Hedman, "Dynamic reserve zones for day-ahead unit commitment with renewable resources," *IEEE Transactions on Power Systems*, vol. 30, no. 2, pp. 612-620, Mar. 2015.

[6] J. Lyon, M. Zhang, and K. W. Hedman, "Locational reserve disqualification for distinct scenarios," *IEEE Transactions on Power Systems*, vol. 30, no. 1, pp. 357-364, Jan. 2015.

[7] C. Li, M. Zhang, and K. W. Hedman, "Extreme ray feasibility cuts for unit commitment with uncertainty," *European Journal of Operations Research*, under review.

Volume 1 Student Theses:

[8] Fengyu Wang, "Improving deterministic reserve requirements for security constrained unit commitment and scheduling problems in power systems," PhD Dissertation, Arizona State University, Tempe, AZ (partially supported by the PSERC Future Grid Initiative and NSF project CMMI 1333646).

[9] Joshua Lyon, "Deterministic scheduling for transmission-constrained power systems amid uncertainty," PhD Dissertation, Arizona State University, Tempe, AZ (partially supported by the PSERC Future Grid Initiative and NSF project CMMI 1333646).

[10] Chao Li, "Unit commitment with uncertainty," PhD Dissertation, Arizona State University, Tempe, AZ (partially supported by the NSF project CMMI 1333646).

Volume 2 Summary, Part 4:

Volume 2 reports work conducted by Carnegie Mellon University. Dr. Marija Ilic's research focused on exploring the use of stochastic SCUC models to represent the uncertainty of resource availability and provide better allocation of ancillary services. In particular, the work concentrated on the optimization of contingency reserves.

Part IV: Day-Ahead Stochastic Co-optimization of Energy and Locational Contingency Reserves

Scheduling spare generation capacity as contingency reserve in power systems is necessary to preserve the security of real-time operations. In this report we develop a stochastic security-constrained unit commitment model to co-optimize energy and the contingency reserves required to respond to a set of likely but uncertain generation contingencies. This model is used to allocate contingency reserves throughout a power grid in order to strictly comply with the N-1 security criterion under transmission congestion, minimizing expected pre contingency dispatch and post contingency redispatch costs. The proposed method efficiently assigns locational reserves in day-ahead markets and it is based on a compact formulation of the stochastic unit commitment problem that is consistent with actual operational practices. We simulated the distribution of locational contingency reserves on the IEEE RTS96 system and compared the results with the traditional global and deterministic allocation method. We found that assigning locational spinning reserves can guarantee an N-1 secure dispatch with transmission congestion at a reasonable extra cost. We also tested the effect of including downward spinning reserves and of co-optimizing spinning and nonspinning reserves. The simulations showed little value of having downward reserves but sizable operating savings from co-optimizing locational spinning and nonspinning reserves. Overall, the results indicate the computational tractability of the proposed method, which can be applied by system operators to improve the reliability and efficiency of scheduling generation and contingency reserves in bulk power systems.

Volume 2 Project Papers and Publications:

[1] J. F. Prada and M. D. Ilic, "Locational allocation and pricing of responsive contingency reserves," *IEEE Power & Energy Society General Meeting*, Denver, Colorado, July 26-30, 2015.

[2] J. F. Prada and M. D. Ilic, "Day-ahead stochastic co-optimization of energy and locational contingency reserves," CMU EESG Working Paper, 2016 (manuscript being submitted to the *IEEE Transactions on Power Systems*).

Volume 2 Student Thesis:

[3] J. F. Prada, "Markets for electricity ancillary services under uncertainty: stochastic allocation and pricing of energy and locational contingency reserves," PhD Dissertation, Engineering and Public Policy Department, Carnegie Mellon University, Pittsburgh, PA.

Intentionally Blank Page

Part I

Market Implications and Pricing of Dynamic Reserve Policies for Systems with Renewables

Fengyu Wang
Joshua Lyon
Kory W. Hedman
Muhong Zhang

Arizona State University

For information about this project, contact

Kory W. Hedman
Arizona State University
School of Electrical, Computer, and Energy Engineering
P.O. BOX 875706
Tempe, AZ 85287-5706
Phone: 480 965-1276
Fax: 480 965-0745
Email: kory.hedman@asu.edu

Power Systems Engineering Research Center

The Power Systems Engineering Research Center (PSERC) is a multi-university Center conducting research on challenges facing the electric power industry and educating the next generation of power engineers. More information about PSERC can be found at the Center's website: http://www.pserc.org.

For additional information, contact:

Power Systems Engineering Research Center
Arizona State University
527 Engineering Research Center
Tempe, Arizona 85287-5706
Phone: 480-965-1643
Fax: 480-965-0745

Notice Concerning Copyright Material

Table of Contents

List of Figures

List of Tables

Nomenclature

Sets:

C	Generator contingencies; $C(j) \subseteq C$ are in zone j.
G	Generators and reserve providers; $\mathcal{G}(k) \subseteq G$ are in zone k and $G(n) \subseteq G$are at node n.
L	Transmission lines and transformers.
N	Nodes; $n(g) \in N$ is the node of generator g.
T	Time periods.
W	Wind scenarios.
Z	Zones; $z(g) \in Z$ is the zone of generator g.

Parameters (index t denotes period):

F_l	Power flow limit on line l.
I_{nt}^c	Net injection at node n after contingency c but prior to re-dispatch.
$PTDF_{nl}$	Sensitivity of flow on line l to injection at node n.
QOS_{ht}^c	Proportion of reserve from resource h cleared in the day-ahead market that is deliverable in real-time for contingency c.
R_{gt}^+, R_{gt}^-	Available up and down reserve from generator g.
π_l	Weight indicating the criticality of line l.
Γ_{gt}^c	Reserve disqualification indicator for generator g ($\Gamma_{gt}^c = 0$ means g is disqualified for contingency c).
Δ_{gt}^c	Reserve quantity from generator g that receives payment for contingency c.
Φ_{gt}	Total reserve payment to generator g.

Variables (index t denotes period):

i_{nt}^c	Net injection at node n following re-dispatch for contingency c.
p_{gt}	Power produced by generator g.
r_{gt}	Reserve provided by generator g.
$\tilde{r}_{kt}^c$	Total reserve designated as deliverable from zone k to contingency c.
S_{kt}^j	Reserve import capability from zone k to zone j.
s_{ht}^c	Cleared reserve from resource h that cannot be dispatched in response to contingency c.
x_{gt}^{c+}, x_{gt}^{c-}	Up and down reserve deployment from generator g in response to contingency c.
λ_{kt}^c	Dual variable for the constraint classifying reserve in zone k as deliverable for contingency c.

1. Introduction

1.1 Research Premise

Independent system operators (ISOs) manage the power grid with the goal of maximizing the market surplus. The day-ahead markets (DAM) and the real-time markets (RTM) are cleared using security-constrained unit commitment (SCUC) and security-constrained economic dispatch (SCED) models. Important physical constraints include generator capacity, generator ramping, and transmission limits. Important operational constraints include ancillary services requirements, such as reserves, which help avoid the need for load curtailment due to random disturbances. Operations may benefit from improved models that better address the stochastic aspects of SCUC because it is difficult for existing constraints to optimally protect against the many contingencies and forecast deviations that may occur.

Ancillary services include various types of reserves, i.e., backup capacities that can be dispatched within a given amount of time, to handle uncertainty. Quick-reserve products respond frequently to load and renewable fluctuations, ten-minute reserves respond to contingencies (and may be used for larger load following deviations), and thirty-minute reserves are used to replace deployed reserves from other reserve categories. Reserve requirements ensure a minimum level of generation flexibility to respond to uncertainty. However, there is no guarantee that reserves can be delivered without violating transmission constraints. To mitigate this issue, ISOs use zonal reserve market models to distribute reserves across the grid. Zonal models are imprecise because they treat all locations in the same zone as equal, ignoring intra-zonal congestion and approximating inter-zonal flows [1]. The evolution from zonal to nodal *energy* markets in the USA is widely recognized as an improvement; however, no such transition has occurred for ancillary services yet. The recent literature has proposed more precise scheduling models that consider the effect of re-dispatch decisions on power flows [2]–[8], but such models are not yet scalable enough for large systems and pose new challenges for market integration.

Instead, operators use approximate models to schedule and to price scarce resources and then adjust the solution after the fact as needed to account for model inaccuracies [9]-[10]. Such out-of-market corrections are referred to as exceptional dispatches in CAISO and out-of-merit energy/capacity in ERCOT [11], [12]. Operators may be forced to commit additional generators or hold back flexible resources to compensate for reserve deliverability issues. MISO and ISO-NE accomplish this by manually disqualifying "Not Qualified" reserves and then procuring more reserve from favorable locations [13]–[15]. The need for such actions, which are made outside the market, may distort price signals [16], increase costs, and cause a market separation between the forward DAM and the spot RTM.

Several deterministic policies have been proposed to address reserve deliverability. References [16], [17] constrain power flows based on participation factors that estimate how generators will respond for different scenarios. Reference [18] proposes an optimization tool for disqualifying undeliverable reserves in the style of MISO and ISO-

NE. MISO has also shown interest in updating reserve zones daily or even hourly (instead of every few months [19]) so that the market model can better address changing conditions [20]. Reference [21] proposes a mathematical framework for such frequent zone updates. One barrier to updating zones more frequently is stakeholder opposition due to uncertainty regarding their participating zone(s). However, this practice may also improve market efficiency and reduce the need for uneconomic out-of-market corrections, like reserve disqualification, which distort the market.

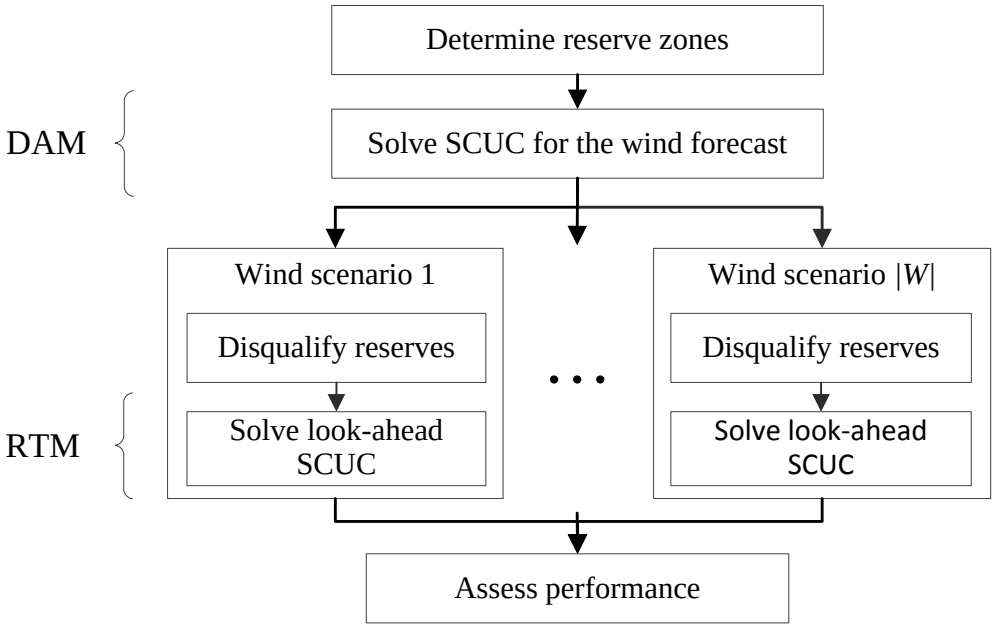

Figure 1. Summary of analysis of different zonal inputs for a single day.

This report examines the market implications of using dynamic reserve zones (that change by hour) to improve contingency reserve deliverability in systems with wind generation. The first hypothesis is that dynamic reserve zones help the DAM determine which resources will be able provide better contingency support in real-time. Following the flowchart in Figure 1, the model of [21] is first used to determine hourly zones that are fed into SCUC to clear the DAM. Unreliable market solutions are repaired for each wind scenario by using the model of [18] to disqualify undeliverable reserves. A look-ahead SCUC is finally solved to simulate the real-time market clearing and to simulate the downstream commitment of fast generators, which can occur during real-time operations or during the adjustment period. The aggregate market outcomes are assessed using a new metric named “quality of service” (QOS) that evaluates the real-time performance of reserves procured in the DAM.

In addition, a market settlement scheme is proposed for use with the reserve disqualification model of [18]. This approach accommodates locational ancillary service prices. Reserves are procured on a per-contingency basis, which allows reserves to be disqualified for a subset of contingencies. The proposed settlement scheme derives prices

with a separate component from each contingency, so that reserve providers cleared in the RTM are only compensated for contingencies for which they are qualified to provide ancillary service. This provides a more precise and exact payment scheme that can result in different reserve prices for resources in the same zone.

1.2 Report Organization

The remainder of this report is organized as follows: Section 2 reviews the reserve literature. Section 3 describes a procedure to determine dynamic zones that is a variant of [21]. Section 4 proposes a new settlement scheme for the model of [18]. Section 5 introduces an algorithm that measures the quality of service of reserves cleared in the DAM. Section 6 analyzes the market results of static reserve policies as well as dynamic reserve policies on the IEEE RTS-96 test case. Section 7 concludes the report.

2. State of the Art Reserve Policies

2.1 Zonal Reserve Quantity

Reserve requirements ensure reserve is on standby to respond to random disturbances. Requirements are usually based on the desire to satisfy certain reliability thresholds, e.g., protection against any single contingency (*N*-1) or probabilistic criteria [22]–[27]. Operators encourage reserve deliverability by applying requirements within zones that represent areas with relatively little congestion. Zones provide a useful approximation of where reserve needs to be without needing to identify a response for every scenario. Zonal reserve requirements may take the form,

$$\sum_{g \in \mathcal{G}(k)} r_{gt} \geq Q_{kt}, \quad \forall k \in Z, t \in T \tag{1}$$

where r_{gt} is the reserve of generator g in period t and Q_{kt} is the minimum quantity for zone k. Many ISOs use constraint relaxation to adjust Q_{kt} as the reserve price changes [17]. For simplicity, constraint relaxation is not used in this report.

Different reserve products protect against different types of disturbances [28]. This report focuses on ten-minute reserve requirements to protect against generator contingencies. Some ISOs are also introducing RTM products that protect against wind uncertainty in the 10–30 minute time frame [28]. Such requirements would be applied on top of the contingency reserves studied in this report.

2.2 Zonal Reserve Sharing

Reserve sharing is a practice of quantifying how much reserve can be transferred between zones. These models rely heavily on off-line studies. For example, MISO determines contingency requirements two days ahead by simulating reserve deliverability between zones [19]. Some operators update sharing capability estimates based on the interface flows in the current solution. For example, PJM and ISO-NE require additional reserve in zones that import more power than expected and vice versa [29], [30]. The reserve sharing model used by [18] is,

$$\sum_{k \in Z} \tilde{r}_{kt}^{j} \geq p_{ct} + r_{ct}, \quad \forall j \in Z, c \in C(j), t \in T \tag{2}$$

$$\tilde{r}_{kt}^{j} \leq \sum_{g \in \mathcal{G}(k)} r_{gt}, \quad \forall j \in Z, k \in Z, t \in T \tag{3}$$

$$\tilde{r}_{kt}^{j} \leq S_{kt}^{j}, \quad \forall j \in Z, k \in Z, t \in T \tag{4}$$

where $\tilde{r}_{kt}^{j}$ represents how much reserve in zone *k* is classified as deliverable to zone *j* in period t. Equation (2) requires reserve to cover the loss of any generator contingency c, (3) models reserve held within the zones, and (4) limits how much reserve may be shared between zones. The sharing bounds S may be based on off-line analysis and dynamically updated as flows change across zonal interfaces [30].

2.3 Reserve Disqualification

Zonal reserve requirements (2)–(4) do not locate reserves from within zones. Operators may improve reliability by forcing reliability must run (RMR) units to be committed at certain locations. Conversely, operators may disqualify reserves that are not expected to be deliverable: only qualified resources may then contribute toward reserve requirements the next time the schedule is updated. The updated reserve sharing formulation from [18] is,

$$\sum_{k \in Z} \tilde{r}_{kt}^{c} \geq p_{ct} + r_{ct}, \quad \forall c \in C, t \in T \tag{5}$$

$$\tilde{r}_{kt}^{c} \leq \sum_{g \in \mathcal{G}(k)} \Gamma_{gt}^{c} r_{gt}, \quad \forall c \in C, k \in Z, t \in T \tag{6}$$

$$\tilde{r}_{kt}^{c} \leq S_{kt}^{z(c)}, \quad \forall c \in C, k \in Z, t \in T \tag{7}$$

where the binary parameter Γ_{gt}^{c} designates if resource g is qualified to offer reserve for contingency c in period t. Note that the reserve sharing variable $\tilde{r}_{kt}^{c}$ is now indexed by destination contingency c instead of destination zone j. The formulation is equivalent to (2)–(4) when no reserve has been disqualified, i.e., when all $\Gamma_{gt}^{c} = 1$. Note that parameter Γ may be treated as a continuous parameter that takes on any value between zero and one; the binary restriction is used here to make the model more intuitive and consistent with traditional reserve disqualification practices. The main development here over traditional models is that reserve disqualification is scenario-specific and, therefore, able to address the different congestion patterns that emerge for distinct contingency scenarios.

Equations (5)–(7) enable finer management of reserve locations, provided that proper values for Γ can be determined. This report uses the algorithm of [18] to disqualify reserves whenever the zonal model provides a solution that is not *N*-1 reliable. The algorithm simulates post-contingency actions and disqualifies reserves that are not deliverable during a coordinated dispatch. Details are left to the reader to explore in [18].

3. Dynamic Reserve Zone Determination

In some systems, reserve zones are determined by grouping nodes together based on some centrality measure [19], [31]–[35]. One such measure, "weighted power transfer distribution factor difference" (WPTDFD), describes whether nodes i and n have a similar influence on critical lines [31]:

$$WPTDFD_{in} = \sum_{l \in L} \pi_l |PTDF_{il} - PTDF_{nl}| \quad (8)$$

where π_l is a weight used to emphasize critical lines, and $|PTDF_{il} - PTDF_{nl}|$ is the absolute difference of flow on line l between a MW injection at node i and node n. This measure is fed into a statistical clustering algorithm that groups nodes together that have small WPTDFDs. Large weights are generally given to transmission bottlenecks so that reserve can replace disturbances in the same zone without aggravating the flow on critical paths. A similar approach to this is also used by MISO and ERCOT to update zones [19], [33].

Reserve zones are reevaluated quarterly in MISO and yearly in ERCOT using historical information to determine line weights [19], [33]. Reference [21] uses a probabilistic analysis to determine line weights by simulating dispatch given the latest system forecasts and scheduled outages. This procedure helps operators to anticipate transmission bottlenecks and to update zones on a more frequent basis.

A variation of the algorithm of [21] is used in this report to update zones on an hourly basis. The main difference is that line weights are calculated relative to post-contingency flows. The algorithm first simulates operations across many wind scenarios and contingencies. Larger weights π_l are then given to lines that frequently operate close to their limits during contingencies. The weights contribute to the WTPTDFs and zones are determined with respect to this metric using the K-means clustering algorithm. This approach helps improve reserve deliverability by better managing reserve locations with respect to critical lines. Details on the underlying framework are left to the reader to explore in [21].

4. Ancillary Service Market Settlement

Most ISOs clear energy and ancillary services together using a model that includes both energy and reserve bids in the objective function [3]. The optimization engine clears the lowest bids that satisfy all physical, operational, and security constraints. Prices are based on dual variables from the market model. After the scheduling run has completed, all binary variables are fixed so that dual variables can be derived from a pricing run [36]. Service providers are compensated based on dual variables, e.g., locational marginal prices (LMPs) are used to settle energy and reserve marginal prices (RMPs) are used to settle reserves. RMPs increase as reserve bids increase and when locational reserves are scarce. Note that there are varying practices for pricing reserve across the ISOs.

Reserve sharing complicates reserve valuation at varying locations. ISO-NE uses a settlement policy that rewards resources at preferred locations. ISO-NE's nested zone model assumes only transmission restricts reserve sharing into child zones, which are load pockets [30]. Resources are not compensated for ancillary services to child zones because outside reserve is assumed to be undeliverable. This type of policy is appropriate when operators can predict the binding network constraints. Otherwise, a more general mechanism is necessary that acknowledges service provided to neighboring zones *only* when marginal reserves are deliverable. With the increase in stochastic resources, such general mechanisms are needed. Such a payment scheme is provided by (9).

$$\phi_{gt} = -\sum_{c \in C} \Gamma^{c}_{gt} r_{gt} \lambda^{c}_{z(g),t} \tag{9}$$

$\Gamma^{c}_{gt} r_{gt}$ is the amount of qualified cleared reserve and λ^{c}_{kt} is the dual variable for (6). Economic theory specifies that λ^{c}_{kt} is a shadow price that reflects the marginal value of reserve in zone k for contingency c [36]. The payments in (9) compensate reserve providers based on service for individual contingencies. Service may be valuable even for a small contingency if other resources are disqualified for that contingency.

The reserve price for resource g in period t is effectively $\left|\sum_{c \in C} \Gamma^{c}_{gt} \lambda^{c}_{z(g),t}\right|$. Reserve disqualification changes Γ and can lead to different prices for resources in the same zone. With this pricing structure, resources receive higher prices if their reserve is qualified for contingencies with substantial shadow prices. This is in contrast to traditional policies that derive a single reserve price for each zone. The locational prices reflect congestion because reserve is disqualified only when it is labelled as not deliverable.

The reserve disqualification algorithm is designed to disqualify a minimal amount of reserve. This feature helps to avoid situations where reserves are unnecessarily disqualified and remunerated a lower price than other resources that provide comparable services. Equation (10) describes the quantity of cleared reserve for which the pricing run attributes some value. In the next section, an algorithm is proposed to measure how much of this cleared reserve is available and deliverable in real-time.

$$\Delta^{\square}_{\square\square} = \begin{cases} \Gamma^{c}_{gt} r_{gt} & \text{if } \lambda^{c}_{z(g),t} \neq 0 \\ 0 & \text{otherwise} \end{cases} \tag{10}$$

5. Measuring Quality of Service

Model ($MQOS_h$) measures the quality of service from reserve provider h. The model assesses real-time reserve availability using a full-network representation. More precisely, it identifies reserves that are not dispatchable when the DAM anticipated they would be dispatchable.

($MQOS_h$):

$$\text{Min} \sum_{c\in C} \sum_{t\in T} \left(s_{ht}^{c} + M \sum_{g\in G} x_{gt}^{c-}\right) \tag{11}$$

$$\sum_{n\in N} i_{nt}^{c} = 0, \quad \forall c \in C, t \in T \tag{12}$$

$$-F_l \le \sum_{n\in N} PTDF_{nl} i_{nt}^{c} \le F_l, \quad \forall l \in L, c \in C, t \in T \tag{13}$$

$$i_{nt}^{c} = I_{nt}^{c} + \sum_{g\in G(n)} \left(x_{gt}^{c+} - x_{gt}^{c-}\right), \quad \forall n \in N, c \in C, t \in T \tag{14}$$

$$R_{gt}^{-} \le x_{gt}^{c+} - x_{gt}^{c-} \le R_{gt}^{+}, \quad \forall g \in G, c \in C, t \in T \tag{15}$$

$$x_{ht}^{c+} + s_{ht}^{c} \ge \Delta_{ht}^{c}, \quad \forall\, c \in C \setminus h, t \in T \tag{16}$$

$$x_{gt}^{c+}, x_{gt}^{c-}, s_{ht}^{c} \ge 0, \quad \forall\, c \in C, g \in G, t \in T \tag{17}$$

Model ($MQOS_h$) assesses reserve availability from resource h for generator contingencies $c \in C$. Parameter F_l is the flow limit for line l and parameter I_{nt}^{c} is the net injection (generation minus load) at node n after the contingency but prior to reserve dispatch. Parameters R_{gt}^{+} and R_{gt}^{-} are the available up and down reserves and x_{gt}^{c+} and x_{gt}^{c-} are the dispatched up and down reserves from resource g. Index g is used for generators in general and index h is for the specific resource being evaluated. Equations (12) and (13) are flow balance and linear transmission constraints, which are common for power system scheduling [37]. Equation (14) models locational injections and (15) models reserve availability. The model above considers spinning reserves but can be generalized to include other reserve products, such as non-spinning reserve or demand response.

Ideally, a resource paid to provide Δ_{ht}^{c} of reserve for contingency c should be able to dispatch that amount. If this amount of reserve cannot be exercised during a coordinated re-dispatch, then the resource provides a lower quality of service than anticipated by the zonal reserve model. Equation (16) measures how much reserve is dispatched from resource h, where s_{ht}^{c} represents the shortfall below Δ_{ht}^{c}. The objective function (11) encourages a small shortfall: if the optimal solution is zero, then reserve from resource h can be dispatched up to the anticipated level. A large penalty M is included in the objective function to prevent generators from ramping down unless absolutely necessary to ensure feasibility. Note that this assumption is not made to reflect actual operations, only to measure the quality of service provided by resource h relative to its ability to deliver its procured reserve.

The proportion of reserve properly characterized as deliverable for each contingency is shown by QOS (quality of service) in (18). Reserve policies that result in low values for QOS_{ht}^{c} poorly anticipate the quality of service provided by resource h. This implies that resource h was compensated for reserve that was unavailable or undeliverable in real time. Equation (19) defines the average quality of service $\overline{QOS}$ across all reserve providers, contingencies, and periods. Efficient models should have $\overline{QOS}$ closer to one,

indicating that a large portion of reserves procured in the DAM are deliverable in real-time.

$$QOS_{ht}^{c} = 1 - \frac{s_{ht}^{c}}{\Delta_{ht}^{c}} \tag{18}$$

$$\overline{QOS} = 1 - \frac{\sum_{t\in T}\sum_{h\in G}\sum_{c\in C} s_{ht}^{c}}{\sum_{t\in T}\sum_{h\in G}\sum_{c\in C} \Delta_{ht}^{c}} \tag{19}$$

Note that $\mathrm{QOS}_{\mathrm{ht}}^{\mathrm{c}}$ is designed to reflect reserve deliverability and it is not meant to capture the market value of reserve. For example, resource h may provide an overall lower QOS than resource $\bar{\mathrm{h}}$ and still deserve more compensation. This may occur when reserve from h is being used to cover more critical contingencies, e.g., large outages within import-constrained areas. Therefore, there need not be a strong relationship between QOS, the reserve price, and the overall compensation. Rather, the overall compensation should be a reflection of both QOS and the shadow prices (λ_{zt}^{c} values) of the contingencies the reserve is meant to satisfy. Furthermore, QOS is a measure of model precision; precise models may be expected to avoid incidences of clearing reserves, which become undeliverable or otherwise unavailable in real-time.

6. Results and Analysis

The analysis in this report evaluates static and dynamic zones using the process described in Figure 1. After reserve zones have been determined, SCUC is solved based on the forecasted wind availability to produce the DAM solution. Several things occur between the DAM and RTM clearings. First, the wind forecast improves dramatically as operations move closer to real-time [38]. Operators respond to forecast updates by re-dispatching the system and committing additional generators if needed. Operators may also disqualify reserves, if congestion is found to threaten reliability, and then procure additional reserves at preferred locations. All of these changes occur prior to the RTM, which is a spot market that is cleared near real-time.

This report uses the process in Figure 2 to simplify operations following the DAM. It is assumed that wind uncertainty is revealed all at one time and a 24-hour SCUC is solved to dispatch the system. Additional commitments are allowed for generators that have minimum down times of less than five hours. The SCUC solution will represent the RTM solution if it passes contingency analysis without violations. Otherwise, the algorithm of [18] is used to disqualify undeliverable reserves and the process is repeated until a reliable solution is found. This approach simplifies actual operations in that 1) the RTM is solved with an hourly time resolution instead of a five minute period and 2) the RTM is cleared with a 24 hour model instead of a series of shorter problems with a rolling horizon. This simplified process approximates the effect of hourly deviations from the day-ahead forecast.

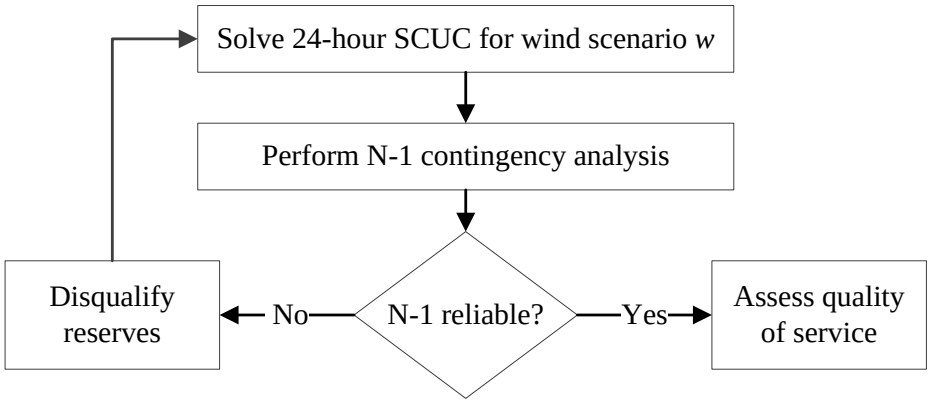

Figure 2. Simulation of the corrections made to the DAM solution in order to satisfy *N*-1 reliability for an individual wind scenario.

6.1 IEEE RTS 96 Test Case

A modified IEEE Reliability Test System (RTS)-96 is used to examine the market impact of the proposed dynamic reserve policies. The system has 73 nodes, 99 units, 117 lines, and 51 loads [39], [40]. Modifications to the test case follow [17], [18]: line (11–13) is removed; 480 MW of load is shifted from nodes 14, 15, 19, and 20 to node 13; and the

capacity of line (14–16) is decreased to 350 MW. These modifications affect each of the three identical areas within the system. A small amount of congestion is induced by tripling the capacity of inexpensive hydro power in the area consisting of nodes 1–24 and removing hydro from all other areas.

Wind farms with 1000 MW of capacity are placed at nodes 23 and 47, which are both central locations containing 660 MW of coal generation each. The wind is placed at central parts of the system because isolated areas may require additional transmission investments that are beyond the scope of this report. These two wind farms comprise about 16% of the installed capacity. Wind energy has a production bid of zero and can be accepted up to the forecasted amount.

Dynamic zones are determined using statistical clustering based on WPTDFDs (8), where the line weights are derived from the dispatch solution from a single-zone model. Seasonal zone weights are based on average line utilizations over a season as in [21]. The three seasonal zones are shown in Figure 3; the smaller zones are usually import-constrained because they lack cheap generation from wind and hydro. Dynamic zone weights are based on post-contingency flows as described in Section 3. For each hour of the dynamic reserve zone process, the number of zones is one if there are no post-contingency violations and, otherwise, the number of zones is three.

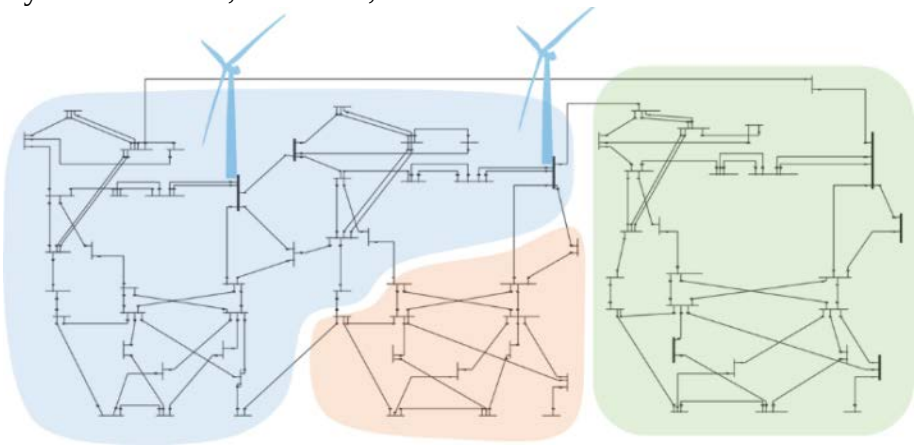

Figure 3. RTS-96 two wind locations and three seasonal reserve zones.

Reserve sharing is limited by constraint (7). Like in [18] and [30], the sharing capability S_{kt}^{j} is a variable defined as the interface capacity between zones k and j minus the scheduled power flows in period t. The interface capacity is taken here to be 95% of the component lines because it may be impossible to fully utilize the interface during contingency response. This is a simplified representation of the more sophisticated reserve sharing limits used by ISO-NE [30].

Only spinning contingency reserves are considered in this analysis. Each generator's reserve bid is 25% of the energy bid as in [41]. All testing is performed using CPLEX v12.6 on an 8-core 3.6 GHz computer, and SCUC is terminated after 10 minutes or upon reaching an optimality gap of 0.1%.

6.2 Wind Scenarios

Autoregressive integrated moving average (ARIMA) models are popular for describing how wind speed changes over time [42]. They are particularly convenient for simulation because movement is dictated by Gaussian error terms that are producible through a random number generator. ARIMA generalizes autoregressive (AR) and moving average (MA) models, which capture temporal correlation present in the data. Reference [43] proposes an efficient way to also account for spatial correlation between wind sites by generating statistically dependent error terms across locations. This report adopts the methodology of [43] to generate wind scenarios that have both spatial and temporal correlations.

The historical wind data is taken from NREL's Western Wind dataset for the first three weeks of August 2005 [44]. Figure 4(a) maps 510 turbines distributed across two clusters; these clusters are aggregated in this report to create two separate wind locations. Hourly ARIMA models are fit for each location based on wind speed, and the time series are later converted to power using an estimate of the aggregate power curves. The model is selected based on goodness of fit and the distribution of residuals. The adopted model includes one AR and MA term for the most recent hour and a 24-hour MA term with seasonal differencing for daily seasonality. The seasonality captures how wind varies by time of day: ramping up in the early morning and dropping off in the afternoon. The model's ability to capture temporal correlation is validated using the Ljung-Box test, which fails to reject the null hypothesis of independent errors with a statistical p-value greater than 0.10 for the first twenty time lags. Therefore, the time-series model does a reasonable job capturing the autocorrelation across most hours of the day.

Since the model is fit using only historical data, the deviation between samples tends to exceed forecast errors seen in practice [45]. This bias is corrected by normalizing the sampled wind speeds with the average so that the power stays within 20% of the mean approximately 80% of the time. Without this adjustment, the variability between scenarios is much greater than would be seen in practice. Figure 4(b) shows the available wind power for the first 15 scenarios generated using this approach. The forecast adopted in the DAM is assumed to follow the mean value of the simulated time series.

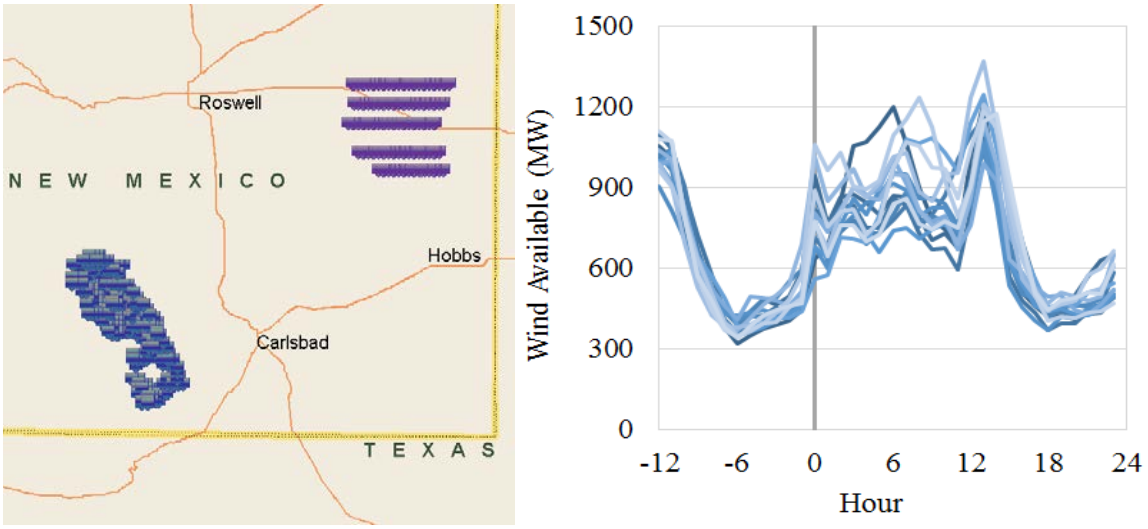

Figure 4. (a) Wind data locations. (b) Sample of fifteen wind scenarios.

6.3 Dynamic and Seasonal Zone Comparison

The seasonal and dynamic zones are analyzed across all seven days of the peak week. Each day is tested against the same 100 wind scenarios; therefore, uncertainty is highest on the weekend days 356 and 357. The peak day has 11% energy from wind and the lowest load day has 15% energy from wind.

Figure 5(a) shows the number of reserve disqualifications performed the make the solution reliable; each marker represents a single wind scenario for a day. There are $992 \times 24 > 235\ 000$ potential reserve disqualifications because the model contains 99 generators and 99 contingencies over 24 hours. Dynamic zones require far fewer disqualifications: only one dynamic zone simulation exceeds 25 disqualifications whereas half of the seasonal zone simulations exceed this amount. More disqualifications are required as wind increases relative to load, which suggests that dynamic zones become more beneficial as wind penetration increases.

The size of the markers in Figure 5(a) represents the sum of contingency violations across scenarios prior to any reserve disqualification. For example, the daily sum of violations (across all periods, wind scenarios, and contingencies) averages over 300 MW using seasonal zones but averages under 2 MW using dynamic zones. These results demonstrate that dynamic zones can significantly improve reliability and reduce the need for reserve disqualification.

Figure 5(b) shows the average quality of service $\overline{(\mathrm{QOS})}$ between seasonal and dynamic zones. Values closer to one indicate that more reserve procured from the DAM is deliverable in real-time. The upward slope in Figure 5(b) suggests that more reserve can be delivered when the system is lightly loaded and during scenarios where wind is abundant. $\overline{(\mathrm{QOS})}$ tends to improve when wind exceeds the forecast because conventional generators are left with more reserve to respond to contingencies. The improvement to quality of service provided by high wind is contingent on reserve being deliverable without needing reserve disqualification.

The size of the markers in Figure 5(b) represents the number of reserve disqualifications. As reserve disqualifications increase, $\overline{(QOS)}$ can be seen to drop relative to scenarios with a similar amount of wind. This shows that $\overline{(QOS)}$ is inversely related the number reserve disqualifications. The results indicate that dynamic zones help SCUC anticipate what reserves will be available in real time.

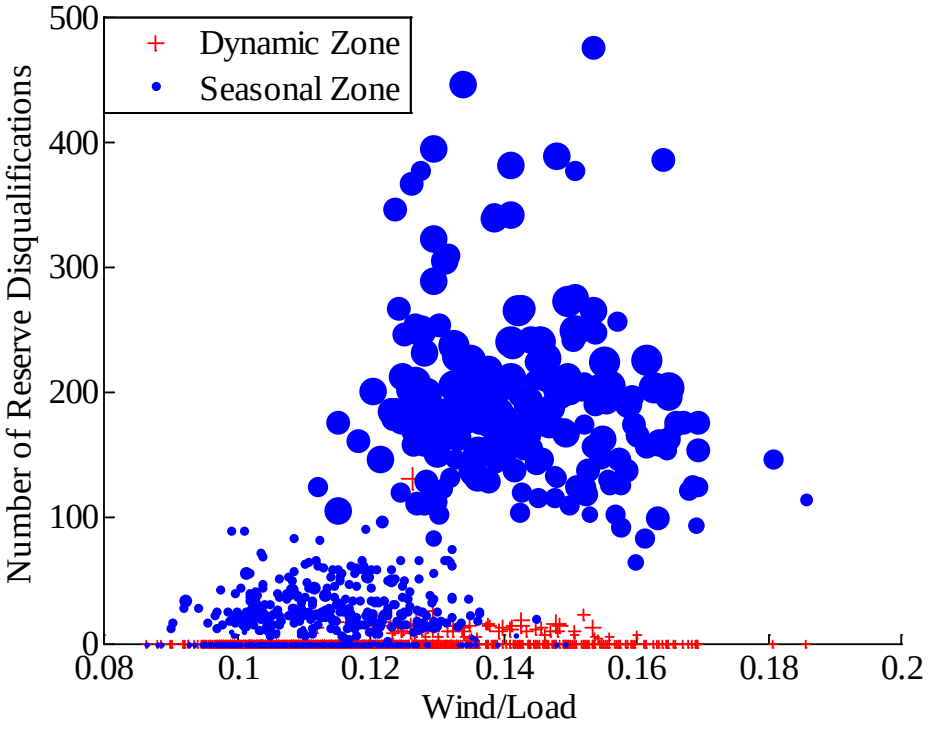

Figure 5(a). The number of reserve disqualifications for different wind scenarios, where marker size represents the sum of violations (MW) across contingencies prior to reserve disqualification.

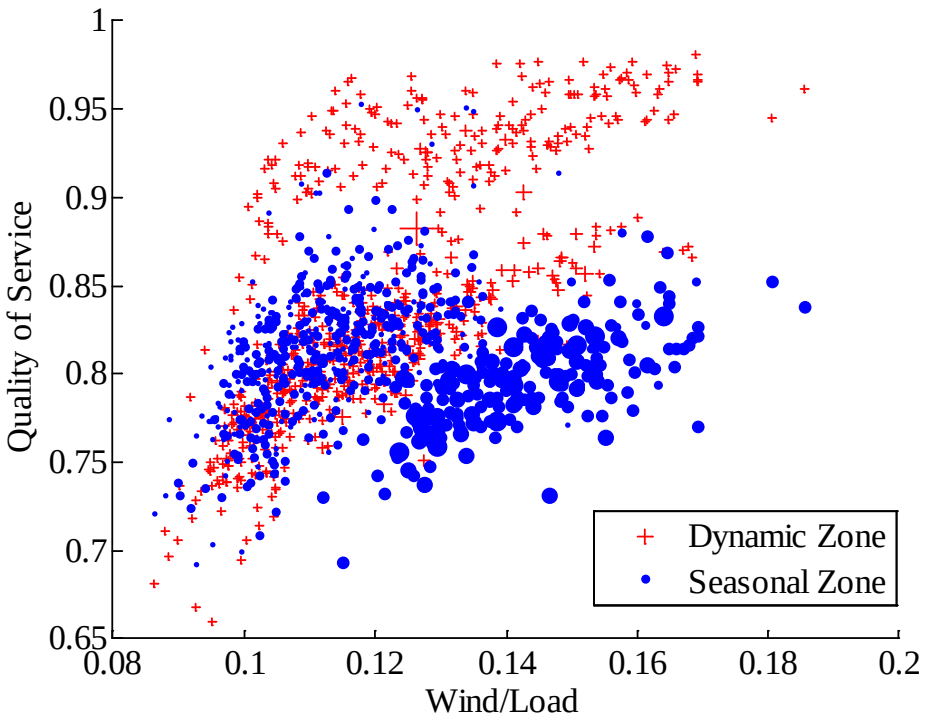

Figure 5(b). Quality of service ($\overline{\text{QOS}}$), where marker size represents the number of reserve disqualifications.

Table 1 summarizes the average market results over the 100 wind scenarios. Seasonal zones are able to achieve a reasonable (similar) production cost relative to the dynamic zones; this is primarily due to the efficiency of the reserve disqualification procedure to identify reserves that are not deliverable. However, in practice, the dynamic reserve zones are still valuable since they dramatically reduce the number of reserve disqualifications, which are generally costly out-of-market corrections (that can cause market distortion) manually implemented by the operator. From Table 1, the biggest improvement comes on days where wind provides a larger proportion of the energy. As shown in Table 2, this observation is validated by doubling the wind penetration: then dynamic zones improve the average cost by 3% compared to the seasonal approach. The cost improvements, when the wind penetration is doubled, are a result of there being less reliance on reserve disqualifications. Thus, dynamic reserve zones are even more beneficial with higher wind penetration levels.

The load payments, energy and reserve revenues are calculated based on the multi-settlement policy described by [46]. Transactions occur in the DAM based on the marginal energy and reserve prices. Trans-actions occur in the RTM relative to the DAM outcomes, e.g., generators cleared at 100 MW in the DAM and 101 MW in the RTM only receive the real-time price for the last MW. In this analysis, individual generators receive a make-whole uplift payment if their cleared bid costs exceed revenue from energy and ancillary services combined.

Tables 1 and 2 describe the aggregate market settlements for the baseline and the double wind penetration cases. The relative outcomes depend on the day and the amount of wind. For example, there is an overall wealth transfer towards suppliers in Table 1 and towards consumers in Table 2. No general conclusion can be drawn as to whether dynamic zones raise or lower market prices compared to seasonal zones; instead of a motive to either raise or lower prices, the motivation is to create a dynamic reserve policy that is efficient and enables price signals that are better at reflecting the true quality of service provided by suppliers. While the aggregate market results are relatively similar, the results in Figures 5(a) and 5(b) demonstrate that the dynamic zones require substantially fewer reserve disqualifications and that solutions with fewer disqualifications tend to result in a better $\overline{QOS}$. The higher quality of service indicates an improvement in market performance because less reserve payments are made toward resources that cannot provide the service in real-time. Moreover, the proposed dynamic reserve policies are better at achieving a reliable market solution, meaning that the market prices and settlements will better reflect how different decisions influence the cost of achieving reliability.

Table 1. Average system results over one hundred wind scenarios (millions $).

Day	Forecasted Wind/Load	Production Cost		Load Payment		Uplift Payments	
		Seasonal	Dynamic	Seasonal	Dynamic	Seasonal	Dynamic
351	11.6%	$1.969	$1.965	$8.924	$9.128	$0.007	$0.010
352	10.8%	$2.630	$2.624	$13.002	$14.010	$0.004	$0.004
353	11.1%	$2.427	$2.424	$10.897	$10.754	$0.023	$0.027
354	11.3%	$2.237	$2.236	$9.089	$9.651	$0.069	$0.041
355	11.5%	$2.058	$2.054	$8.341	$8.398	$0.042	$0.040
356	14.1%	$1.033	$1.026	$2.269	$2.301	$0.010	$0.005
357	14.5%	$0.971	$0.966	$2.464	$2.147	$0.001	$0.003
Ave.	12.0%	$1.903	$1.899	$7.855	$8.056	$0.022	$0.019
Day	Forecasted Wind/Load	Energy Revenue		Reserve Revenue			
		Seasonal	Dynamic	Seasonal	Dynamic		
351	11.6%	$8.165	$8.348	$0.138	$0.177		
352	10.8%	$11.935	$12.889	$0.156	$0.157		
353	11.1%	$9.987	$9.838	$0.116	$0.173		
354	11.3%	$8.303	$8.810	$0.124	$0.190		
355	11.5%	$7.616	$7.667	$0.098	$0.113		
356	14.1%	$1.974	$2.013	$0.094	$0.099		
357	14.5%	$2.150	$1.873	$0.100	$0.102		
Ave.	12.0%	$7.162	$7.348	$0.118	$0.144		

Table 2. Double wind: average system results
over one hundred scenarios (millions $).

Day	Forecasted Wind/Load	Production Cost		Load Payment		Uplift Payments	
		Seasonal	Dynamic	Seasonal	Dynamic	Seasonal	Dynamic
351	23.3%	$1.623	$1.606	$4.755	$4.338	$0.020	$0.022
352	21.6%	$2.223	$2.185	$8.716	$8.686	$0.013	$0.013
353	22.2%	$2.237	$2.014	$8.716	$7.500	$0.013	$0.020
354	22.6%	$1.907	$1.841	$7.014	$7.224	$0.014	$0.011
355	23.0%	$1.711	$1.670	$4.721	$4.949	$0.024	$0.020
356	28.2%	$0.776	$0.781	$2.037	$2.043	$0.001	$0.001
357	29.0%	$0.731	$0.725	$1.959	$1.871	$0.001	$0.001
Ave.	24.0%	$1.601	$1.546	$5.417	$5.230	$0.012	$0.013
Day	Forecasted Wind/Load	Energy Revenue		Reserve Revenue			
		Seasonal	Dynamic	Seasonal	Dynamic		
351	23.3%	$3.945	$3.573	$0.011	$0.011		
352	21.6%	$7.434	$7.376	$0.034	$0.021		
353	22.2%	$7.442	$6.310	$0.045	$0.011		
354	22.6%	$5.933	$6.059	$0.051	$0.013		
355	23.0%	$3.348	$3.131	$0.033	$0.011		
356	28.2%	$1.549	$1.558	$0.074	$0.088		
357	29.0%	$1.486	$1.419	$0.090	$0.090		
Ave.	24.0%	$4.448	$4.204	$0.048	$0.035		

6.4 Locational Reserve Prices

The reserve settlement scheme shown in (9) compensates resources for service to individual contingencies. The proposed policy can provide locational prices if reserves have been disqualified. This section illustrates such locational prices for one time period under a single wind scenario.

Figure 6(a) shows the flowgate marginal prices (FMPs) for hour one of day 357 when using seasonal zones. The FMP is defined as the dual variable for the flow limit on the respective line. Two lines are congested in this case before any contingency occurs: the line connecting node 73 to 21 and the line connecting node 22 to 21. As may be expected, one of these lines is already part of a zonal interface (see the zonal layout in Figure 3). The reserve sharing constraints mitigate congestion on this line by ensuring reserve is held within the import-constrained region. However, reserve zones cannot control the location of reserve around line (22-21) because this line is located completely within one of the zones. Reserve deliverability is generally harder to ensure when such intra-zonal congestion exists.

Indeed, congestion is a limiting factor and reliability is only obtained after disqualifying 37 reserve-contingency pairs. Figure 6(b) shows the reserve locations and prices in the resulting RTM solution. Reserve in the rightmost regions is valued high because it can serve more contingencies without overloading transmission. Reserve in the leftmost region is valued low because it provides limited service to outside areas. The one exception is reserve at node 21, which is valued relatively high because it counters

congestion on line (22-21). Even though nodes 21 and 22 are in the same zone, they have very different prices because they straddle a congested line. The settlement scheme still provides some payment to node 22 because the model recognizes that the reserve is deliverable for a subset of contingencies. This example demonstrates what would be expected of locational pricing: the procedure rewards market participants that are at key locations relative to congested lines. Traditional reserve zones do not provide this level of precision.

The analysis in this report uses reserve disqualification to repair unreliable solutions after the DAM. Therefore, the locational prices only reflect the RTM results. Reserve disqualification may also be integrated within the DAM structure to further improve market settlements.

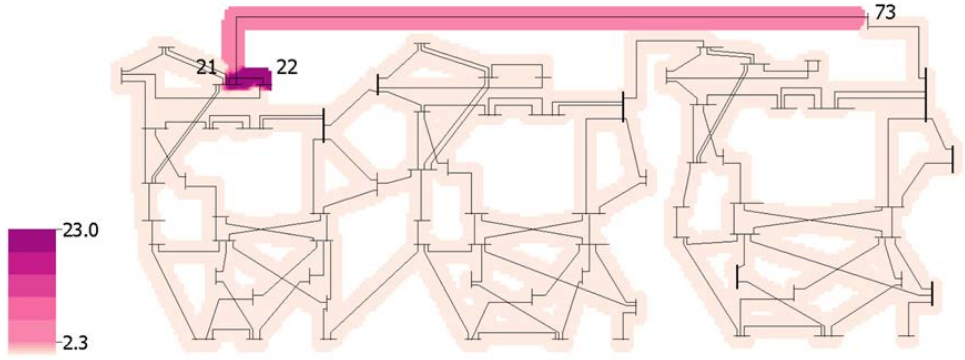

Figure 6(a). RTM results for a single wind scenario during hour one of day 357. Flowgate marginal prices.

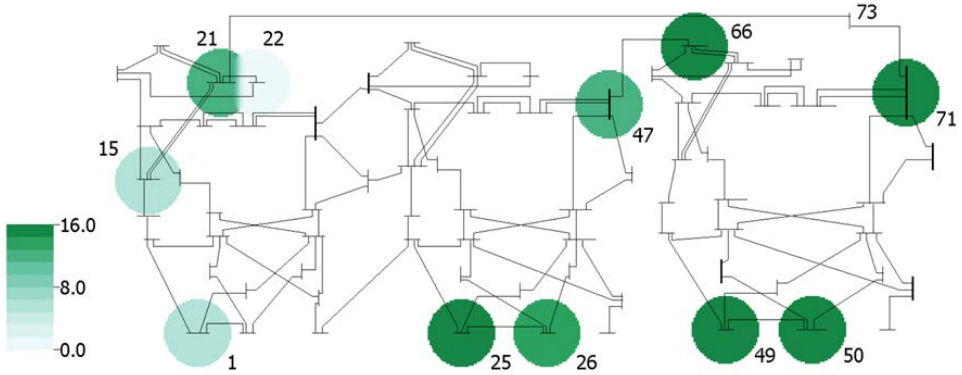

Figure 6(b). RTM results for a single wind scenario during hour one of day 357. Reserve locations and prices.

6.5 Market Complexity versus Market Transparency

Market complexity is important to consider [47]. Should the markets be simple and transparent or should they be complex and better reflect operational realities? Inaccurate DAM policies require costly uneconomic adjustments outside of the market (i.e., out-of-market corrections) in order to obtain a reliable solution. For instance, operators may procure additional generation headroom in the DAM to mitigate large day-ahead uncertainties [48]. This excess capacity can suppress market prices, only to be stripped away by reserve disqualification procedures (if the reserve is not deliverable) outside of the market environment. The advanced reserve policies investigated in this report are anticipated to produce price signals that better reflect the true value of ancillary services as compared to existing reserve policies. The market benefits should be considered against the increased market complexity brought on by these policies.

Some operators have expressed interest in reducing the number of reserve disqualifications [16]. This research shows that dynamic zones are a viable means in which to reduce reserve disqualifications. Furthermore, while this report applies the reserve disqualification algorithm after the DAM, the generalized reserve disqualification algorithm, [18], could be used within the DAM model itself. Such an execution within the DAM is expected to further improve market efficiency as well as reduce the price separation between the DAM and the RTM.

7. Conclusions

Ancillary service markets are used to procure standby reserves that provide operators with additional flexibility to respond to random disturbances. However, this flexibility is wasted when reserves are not deliverable. It is important to anticipate how uncertainty from intermittent renewable resources will affect congestion. It is desirable for the market model to anticipate what reserves will be deliverable in order to make efficient decisions and set prices that reflect the true locational scarcity of reserves.

Zonal reserve requirements ensure reserve is held within import-constrained areas. However, congestion may still prohibit the deliverability of reserve. In such cases, operators may adjust the schedule by disqualifying reserves that are hindered by transmission limitations. These adjustments occur outside of the DAM model and, therefore, are not reflected in day-ahead prices. Analysis on the IEEE RTS-96 test case demonstrates how updating zones on a more frequent basis can reduce the need for reserve disqualification and improve the real-time value of reserves procured in the DAM. The benefit of dynamic zones is magnified as the percentage of energy provided by uncertain resources (e.g., wind) increases.

This report introduces two further contributions that may also contribute to future research. The first is a mathematical program to evaluate the performance of reserve procured in the DAM. This approach may find further applications as a market assessment tool. The second contribution is a reserve settlement scheme for the generalized reserve disqualification model introduced by [18]. This settlement scheme includes a price component from each contingency based on their individual needs. The outcome is locational reserve prices based on the anticipated post-contingency congestion. Future research should study how this settlement scheme may impact market power and reserve bidding strategies.

Future work may extend the proposed approaches to address other forms of uncertainty. The application can support policies that are being investigated to mitigate wind uncertainty in the 5–30 min time range [28]. There is also potential to protect against multiple contingencies using a probabilistic framework. The methods discussed in this report can improve the locational modeling of such reserve products.

References

[1] K. Purchala, E. Haesen, L. Meeus, and R. Belmans, "Zonal network model of European interconnected electricity network," in *CIGRE/IEEE PES Int'l Symp.*, New Orleans, Louisiana, Oct. 2005.

[2] J. M. Arroyo and F. D. Galiana, "Energy and reserve pricing in security and network-constrained electricity markets," *IEEE Trans. Power Syst.*, vol. 20, no. 2, pp. 634–643, May 2005.

[3] F. D. Galiana, F. Bouffard, J. M. Arroyo, and J. F. Restrepo, "Scheduling and pricing of coupled energy and primary, secondary, and tertiary reserves," *Proc. IEEE*, vol. 93, no. 11, pp. 1970–1983, Nov. 2005.

[4] F. Bouffard, F. D. Galiana, and A. J. Conejo, "Market-clearing with stochastic security – part I: Formulation," *IEEE Trans. Power Syst.*, vol. 20, no. 4, pp. 1818–1826, Nov. 2005.

[5] L. Wu, M. Shahidehpour, and T. Li, "Stochastic security-constrained unit commitment," *IEEE Trans. Power Syst.*, vol. 22, no. 2, pp. 800–811, May 2007.

[6] L. Wu, M. Shahidehpour, and T. Li, "Cost of reliability analysis based on stochastic unit commitment," *IEEE Trans. Power Syst.*, vol. 23, no. 3, pp. 1364–1374, Aug. 2008.

[7] K. W. Hedman, M. C. Ferris, R. P. O'Neill, E. B. Fisher, and S. S. Oren, "Co-optimization of generation unit commitment and transmission switching with *N*-1 reliability," *IEEE Trans. Power Syst.*, vol. 25, no. 2, pp. 1052–1063, May 2010.

[8] H. A. Hejazi, H. R. Mohabati, S. H. Hosseinian, and M. Abedi, "Differential evolution algorithm for security-constrained energy and reserve optimization considering credible contingencies," *IEEE Trans. Power Syst.*, vol. 26, no. 3, pp. 1145–1155, Aug. 2011.

[9] Y. Al-Abdullah, M. Abdi-Khorsand, and K. W. Hedman, "Analyzing the impacts of out of market corrections," *IREP Symp. - Bulk Power System Dynamics and Control* – IX, Aug. 25-30 2011.

[10] Y. M. Al-Abdullah, M. Abdi-Khorsand, and K. W. Hedman, "The role of out-of-market corrections in day-ahead scheduling," *IEEE Trans. Power Syst.*, vol. 30, no. 4, pp. 1937-1946, Jul. 2015.

[11] CAISO, "2012 annual report on market issues & performance," Apr. 2013. [Online]. Available: http://www.caiso.com/Documents/2012AnnualReport-MarketIssue-Performance.pdf.

[12] ERCOT, "Report on existing and potential electric system constraints and needs," Dec. 2007. [Online]. Available: http://www.ercot.com/ content/news/presentations/2013/2012%20Constraints%20and%20Needs %20Report.pdf.

[13] FERC, "Docket no. ER11-2794-000 – Order conditionally accepting tariff revisions – MISO," Jun. 2011. [Online]. Available: http://www.ferc.gov/ EventCalendar/Files/20110628160939-ER11-2794-000.pdf.

[14] ISO-NE, SOP-RTMKTS.0060.0020, "Monitor system security v57," Feb. 2013. [Online]. Available: http://www.iso-ne.com/rules_proceds/operating/sysop/rt_mkts/sop_rtmkts_0060_0020.pdf.

[15] ISO-NE, SOP-RTMKTS.0120.0030, "Implement transmission remedial action v20," Jun. 2012. [Online]. Available: http://www.iso-ne.com/rules_proceds/operating/sysop/rt_mkts/sop_rtmkts_0120_0030.pdf.

[16] Y. Chen, P. Gribik, and J. Gardner, "Incorporating post zonal reserve deployment transmission constraints into energy and ancillary services co-optimization," *IEEE Trans. Power Syst.*, vol. 29, no. 2, pp. 537–549, Feb. 2014.

[17] J. D. Lyon, K. W. Hedman, and M. Zhang, "Reserve requirements to efficiently manage intra-zonal congestion," *IEEE Trans. Power Syst.*, vol. 29, no. 1, pp. 251–258, Jan. 2014.

[18] J. D. Lyon, M. Zhang, and K. W. Hedman, "Locational reserve disqualification for distinct scenarios," *IEEE Trans. Power Syst.*, vol. 30, no. 1, pp. 357-364, Jan. 2015.

[19] MISO, "MISO energy and operating reserve markets, business practices manual," BPM-002-r11, Jan. 2012. [Online]. Available: https://www.misoenergy.org/Library/BusinessPracticesManuals/Pages/BusinessPracticesManuals.aspx.

[20] M. Shields, M. Boughner, R. Jones, and M. Tackett, "Market subcommittee minutes/asm market design," MISO, printed copy, Aug. 2007.

[21] F. Wang and K. W. Hedman, "Dynamic reserve zones for day-ahead unit commitment with renewable resources," *IEEE Trans. Power Syst.*, vol. 30, no. 2, pp. 612-620, Mar. 2015.

[22] H. Gooi, D. Mendes, K. Bell, and D. Kirschen, "Optimal scheduling of spinning reserve," *IEEE Trans. Power Syst.*, vol. 14, no. 4, pp. 1485–1492, Nov. 1999.

[23] H. Wu and H. B. Gooi, "Optimal scheduling of spinning reserve with ramp constraints," in *Proc. IEEE PES Winter Meeting*, vol. 2, pp. 785–790, Jan. 1999.

[24] D. Chattopadhyay and R. Baldick, "Unit commitment with probabilistic reserve," in *Proc. IEEE PES Winter Meeting*, vol. 1, pp. 280–285.

[25] L. M. Xia, H. B. Gooi, and J. Bai, "Probabilistic spinning reserves with interruptible loads," in *Proc. IEEE PES General Meeting*, vol. 1, pp. 146–152, 2004.

[26] L. M. Xia, H. B. Gooi, and J. Bai, "A probabilistic reserve with zero-sum settlement scheme," *IEEE Trans. Power Syst.*, vol. 20, no. 2, pp. 993–1000, May 2005.

[27] F. Aminifar, M. Fotuhi-Firuzabad, and M. Shahidehpour, "Unit commitment with probabilistic spinning reserve and interruptible load considerations," *IEEE Trans. Power Syst.*, vol. 24, no. 1, pp. 388–397, Feb. 2009.

[28] H. Holttinen *et al.*, "Methodologies to determine operating reserves due to increased wind power," *IEEE Tran. Sust. Energy.*, vol. 3, no. 4, pp. 713–723, Oct. 2012.

[29] PJM, "2013 PJM reserve requirement study," [Online]. Available: http://www.pjm.com/~/media/committees-groups/committees/mrc/20131024/20131024-item-04-irm-study.ashx.

[30] T. Zheng and E. Litvinov, "Contingency-based zonal reserve modeling and pricing in a co-optimized energy and reserve market," *IEEE Trans. Power Syst.*, vol. 23, no. 2, pp. 277–286, May 2008.

[31] F. Wang and K. W. Hedman, "Reserve zone determination based on statistical clustering method," in *Proc. North American Power Symp.*, 2012.

[32] A. Kumar, S. C. Srivastava, and S. N. Singh, "A zonal congestion management approach using real and reactive power rescheduling," *IEEE Trans. Power Syst.*, vol. 19, no. 1, pp. 554–562, Feb. 2004.

[33] ERCOT, "ERCOT protocols, section 7: congestion management," July, 2010 [Online]. Available: www.ercot.com/content/mktrules/protocols/current/07-070110.doc.

[34] Z. Wang, A. Scaglione, and R. J. Thomas, "Electrical centrality measures for electric power grid vulnerability analysis," in *49th IEEE Conf. on Decision and Control*, Atlanta, GA, Dec. 15–17, 2010.

[35] E. Cotilla-Sanchez, P. D. Hines, C. Barrows, S. Blumsack, and M. Patel, "Multi-attribute partitioning of power networks based on electrical distance," *IEEE Trans. Power Syst.*, vol. 28, no. 4, pp. 4979–4987, Nov. 2013.

[36] R. P. O'Neill, P. M. Sotkiewicz, B. F. Hobbs, M. H. Rothkopf, and W. R. Stewart, "Efficient market-clearing prices in markets with nonconvexities," *Eur. Journal of Oper. Res.*, vol. 164, pp. 269–285, Dec. 2003.

[37] B. Stott, J. Jardim, and O. Alsac¸, "DC power flow revisited," *IEEE Trans. Power Syst.*, vol. 24, no. 3, pp. 1290–1300, Aug. 2009.

[38] J. Lerner, M. Grundmeyer, and M. Garvert, "The importance of wind forecasting," *Renewable Energy Focus*, vol. 10, no. 2, pp. 64–66, 2009.

[39] C. Grigg *et al.*, "The IEEE reliability test system – 1996," *IEEE Trans. Power Syst.*, vol. 14, no. 3, pp. 1010–1020, Aug. 1999.

[40] Univ. of Washington, "Power systems test case archive," 1999. [Online]. Available: http://www.ee.washington.edu/research.

[41] F. Bouffard, F. D. Galiana, and A. J. Conejo, "Market-clearing with stochastic security—Part II: Case studies," *IEEE Trans. Power Syst.*, vol. 20, no. 4, pp. 1818–1826, Nov. 2005.

[42] M. Lei, L. Shiyan, J. Chuanwen, L. Hongling, and Z. Yan, "A review of the forecasting of wind speed and generated power," *Renewable and Sustain. Energy Reviews*, vol. 13, pp. 915–920, Feb. 2009.

[43] J. M. Morales, R. Minguez, and A. J. Conejo, "A methodology to generate statistically dependent wind speed scenarios," *Applied Energy*, vol. 87, pp. 843–855, Sep. 2009.

[44] NREL, "Western wind resource dataset," Jan. 2014. [Online]. Available: wind.nrel.gov/Web_nrel/.

[45] B. Hodge, A. Florita, K. Orwig, D. Lew, and M. Milligan, "A comparison of wind power and load forecasting error distributions," in *World Renewable Energy Forum*, May 2012.

[46] R. E. Kurlinski, "Real-time revenue imbalance in CAISO markets," CAISO Dept. of Mkt. Mon., Tech. Rep., Apr. 2013. [Online]. Available:

http://www.caiso.com/Documents/DiscussionPaper-Real-timeRevenueImbalance_CaliforniaISO_Markets.pdf .

[47] C. Vournas and T. Bakirtzis, “Oral discussions on session: markets – part II,” I*REP Symposium – Bulk Power Syst. Dynamics and Control –IX (IREP)*, Rethymnon, Greece, Aug. 25-28, 2013.

[48] D. B. Patton, P. LeeVanSchaick, and J. Chen, “2011 assessment of the ISO New England electricity markets,” Potomic Economics, 2012. [Online]. Available: http://www.iso-ne.com/markets/mktmonmit/rpts/ind_mkt_advsr/emm_mrkt_rprt.pdf.

Part II

A Statistical Evaluation of Dynamic Reserve Policies with Consideration of Stochastic Resources

Fengyu Wang
Kory W. Hedman

Arizona State University

For information about this project, contact

Kory W. Hedman
Arizona State University
School of Electrical, Computer, and Energy Engineering
P.O. BOX 875706
Tempe, AZ 85287-5706
Phone: 480 965-1276
Fax: 480 965-0745
Email: kory.hedman@asu.edu

Power Systems Engineering Research Center

The Power Systems Engineering Research Center (PSERC) is a multi-university Center conducting research on challenges facing the electric power industry and educating the next generation of power engineers. More information about PSERC can be found at the Center's website: http://www.pserc.org.

For additional information, contact:

Power Systems Engineering Research Center
Arizona State University
527 Engineering Research Center
Tempe, Arizona 85287-5706
Phone: 480-965-1643
Fax: 480-965-0745

Notice Concerning Copyright Material

Table of Contents

List of Figures

List of Tables

Nomenclature

Sets:

I	Transmission constrains; $i \in I$.
J	Resources; $j \in J$. $J^k \subseteq J$ are resources in zone; $J^c \subseteq J$ are conventional resources; J^w are wind resources.
K	Set of reserve zones; $k, k' \in K$.
N	Nodes; $n_j \in N$ is the node of resource j.
S	Set of net load scenarios; $s \in S$.
T	Time periods; $t, t' \in T$.
X	Set of reserve categories {*REG, SPIN, SUPP*}, $x \in X$.

Parameters (index t denotes period):

$PTDF_{i,n}$	PTDF for transmission asset i, based on an injection at node n and a withdrawal at the reference bus.
$PTDF_{i,LC}$	PTDF of the flow on transmission asset i to injection at the load center LC and withdrawal at the reference bus.
$PTDF_{i,k,t}$	Aggregated PTDF of the flow on transmission asset i to zone k and withdrawal at the reference bus.
$PTDF_{i,k}^{TRIP}$	Aggregated PTDF of the flow on transmission asset i to the largest contingency event in zone k with injections at the locations used to model the outage and withdrawal at the reference bus.
$\mathrm{C}_j^{SU}, \mathrm{C}_j^{SD}$	Start-up and shut-down costs of resource j.
C_j^{NL}	No-load cost of resource j.
$\mathrm{C}_{j,t}^{P}(\cdot)$	Energy offer cost function of $p_{j,t}$ from resource j, in \$/MWh.
$Y_{n,t}$	Demand at node n.
$\mathrm{D}_{k,t}^{SPIN}, \mathrm{D}_{k,t}^{SUPP}$	Spinning and supplemental reserve deployment factors under the largest contingency event in zone k.
DT_j, UT_j	Minimum down- and up- time of resource j.
$E_{k,t}$	Largest contingency event size in zone k.
$\overline{F}_{i,t}, \overline{\overline{F}}_{i,t}$	Normal and contingency limits for transmission limit i.
$R_{MKT,t}^{x}$	Market-wide requirement for reserve x.
$R_{j,t}^{x}$	Maximum amount of reserve x that can be cleared on resource j.
$O_{j,t}^{x}$	Resource j available offer price for reserve x, in \$/MWh.
L_t	Interval length of interval *t*, in minutes.
$\bar{P}_{j,t}, \underline{P}_{j,t}$	Resource j maximum and minimum power output.
$PTDFD_{mn}$	PTDF difference between node *n* and *m.*
$V_{j,t}^{UP}, V_{j,t}^{DOWN}$	Resource j up and down ramp rate in MW/min.
$W_{j,t}$	Forecasted wind output for resource j.
$WPTDFD_{mn}$	Weighted PTDF difference between node *n* and *m.*
$\alpha_{i,t}$	Expected power flow on transmission asset i.
$\pi_{i,t}$	Weighted factor of PTDF difference for transmission asset i.

$\sigma_{i,t}$ Standard deviation of flow on transmission asset i.

Variables (index t denotes period):

$f_{i,t}$ Power flow on transmission asset i.
$l_{n,t}$ Net fixed injection at node n.
$p_{j,t}$ Cleared energy on resource j.
$r_{j,t}^{x}$ Cleared reserve x on resource j.
$r_{k,t}^{x}$ Solved zone k requirement for reserve x.
$su_{j,t}, sd_{j,t}$ Start-up / shut-down variable of resource j.
$u_{j,t}$ Commitment variable for resource j.
$w_{j,t}$ Wind spillage for resource j.

Shadow Prices (index t denotes period):

λ_t Shadow price of power balance equation.
γ_t^{MRR} Shadow price of the market-wide regulating reserve requirement constraint.
γ_t^{MRS} Shadow price of the market-wide regulating plus spinning reserve requirement constraint.
γ_t^{MOR} Shadow price of the market-wide operating reserve constraint.
γ_t^{MRR} Shadow price of the market-wide regulating reserve requirement constraint.
$\gamma_{k,t}^{ZRR}$ Shadow price of the minimum zonal regulating reserve requirement constraint k.
$\gamma_{k,t}^{ZRS}$ Shadow price of the minimum zonal regulating plus spinning reserve requirement constraint k.
$\gamma_{k,t}^{ZOR}$ Shadow price of the minimum zonal operating reserve requirement constraint k.
$\mu_{i,t}$ Shadow price of transmission constraint i.
$\mu_{i,t}^{REGDN}$ Shadow price of transmission constraint i under post regulating reserve down deployment.
$\mu_{i,t}^{REGUP}$ Shadow price of transmission constraint i under post regulating reserve up deployment.

Market Clearing Prices:

$MCP_{k,t}^{x}$ Zonal MCP for reserve *x* zone k.
$LMP_{n,t}$ Locational marginal price at node n.

1. Introduction

1.1 Research Premise

Due to global climate change and increasing electricity demand, the amount of renewable resources is expected to increase substantially in order to lower greenhouse gas emissions and the use of fossil fuel generators. However, there are three aspects that create new challenges for power system engineers to maintain system reliability without degrading the market efficiency. First, renewable generation (wind and solar) is unpredictable and highly variable. Even though the diversity of wind locations can lower the uncertainty, there is still the chance of a sudden fleet drop or increase in wind output; compared to wind output, solar output can drop even more drastically due to the change in cloud coverage. As a result, existing deterministic scheduling tools should be updated to improve their handling of such continuous uncertainties. Second, renewable generation is non–dispatchable or semi-dispatchable, unlike conventional generators; with an increasing percentage of the fleet being renewable, there is an increased reliance on conventional generators to provide ancillary services. Third, bulk energy storage is still expensive and the installed energy storage capacity is small; until bulk storage is substantially cheaper, the challenge to efficiently manage high levels of renewables, while maintaining reliability, will remain.

Uncertainties, such as renewables, load, and contingencies, can cause imbalance between load and generation, which will lead to frequency fluctuations. Operating reserves are one key ancillary service, which are necessary to operate the grid reliably. Operating reserve is a dispatchable backup capability that is used to maintain system frequency as well as to stay within various operating limits. Operating reserves can be called upon due to fluctuations in demand, renewable production, or to respond to a contingency. Based on the response time and functionality, reserve can be categorized into three types: primary reserve, secondary reserve, and tertiary reserve [1]. Primary reserve is using system inertia to resist system frequency change. Secondary reserve, which is also recognized as regulation reserve, is used to change the generation based on the feedback of area control error (ACE) and it is also referred to as automatic generation control (AGC). Tertiary reserve, which is recognized as contingency reserve, is used to sustain the system frequency against larger system disturbances, such as contingencies. Based on basic decision making theory, and as stated in [1], optimizing the energy and ancillary services (e.g., reserve) simultaneously is better than optimizing these services sequentially since a single, simultaneous decision making process will result in a more efficient (or the same) solution as a sequential approach.

Different reserve policies can be used to quantify the amount of operating reserve. For instance, the National Renewable Energy Laboratory (NREL) proposed a heuristic rule, which is the reserve should be no less than 3% of load and 5% of forecasted renewable generation [2]-[3]. However, due to the uncertainty of renewable resources, such basic, static reserve policies may not be economical or reliable. A good reserve policy should determine, efficiently, the location and quantity of operating reserve while ensuring reliability. Some reserve policies dynamically determine the amount of reserve

as the system operating conditions change [4]-[6]. Reference [4] procures operating reserve on an hourly basis with consideration of expected wind power output to lower the operating cost while maintaining system reliability**.** In [5]-[6], the authors determine the reserve requirements based on probabilities such that reserve is acquired in an attempt to balance the operating cost and the expected energy not served cost. References [4]-[6] address the optimal quantity of operating reserve, but the location of reserve and reserve deliverability are not studied. Post-contingency congestion may inhibit the deliverability of reserve and renewables will make post-contingency congestion even more unpredictable. Thus, even if an adequate quantity of reserve is acquired, system reliability may not be guaranteed. Therefore, if congestion exists in the system, the "right" location of reserve may be preferred over acquiring an "excessive" quantity of reserve.

Uncertainties can be *endogenously* modelled within stochastic unit commitment (UC) such that the quantity and location of reserve is *implicitly* acquired [1], [7]-[8]. Reference [1] proposed a stochastic model to balance the operating cost and reliability cost with the consideration of probabilities of system disturbances; [1] uses what is known as a deterministic equivalent (extensive form) stochastic programming formulation to explicitly represent contingencies (scenarios) and suggests a pricing structure for such a stochastic market. While stochastic programming produces an optimal solution (with respect to the modeled uncertainties), the concerns are as follows:

1) Limitation of stochastic information. Modelling all the continuous and discrete uncertainties in the UC formulation is impossible today and usually selected "scenario trees" are modelled. The inclusion of more scenarios in the optimization formulation will improve the representation of the uncertainties but this also increases the computational time. The modelled uncertainties in the day-ahead may be quite different from true scenarios.

2) Scalability issues. Even though some alternative formulations or decomposition approaches are investigated [9]-[10], the computational times for most stochastic UC problems increases significantly (an order of 10 or more) compared to a deterministic UC problem, depending on the formulation structure, problem size, and the number of scenarios modelled. Decomposition techniques can break the original stochastic problem into smaller problems, which may be easier to solve and, depending on the decomposition approach, those smaller problems may be parallelizable; such approaches are known to improve the computational performance over solving an extensive form stochastic program. However, there are still some practical issues for those decomposition techniques. For instance, Benders' decomposition has a bloat problem; the master problem size increases at each iteration and there is no guarantee that the master problem does not grow to a size that it is not any less difficult to solve than the original problem or that it does not require as much memory.

3) Pricing issues. There is an ongoing debate on how to design a market where the internal mathematical program is a stochastic program. Therefore, stochastic UC is being considered for problems such as residual unit commitment but there is still hesitation due to the market complexities it adds to existing markets.

Implementing stochastic programming will, therefore, be a greater challenge. Instead of implementing stochastic programming, approximations, such as reserve requirements, are used in existing UC frameworks without incurring excessive computational time. Operators determine the quantity of reserve by specifying a minimum quantity of reserve on a system-wide and/or a zonal basis. For instance, Midcontinent Independent System Operator (MISO) implements zonal reserve requirements and evaluates its zonal reserve requirements two days ahead [9]. Operators locate the reserve by using reserve zones such that the reserve will be distributed across the grid. Reserve will be shared inside the zone and it is assumed that resources in the zone have the same impact on the system and there is no intra-zonal congestion that inhibits the deliverability of reserves. These assumptions may not be always true. If intra-zonal congestion prohibits reserve deliverability, operators may increase the minimum zonal reserve requirements or manually disqualify undeliverable reserve. However, such procedures may lead to uneconomic solutions and distort the market signal.

It is supposed that resources that have similar impacts on the system transmission bottlenecks are grouped into the same zone. However, operators today rarely update the reserve zone configuration even though the system operating conditions changes continually as well as the transmission bottlenecks. Usually, uncertainties such as contingencies, load, area interchange, and renewable resources are not considered while updating the reserve zone. Today, one of the most common ways to determine reserve zones is based on asset ownership, which is independent from system operating conditions and uncertainties. MISO re-configures its reserve zone partition on a quarterly basis if there is no significant system operating condition change [9]. Distributing reserve in such a static operational rule may result in inefficient market solution.

In [10], PTDF differences (PTDFD) are employed to partition the reserve zones based on statistical clustering techniques; while the method is a heuristic, it is computationally tractable. Buses with similar impacts on the power system will be grouped in the same reserve zones. However, [10] does not account for the impacts of renewable resources.

Reference [11] employs the PTDFD metric in [10] and performs it on a daily basis with the consideration of renewables. The numerical results in [11] show that daily probabilistic reserve zone outperforms the seasonal zone by improving the expected load shedding and expected total operating cost on a probability basis. The expected total cost is calculated based on the assumption that the uneconomic adjustments cost, i.e., the cost to implement reserve disqualification, is a positive linear function of load shedding. However, due to the non-convexities and complexity of unit commitment formulations, this approximation may be inaccurate and the expected total cost does not reflect the true operating cost.

In [12], the market aspects of an hourly reserve zone determination method are evaluated. Updating reserve zones on a more frequent basis enables a more accurate representation of operating conditions, identification of key transmission bottlenecks, the preferred locations for reserves, and better reserve sharing rules across zones.

The work of [10], [11], and [12] are not adequate to produce sufficient incentive for the industry application of the proposed hourly reserve determination method. This report is supposed to bridge the proposed method with real-world system operation by studying

the feasibility of the proposed method's application based on real-life system operational rules and models. The main contributions of this report are:

1) Approximate MISO's security-constrained unit commitment (SCUC) model and look-ahead unit commitment model to better approximate the MISO's market clearing process and to improve the quality and credibility of the numerical results [13].

2) A statistical technique (confidence intervals) is used to provide a proper statistical assessment of the benefits of the proposed reserve rule refinement.

In real-word operations, unreliable market solutions will be adjusted by operators. Evaluating the true operating cost using an assumed fixed value of lost load (VOLL) can be inaccurate. To obtain a better assessment of the cost of out-of-market corrections (reserve disqualifications) [14], unreliable solutions from the market SCUC are corrected based on similar procedures implemented today by ISOs. Reserve disqualifications occur after both the day-ahead SCUC and the look-ahead short-term SCUC. An accurate assessment of the actual costs to correct unreliable solutions is difficult to obtain and is generally overlooked as such ad-hoc practices are not well documented. This report utilizes an algorithm that mimics MISO's reserve disqualification process to accurately account for such reserve disqualification costs.

1.2 Report Organization

The rest of the report is organized as follows. In Section 2, an hourly reserve zone determination method, which utilizes sensitivity difference and probabilistic power flows to model the potential network flows, is presented. Section 3 presents the SCUC, look ahead commitment, and reserve disqualification models. The hourly reserve zone determination method is applied to a modified version of RTS-96 and the results are presented in Section 4. Section 5 concludes this report.

2. Hourly Reserve Zones Based on Probabilistic Power Flows

2.1 Power Transfer Distribution Factors

The sensitivity factor, $PTDF_{i,n,t}$, is the power flow impact on transmission line *i* while injecting 1MW at bus *n* and withdrawing 1MW at the reference bus. To capture the difference in the line flow between two injection points, the absolute power flow change on line *i* is $\left|PTDF_{i,n} - PTDF_{i,m}\right|$. The PTDF difference (PTDFD) between buses *i* and *j*, which is the average absolute power flow change over all transmission lines, is defined as,

$$PTDFD_{mn} = \frac{\sum_{i=1}^{|I|}\left|PTDF_{i,n} - PTDF_{i,m}\right|}{|I|} \quad (1)$$

where $|I|$ represents the number of transmission lines. This metric is meant to capture the impact of injecting reserve at different locations in the network. The primary motivation is to lump nodes together that have similar impacts on transmission assets. While the PTDFD in (1) involves all transmission lines, it can be used to focus on only key transmission bottlenecks. Weights are, thus, used to identify the importance of each line. Suppose there are $|I|$ transmission lines, then the weighted PTDFD (WPTDFD), with weight π_i on transmission line *i* between bus *n* and bus *m*, is shown by (2). Existing reserve zones do not dynamically change even though system operating conditions widely vary. As a result, intuitively, it is expected that such a concept will have substantial impacts on operations, as is shown later with the results.

$$WPTDFD_{mn} = \frac{\sum_{i=1}^{|I|}\pi_i\left|PTDF_{i,n} - PTDF_{i,m}\right|}{|I|} \quad (2)$$

2.2 Hourly Reserve Zone Partitioning Method Based on Probabilistic Power Flows

To determine the reserve zone on an hourly basis, the weight for each transmission line should be updated hourly. The proposed hourly reserve zone determination method is expected to involve the uncertainty and variability of renewable resources (e.g., wind) and load based on a probabilistic power flow model.

To identify the critical transmission lines, two factors should be considerd, the expected power flow and the deviation of power flow. Simulations are conducted to generate sufficienct power flow scenarios based on different wind scenarios and contingencies. Note that contingency analysis generally includes transmission contingencies and generation contingencies. In this report, only generation contingencies are considered; note, however, that it is technically easy to include both types of contingencies. The procedures of generating weights and reserve zones are shown below. Note that, for the ISO to implement this process, the only added computation would be to

conduct contingency analysis (Step 3) and then to generate the reserve zones (Step 5) since Step 1 can be based on the day-ahead market based security constrained unit commitment solution.

Step 1 A deterministic unit commitment is solved based on predetermined zones. The unit commitment solution is then fixed for Step 3.

Step 2 Generate the net load scenarios in order to characterize the uncertainty and variability of wind power output and load. The net scenario generation procedure is presented in Section 4.1.

Step 3 Perform *N*-1 contingency analysis with generated net load scenarios and record the power flows for the various wind scenarios. Note that while there are many power flow results that are generated, each scenario is independent and, thus, it is trivial to parallelize this process. The expected power flow on transmission line *i* at hour *t*, represented by $\alpha_{i,t}$, and the standard deviation of power flow of transmission line *i* at period *t*, i.e., $\sigma_{i,t}$, are calculated for each transmission line. Note that, for this investigation, we solved independent DCOPFs that minimized the post-contingency violations; for implementation, it would be sufficient to conduct contingency analysis (solve many independent power flows) to generate the probabilistic power flow data.

Step 4 Calculate each weight, $\pi_{i,t}$, for transmission line *i*: $\pi_{it} = \left(\left|\frac{\alpha_{i,t}}{\overline{F}_{i,t}}\right| + \frac{2\sigma_{i,t}}{\overline{F}_{i,t}}\right)^2$; the term is squared in order to place more emphasis on the critical paths.

Step 5 If there is any violation at period *t* for any wind scenario and contingency, perform the statistical clustering algorithm (K-means) to partition the reserve zones based on WPTDFD and the weights from Step 4. Otherwise, the reserve zone at period *t* will remain the same as the pre-determined zone.

3. Operational Model with Consideration of Hourly Reserve Zones

3.1 SCUC Formulation

MISO co-optimizes energy and ancillary service in the day-ahead market with energy and reserve bids to ensure adequate generation capacity to serve next day's demand [15].

Before the day-ahead market solution is approved, none of the transmission constraints should be violated, otherwise an adjustment will be made to the SCUC formulation [16]. To lower the expected transmission violation after reserve deployment, in [17], a security constrained economic dispatch (SCED) model is enhanced by incorporating post zonal reserve deployment and modelling the largest contingency in each reserve zone. The post zonal reserve deployment transmission constraints are also used within MISO's SCUC. The proposed SCUC formulation with consideration of post regulation and contingency reserve deployment is shown as below,

$$\text{Min}_{p_{j,t},\, r^{x}_{j,t}, su_{j,t}, sd_{j,t}} \sum_{j\in J, t\in T}\Big\{C^{P}_{j,t}\big(p_{j,t}\big) + C^{SU}_{j}\big(su_{j,t}\big) + C^{SD}_{j}\big(sd_{j,t}\big) + C^{NL}_{j}\big(u_{j,t}\big) + \sum_{x\in X}\big(O^{x}_{j,t}\cdot r^{x}_{j,t}\big)\Big\} \quad (3)$$

Subject to:

$$\sum_{n\in N}\big(l_{n,t}\big) = 0, \qquad (\lambda_t) \quad (4)$$

$$l_{n,t} = \sum_{n_j=n}\big(p_{j,t}\big) + \sum_{n_j=n}\big(W_{j,t} - w_{j,t}\big) - Y_{n,t} \quad (5)$$

$$f_{i,t} \le \overline{F}_{i,t}, \qquad (\mu_{i,t}) \quad (6)$$

$$f_{i,t} = \sum_{n\in N}\big\{l_{n,t} PTDF_{i,n,t}\big\} \quad (7)$$

$$\sum_{k\in K} r^{REG}_{k,t} \ge R^{REG}_{MKT,t}, \qquad (\gamma^{MRR}_{t}) \quad (8)$$

$$\sum_{k\in K}\{r^{REG}_{k,t} + r^{SPIN}_{k,t}\} \ge R^{REG}_{MKT,t} + R^{SPIN}_{MKT,t}, \qquad (\gamma^{MRS}_{t}) \quad (9)$$

$$\sum_{k\in K}\{r^{REG}_{k,t} + r^{SPIN}_{k,t} + r^{SUPP}_{k,t}\} \ge R^{REG}_{MKT,t} + R^{SPIN}_{MKT,t} + R^{SUPP}_{MKT,t}, \qquad (\gamma^{MOR}_{t}) \quad (10)$$

$$\sum_{j\in J^k} r^{REG}_{j,t} \ge r^{REG}_{k,t}, \qquad (\gamma^{ZRR}_{k,t}) \quad (11)$$

$$\sum_{j\in J^k}\{r^{REG}_{jt} + r^{SPIN}_{jt}\} \ge r^{REG}_{k,t} + r^{SPIN}_{k,t}, \qquad (\gamma^{ZRS}_{k,t}) \quad (12)$$

$$\sum_{j\in J^k}\{r^{REG}_{jt} + r^{SPIN}_{jt} + r^{SUPP}_{jt}\} \ge r^{REG}_{k,t} + r^{SPIN}_{k,t} + r^{SUPP}_{k,t}, \qquad (\gamma^{ZOR}_{k,t}) \quad (13)$$

$$f_{i,t} + \sum_{k\in K}\big\{r^{REG}_{k,t} PTDF_{i,k}\big\} - PTDF_{i,LC} R^{REG}_{MKT,t} \le \overline{F}_{i,t}, \qquad (\mu^{REGUP}_{i,t}) \quad (14)$$

$$f_{i,t} - \sum_{k\in K}\big\{r^{REG}_{k,t} PTDF_{i,k}\big\} + PTDF_{i,LC} R^{REG}_{MKT,t} \le \overline{F}_{i,t}, \qquad (\mu^{REGDN}_{i,t}) \quad (15)$$

$$f_{i,t} - E_{k,t} PTDF^{TRIP}_{i,k} + \mathrm{D}^{SPIN}_{k,t} \sum_{k'\in K}\big\{r^{SPIN}_{k',t} PTDF_{i,k'}\big\} + \mathrm{D}^{SUPP}_{k,t} \sum_{k'\in K}\big\{r^{SUPP}_{k',t} PTDF_{i,k'}\big\} \le \bar{\overline{F}}_{i,t}, \qquad (\mu^{CR}_{i,k,t}) \quad (16)$$

$$p_{j,t} + \sum_{x\in X} r^{x}_{j,t} \le u_{j,t}\overline{P}_{j,t} \quad (17)$$

$$p_{j,t} - r^{REG}_{j,t} \ge u_{j,t}\underline{P}_{j,t} \quad (18)$$

$$\sum_{t'=t-UT_j+1}^{t} su_{j,t'} \le u_{j,t}\,, t \in \big(UT_j\,, \ldots, T\big) \quad (19)$$

$$\sum_{t'=t-DT_j+1}^{t} sd_{j,t'} \le 1 - u_{j,t}\,, t \in \big(DT_j\,, \ldots, T\big) \quad (20)$$

$$-L_t V^{DOWN}_{j,t} \le p_{j,t} - p_{j,t-1} \le L_t V^{UP}_{j,t} \quad (21)$$

$$0 \le r^{x}_{j,t} \le \overline{R}^{x}_{j,t} \quad (22)$$

$$u_{j,t} \in \{0,1\}, 0 \le su_{j,t}, sd_{j,t} \le 1 \quad (23)$$
$$0 \le w_{j,t} \le W_{j,t} \quad (24)$$

where,

$$D_{k,t}^{SPIN} = \min\{1, \frac{E_{k,t}}{R_{MKT,t}^{SPIN}}\} \quad (25)$$
$$D_{k,t}^{SUPP} = \max\{0, \frac{E_{k,t} - R_{MKT,t}^{SPIN}}{R_{MKT,t}^{SUPP}}\}. \quad (26)$$

The objective, (3), minimizes the operating cost. Equations (4) and (5) represent the power balance constraint and nodal power injection, respectively. Constraints (6) and (7) are transmission constraints. Constraints (8)-(10) are market-wide regulation, regulation plus spinning, and operating reserve requirements, respectively. Constraints (11)-(13) are zonal regulation, regulation plus spinning, and operating reserve requirements, respectively. Constraints (14) and (15) are post regulating reserve –up and –down deployment constraints, which are used to balance regulation reserve between zones. Constraint (16) is the post zonal contingency event constraint, which is used to balance contingency reserve between zones. Constraints (17) and (18) specify the resource maximum and minimum output. Minimum-up and –down time constraints are modelled by (19) and (20). Constraints (21)-(22) are the resource ramping constraints. Note that the symbol in the bracket after each constraint represents the shadow price of each constraint.

Equations (25) and (26) are based on MISO's practices; (25) is associated to the spinning reserve requirement while (26) is associated to the supplemental reserve requirement. Both (25) and (26) represent participation factors associated to each zone's response for a contingency. The participation factors vary by zone and are determined before the day-ahead market SCUC based on offline analysis.

Based on the concept of marginal pricing [18], the reserve market clearing price and energy price can be calculated as below,

$$MCP_{k,t}^{REG} = \gamma_{kt}^{ZRR} + \gamma_{kt}^{ZRS} + \gamma_{kt}^{ZOR} \quad (27)$$
$$MCP_{k,t}^{SPIN} = \gamma_{kt}^{ZRS} + \gamma_{kt}^{ZOR} \quad (28)$$
$$MCP_{k,t}^{SUPP} = \gamma_{kt}^{ZOR} \quad (29)$$
$$LMP_{n,t} = \lambda_t + \sum_{i \in I}\left\{\left(\mu_{i,t} + \mu_{i,t}^{REGUP} + \mu_{i,t}^{REGDN}\right)PTDF_{i,n}\right\} + \sum_{i \in I}\sum_{k \in K}\left\{\mu_{i,k,t}^{CR} PTDF_{i,n}\right\}. \quad (30)$$

3.2 Look Ahead Commitment

ISOs prefer to have multiple scheduling horizons as compared to a one shot day-ahead scheduling; with more uncertainties, a preferred approach is to use a multi-stage approach to adjust decisions based on the change in the uncertainties [19]. During the transition process from the day-ahead market to the real time market, a look-ahead unit commitment (LAC) is allowed to commit additional generators. PJM implements a two hour LAC model, which focuses on fast-start units [20].

In MISO's scheduling process, units with long lead times will be studied by multi-day forward reliability assessment commitment (FRAC). The majority of commitments decisions are made in the DAM and day-ahead FRAC. Reliability assessment commitment allows to commit additional generation to ensure sufficient capacity and meet reliability criteria considering system load forecasts, net scheduled interchange, and intermittent resources availability. LAC is used to create a bridge between the DAM as well as the reliability assessment commitment (RAC) and the RT-SCED. MISO uses a three hours LAC to ensure sufficient generation and ramp capacity with the most recent uncertainty forecasts and outage scheduler [21]. Intra-day reliability assessment commitment (IRAC) has a similar formulation as RAC, but the time window of IRAC is from the current operating point to the end of the operating day. IRAC and LAC are better equipped with the most recent system operating information to improve commitment decisions.

In this report, to approximate the market clearing process at MISO, LAC is also employed to adjust the DAM commitment decisions of resources whose minimum down time is less than or equal to three hours with consideration of the revealed net load scenarios. The LAC formulation is similar as the SCUC, except that many slow units are fixed.

3.3 Reserve Disqualification

Due to the inaccuracy of existing market models, out-of-market corrections (OMCs) may be required to obtain a reliable solution [14]. The California Independent System Operator (CAISO) defines OMCs as uneconomic adjustments [22]-[23]. CAISO will adjust its market solution if the optimization engine cannot guarantee a feasible solution for credible uncertainties.

MISO also manually adjusts the unreliable market solutions, which result from insufficient generation capacity or congestion [24]. During the day-ahead or real-time operations, some cleared reserve may not be deliverable and available reserve may be insufficient to cover all the credible uncertainties. To ensure adequate deliverable reserve capacity, operators will disqualify undeliverable resources and more resources may be committed. Operators will rank the resources based on the sensitivities of the binding transmission constraints. Top ranked resources will be labeled as "Not Qualified." This process is defined as reserve disqualification at MISO [25]. Such reserve disqualifications are outside the market optimization engine and incur additional operational costs. Furthermore, the manual modifications will impact the market outcomes and distort the price signals. Thus, reserve disqualification is not desirable. Improving existing market models is a way to reduce reserve disqualifications.

In this report, to mimic the reserve disqualification at MISO, for each period, resource with 1MW more power injection that aggravates most of the binding transmission constraints will be disqualified. For each iteration, only one resource can be disqualified for each hour that is not reliable. Reserve disqualification will be repeated until the market solution is reliable.

4. Numerical Results

4.1 Wind and Load Scenario Generation

To simulate the uncertainty and variability of wind output and load in the real world, one hundred wind scenarios and load scenarios are generated. Note that one hundred wind and load scenarios that are used in the real-time market analysis are different from those that are used to generate hourly reserve zones.

To generate wind scenarios, the autoregressive integrated moving average (ARIMA) model is used. The historical wind data is taken from NREL's Western Wind dataset and the first three weeks of August 2005 [26] are used to tune the parameters of the ARIMA model. The error (residuals) of the ARIMA model, which is fit for wind speed, follows a normal distribution. The wind speed scenarios will later be converted to wind power output.

Monte Carlo simulations [27] are used to produce the load scenarios and, for each period *t*, it is assumed that the mean of the probability distribution is the forecasted load; the folded Gaussian distribution is employed to accurately tune the forecasting error, which is 3%. Note that it is assumed that wind scenarios and load scenarios are independent and the wind scenario *s* will be combined with load scenario *s* to produce the net load scenario *s* for each node.

4.2 Proposed Market Clearing Process

Two different reserve zone models, a dynamic reserve zonal model and a seasonal reserve zonal model, are compared in this report. The process of determining dynamic reserve zone follows the algorithm in Section 2.2. The seasonal reserve zone is determined based on historical power flow data, which is generated by running optimal power flow through the winter. The flowchart in Figure 1 presents the proposed market clearing process. The zonal partitions will be inputs to the day-ahead SCUC model at the beginning of proposed market clearing process. The market solution of the SCUC will be adjusted by the reserve disqualification presented in Section 3.3 until it is *N*-1 reliable. Once the market solution of SCUC achieves *N*-1 reliability, the commitments of generators, which has minimum-down time larger than three hours, will be fixed for LAC. It is assumed that all net load scenarios are revealed in the LAC process and the only uncertainties in the real-time market are contingencies. LAC is used to better utilize the most recent system operating information. In Figure 2, to ensure the LAC solution is *N*-1 reliable, reserve disqualification process will be repeated until it is *N*-1 reliable for each net load scenario *s* ($s \in S$). Note that all the contingency studies in the proposed market clearing process are using emergency line limits.

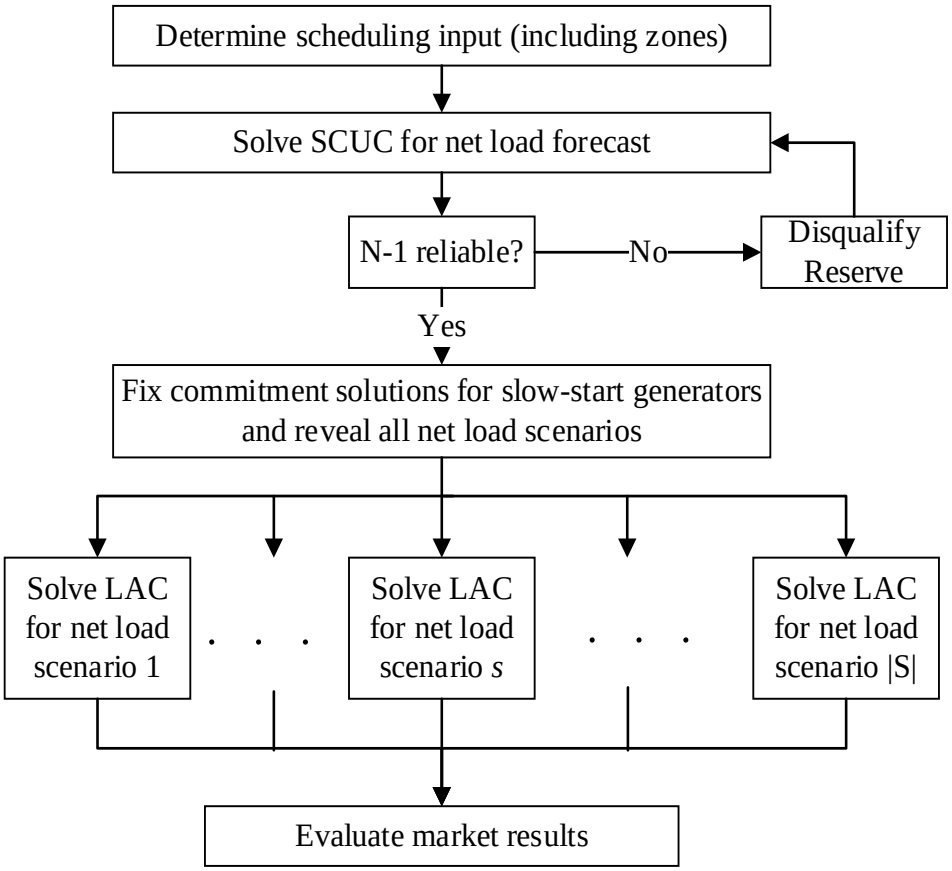

Figure 1. Proposed market clearing process of DAM and RTM.

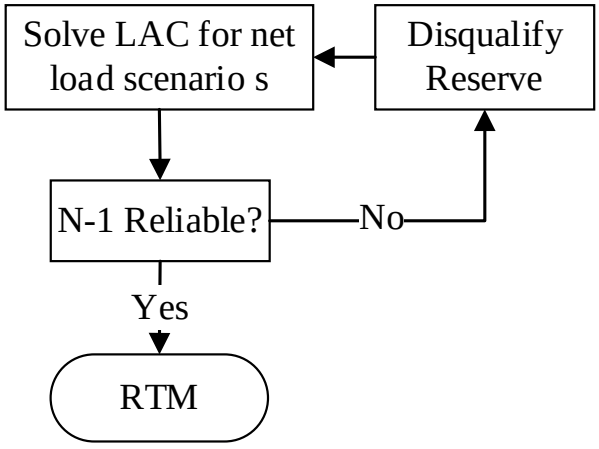

Figure 2. Detailed RTM clearing process.

4.3 IEEE RTS-96 Test Case

A modified IEEE Reliability Test System (RTS)-96, with 73 nodes, 99 units, 117 lines, and 51 loads [28], [29], is used to examine the proposed method. The proposed method is analyzed across all seven days of the peak week, which is from day 351 to day 357.

In this report, reserve bids are incorporated within both DAM and RTM, which is the same practice as in MISO; note that such practices vary from ISO to ISO. It is assumed that each generator's regulation reserve bid is 25% of its energy bid, the spinning reserve bid is 10% of its energy bid, and the supplemental reserve bid is 5% of its energy bid.

The market-wide regulating reserve requirements, regulating reserve plus spinning reserve requirements, and operating reserve requirements are set as 60MW, 150MW, and 400MW respectively. The average wind penetration (wind output/forecasted load capacity) is 12%. All testing is performed using CPLEX v12.6 on a 2-core 2.8 GHz computer with 12 GB RAM.

4.4 Confidence Intervals

In statistics, a confidence interval (CI) is an indicator of estimating the range of the results and it provides the probability of the true population mean falling within the calculated interval [30]. CI is a statistical metric that can be used to analyze the simulation results as well as validate the credibility of the results, over a pool of potential results.

Reserve disqualification will be applied if the LAC solution is not *N*-1 reliable. Table 1 presents the average number of reserve disqualifications for one hundred net load scenarios each day. The dynamic reserve zone dramatically reduces the number of reserve disqualifications.

Based on constraints (14), (15), and (16), the accuracy of zonal sensitivities will impact the quality of these zonal reserve requirements. Therefore, these zonal reserve requirements can be improved via improving reserve zones. Improved zonal reserve requirements can better capture the system operating conditions, i.e., the post-event power flow if the regulation or contingency reserve is deployed. By better constraining the approximate the post-event power flow, the location of the procured reserve tends to have better deliverability.

Table 1. Average number of reserve disqualifications for each day.

Day:	1	2	3	4	5	6	7
Dynamic	0.3	2.1	1.7	16.0	0.65	10.6	8.7
Seasonal	0.9	3.7	4.0	20.6	0.72	15.8	10.7

In Figure 3, the blue dot represents average operating costs after reserve disqualification (*N*-1 reliability approval) of the seasonal model and the red asterisk represents the results for the dynamic zone model. For results of each model, the top of

each bar represents the upper bound of the 95% confidence interval and the bottom of each bar represents the lower bound of the 95% confidence interval. Note that this rule also applies to Figures 3 – 6. It can be observed that the operating cost of the dynamic zone model has a higher probability to be lower comparing with the seasonal model. The average operating cost of the dynamic model for seven days is $1.90 million and that of the seasonal model is $1.95 million. Based on the proposed zone determination method, the dynamic model updates the reserve zone on an hourly basis and the accuracy of zonal PTDFs ($PTDF_{i,k,t}$) will be improved with the consideration of system operating conditions. Thus, the SCUC model will more accurately capture the post-event power flow and determine reserves at preferable locations where reserves are expected to have improved deliverability. As a result, the market solution for the dynamic zone provides a better starting point for LAC and RTM, which results in the lower operating cost. Therefore, the proposed dynamic model has effectively improved the market efficiency and has provided more accurate price signals while also lowering the number of undesirable manual reserve disqualifications, which ensures that the market solution produces a more reliable solution.

From Figures 4 – 6, the 95% confidence interval of load payment, regulation reserve payment, and contingency reserve payment of each day are shown, for both the dynamic and the seasonal models, across seven days and each day has one hundred net load scenarios. To further improve the credibility of the market results in this report, the multi-settlement policy in [9] is used to calculate load payments and reserve revenues. Products cleared in the DAM will receive the DAM prices while products cleared in the RTM relative to DAM cleared amount will receive RTM prices. For instance, a generator that cleared 100MW energy in the DAM and 101MW energy in RTM will receive DAM price for the 100MW and RTM price for the last MW.

Based on Figure 4, the confidence intervals indicate that the dynamic zone model has a higher probability to receive lower load payment compared to the seasonal model. The average load payment for seven days for the dynamic model is $7.11 million and the load payment for the seasonal model is $7.56 million. Another interesting observation is that the confidence interval error margin for the dynamic model for load payment is slightly higher than that of the seasonal model; this is attributed to more frequent updates of the reserve zone partition, which have led to a higher standard deviation in LMPs.

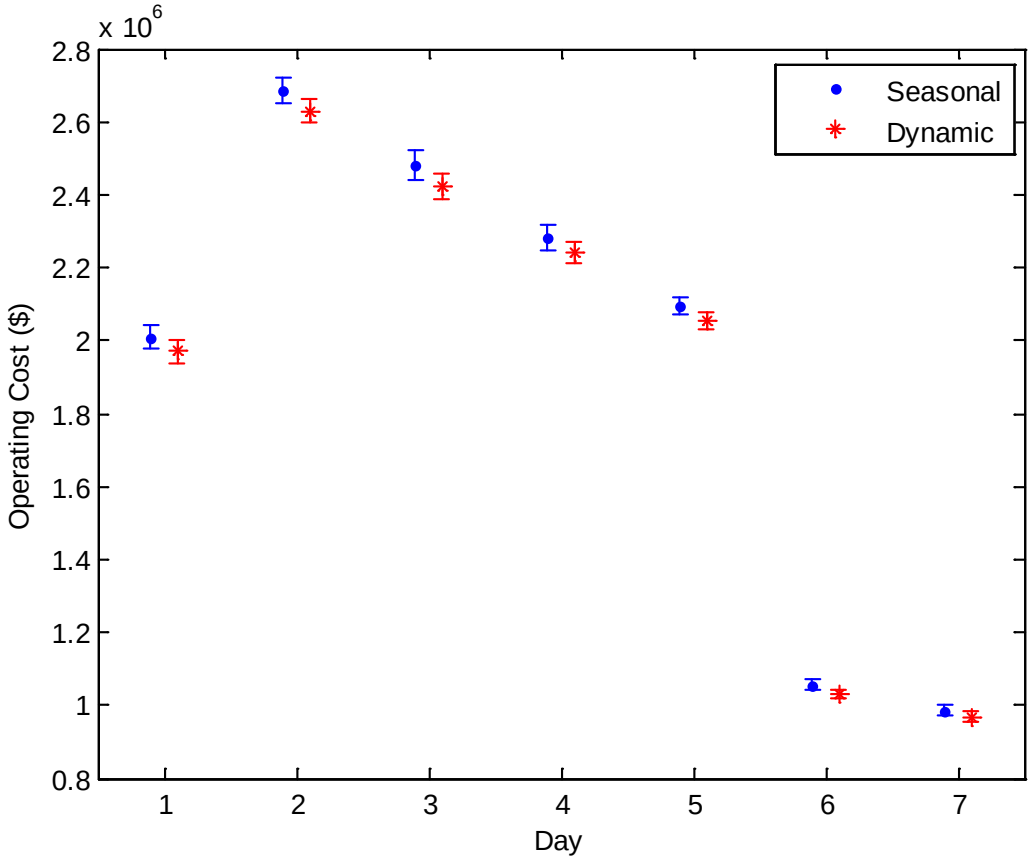

Figure 3. 95% confidence interval of operating cost of each day for dynamic and seasonal model.

In Figure 5, the regulation reserve payment from the dynamic model has 1.2% higher average reserve payments than that of the seasonal model. Also, the lengths of the dynamic model segments are longer than that of the seasonal zone segments. The dynamic zone model experiences more volatility in the regulation reserve price. While price volatility is sometimes not preferred based on risk preference, the purpose of a price is to provide an accurate economic signal, volatile or not, which is why there was the movement from zonal energy markets to nodal energy markets to obtain nodal energy payments, i.e., LMPs.

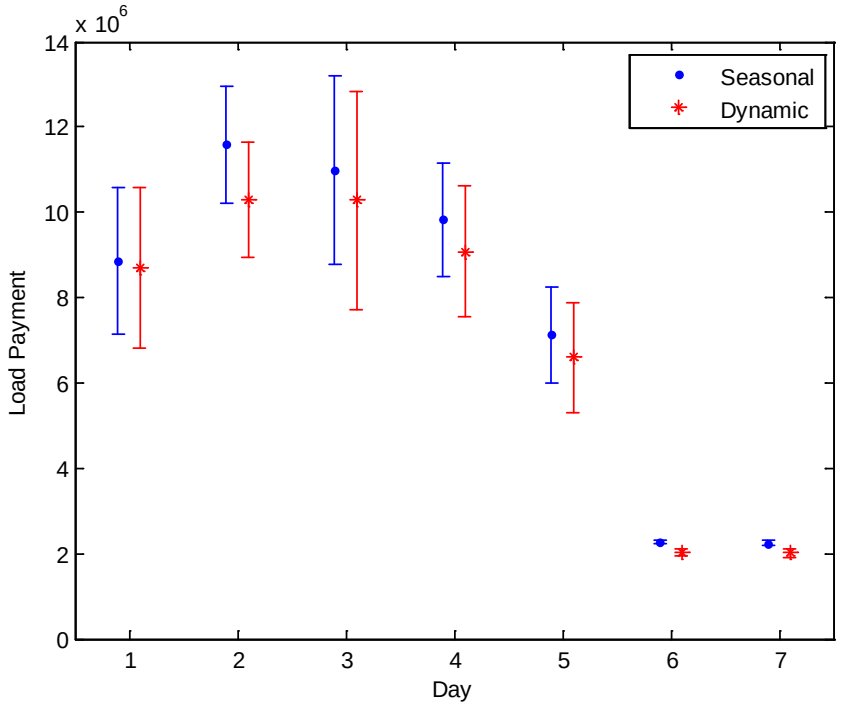

Figure 4. 95% confidence interval of load payment of each day for dynamic and seasonal model.

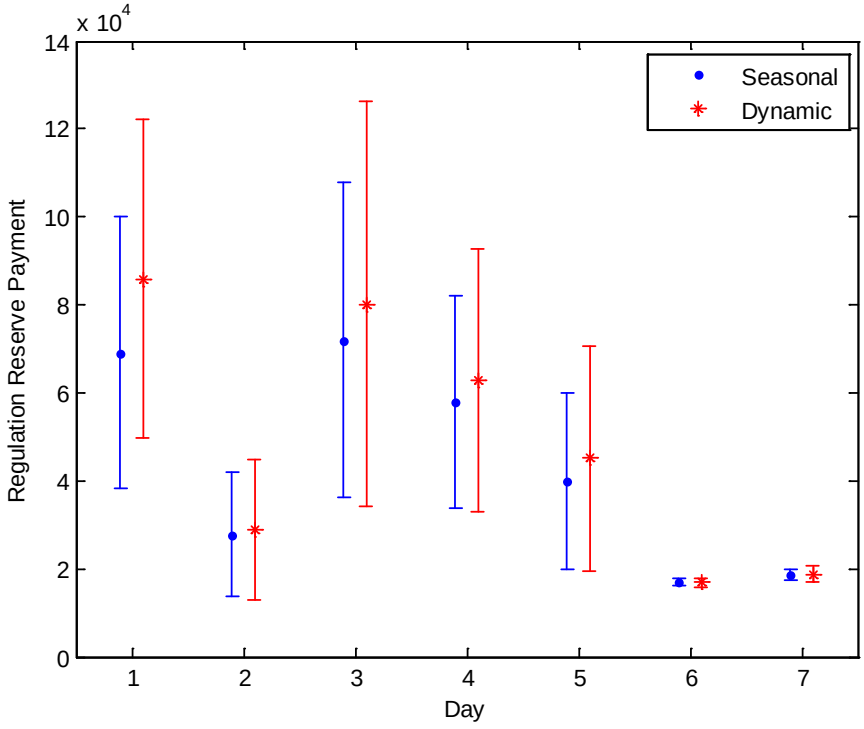

Figure 5. 95% confidence interval of regulation reserve payment of each day for dynamic and seasonal model.

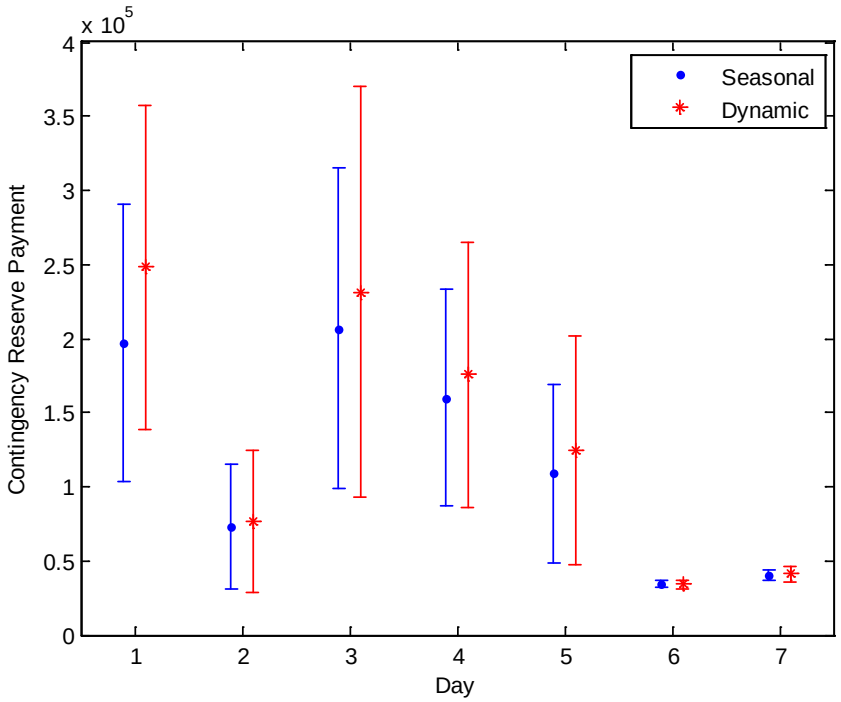

Figure 6. 95% confidence interval of contingency reserve payment of each day for dynamic and seasonal model.

In Figure 6, the contingency reserve payment is the sum of the spinning reserve payment and the supplemental reserve payment. The average of the contingency reserve payment for the dynamic model is $0.17 million and the seasonal model is $0.13 million. Like the results for the regulation reserve payment, the contingency reserve payment also exhibits a larger variability in payment range. As observed, the confidence interval margin of regulation and contingency reserve payment of the dynamic zone model is larger than that of the seasonal zone model. The proposed dynamic reserve model adjusts with the operating states and such additional information is translated into the approach and the results. The resulting regulation and contingency reserve prices better reflect the operating states. This is one key benefit of using more accurate zonal reserve requirements as well as updating the reserve zone on a more frequent, i.e., hourly basis.

5. Conclusions

Existing protocols to determine reserve zones are based on ad-hoc rules such as utility ownership or geographical boundaries. These reserve zones are not adjusted frequently and, thus, they do not reflect the continuous change in the system operating conditions. The main alternative to such ad-hoc existing protocols has been to pursue stochastic programming. However, the computational complexity and market design issues limit its use. This report proposes a deterministic reserve policy; the results demonstrate improvements in market efficiency, the reliability of the proposed market solution, as well as in the price signals. With smart adjustments to existing deterministic reserve policies, sizeable improvements towards all of these concerns have been achieved.

The proposed hourly dynamic reserve zone determination method considers uncertainties caused by renewables, load, and contingencies. To convey the credibility of the numerical results, confidence intervals of the market solutions are presented. The numerical results have shown that the proposed model can lower the operators' manual adjustments, i.e., reserve disqualification. Furthermore, the operating cost is lowered by using the proposed dynamic model. Therefore, the proposed hourly reserve zone improves the market efficiency of the SCUC and LAC stages while also ensuring the market model more accurately captures system reliability.

References

[1] F. Galiana, F. Bouffard, J. M. Arroyo, and J. F. Restrepo, "Scheduling and pricing of coupled energy and primary, secondary, and tertiary reserves," *Proc. IEEE*, vol. 93, no. 11, pp. 1970-1983, Nov. 2005.

[2] H. Holttinen, M. Milligan, E. Ela, *et al.*, "Methodologies to determine operating reserves due to increased wind power," *IEEE Trans. Power Syst*., vol. 3, no. 4, pp. 713–723, Oct. 2012.

[3] National Renewable Energy Laboratory, "Western wind and solar integration study," NREL, Tech. Rep., May 2010. [Online]. Available: http://www.nrel.gov/docs/fy10osti/47434.pdf.

[4] K. De Vos and D. Kriesen, "Dynamic operating reserve strategies for wind power integration," *IET Renew. Power Gen.*, vol. 8, no. 6, pp. 598-610, Aug. 2014.

[5] R. Doherty and M. O'Malley, "A new approach to quantify reserve demand in systems with significant installed wind capacity," *IEEE Trans. Power Syst.*, vol. 20, no. 2, pp. 587–595, May 2005.

[6] M. Ortega-Vazquez and D. Kirschen, "Estimating the spinning reserve requirements in systems with significant wind power generation penetration," *IEEE Trans. Power Syst.*, vol. 24, no. 1, pp. 114–123, Feb. 2009.

[7] A. Papavasiliou, S. S. Oren, and R. P. O'Neill, "Reserve requirements for wind power integration: a scenario-based stochastic programming framework," *IEEE Trans. Power Syst.*, vol. 26, no. 4, pp. 2197-2206, Nov. 2011.

[8] K. W. Hedman, M. C. Ferris, R. P. O'Neill, E. B. Fisher, and S. S. Oren, "Co-optimization of generation unit commitment and transmission switching with *N*-1 reliability," *IEEE Trans. Power Syst.*, vol. 25, no. 2, pp. 1052-1063, May 2010.

[9] MISO, "MISO energy and operating reserve markets, business practices manual," BPM-002-r11, Jan. 2012. [Online]. Available: https://www.misoenergy.org/Library/BusinessPracticesManuals/Pages/BusinessPracticesManuals.aspx.

[10] F. Wang and K. W. Hedman, "Reserve zone determination based on statistical clustering method," in *Proc. North American Power Symp.*, 2012.

[11] F. Wang and K. W. Hedman, "Dynamic reserve zones for day-ahead unit commitment with renewable resources," *IEEE Trans. Power Syst.*, accepted for publication.

[12] J. Lyon, F. Wang, K. W. Hedman, and M. Zhang, "Market implications and pricing of dynamic reserve policies for systems with renewables," *IEEE Trans. Power Syst.*, accepted for publication.

[13] Y. Chen, MISO, Private Communication. Carmel, IN,

[14] Y. M. Al-Abdullah, M. Abdi-Khorsand, and K. W. Hedman, "The role of out-of-market corrections in day-ahead scheduling," *IEEE Trans. Power Syst.*, accepted for publication.

[15] X. Ma, H. Song, M. Hong, J. Wan, Y. Chen, and E. Zak, "The security-constrained commitment and dispatch for Midwest ISO day-ahead co-optimized

energy and ancillary service market," in *Proc. IEEE PES General Meeting*, 2009.
[16] A. Casto, "Overview of MISO day-ahead market," [Online]. Available: http://www.atcllc.com/oasis/Customer_Notices/NCM_MISO_DayAhead111507.pdf.
[17] Y. Chen, P. Gribik, and J. Gardner, "Incorporating post zonal reserve deployment transmission constraints into energy and ancillary services co-optimization," *IEEE Trans. Power Syst.*, vol. 29, no. 2, pp. 537-549, Mar. 2014.
[18] F. C. Schweppe, M. C. Caramanis, R. D. Tabors, and R. E. Bohn, S*pot Pricing of Electricity*. Norwell, MA, USA: Kluwer, 1988.
[19] N. Navid, T. Ramey, and D. Chatterjee, "Operational and practical considerations for stochastic unit commitment solutions," FERC Technical Conference On Increasing Real-Time And Day-Ahead Market Efficiency Through Improved Software, June 23-25, 2014, Washington, DC.
[20] Q. Wang, X. Wang, K. Cheung, Y. Guan, and F. Bresler, "A two-stage robust optimization for PJM look-ahead unit commitment," *IEEE PowerTech Conf.*, Grenoble, France, 16-20 June 2013.
[21] Y. Chen, V. Ganugula, J. Williams, J. Wan, and Y. Xiao, "Resource transition model under MISO MIP based look ahead commitment," in *Proc. IEEE PES General Meeting*, July 2012.
[22] CAISO, "Intra-zonal congestion," CAISO Dept. of Market Monitoring, Tech. Report., Apr. 2007. [Online]. Available: http://www.caiso.com/1bb7/1bb77b241b920.pdf.
[23] CAISO, "Parameter tuning for uneconomic adjustments in the MRTU market optimizations," Dept. Market and Product Development, May 6, 2008. [Online]. Available: http://www.caiso.com/1fbf/1fbfe3a2498e0.pdf.
[24] X. Ma, Y. Chen, and J. Wan, "The security-constrained economic dispatch for Midwest ISO's real-time co-optimized energy and ancillary service market," in *Proc. IEEE PES General Meeting*, 2009.
[25] MISO, "MISO resources not qualified for reserves in real time market," Oct., 2013. [Online]. Available: www.misoenergy.org/Library/Repository/Meeting%20Material/Stakeholdr/MSC/2013/20131001/20131001%20MSC%20Item%2005c%20MISO%20Resources%20Not%20Qualified%20for%20Reserves%20in%20RT%20Market.pdf.
[26] NREL, "Western wind resource dataset," Jan. 2014. [Online]. Available: wind.nrel.gov/Web_nrel/.
[27] R. Billinton and R. Allan, Reliability Evaluation of Power Systems, 2nd ed. New York: Plenum, 1996.
[28] C. Grigg *et al.*, "The IEEE reliability test system – 1996," *IEEE Trans. Power Syst.*, vol. 14, no. 3, pp. 1010–1020, Aug. 1999.
[29] Univ. of Washington, "Power systems test case archive," 1999. [Online]. Available: http://www.ee.washington.edu/research.
[30] M. Kutner, C. Nachtsheim, J. Neter, *et al.*, Applied Linear Statistical Models. New York: McGraw-Hill, 2005.

Part III

Market Implications of Security Requirements

Chao Li
Kory W. Hedman
Muhong Zhang

Arizona State University

For information about this project, contact

Kory W. Hedman
Arizona State University
School of Electrical, Computer, and Energy Engineering
P.O. BOX 875706
Tempe, AZ 85287-5706
Phone: 480 965-1276
Fax: 480 965-0745
Email: kory.hedman@asu.edu

Power Systems Engineering Research Center

The Power Systems Engineering Research Center (PSERC) is a multi-university Center conducting research on challenges facing the electric power industry and educating the next generation of power engineers. More information about PSERC can be found at the Center's website: http://www.pserc.org.

For additional information, contact:

Power Systems Engineering Research Center
Arizona State University
527 Engineering Research Center
Tempe, Arizona 85287-5706
Phone: 480-965-1643
Fax: 480-965-0745

Notice Concerning Copyright Material

Table of Contents

List of Figures

List of Tables

Nomenclature

Sets:

G	Set of generators.
$G(n)$	Set of generators at bus n.
I	Set of extreme rays of dual cone.
L	Set of transmission lines.
N	Set of buses.
S	Set of scenarios.
T	Set of time periods.

Parameters and Functions:

$C_g(\cdot)$	Generation cost function of generator g.
D_n	Forecasted load at bus n.
F_l	Line rating of transmission line l.
$G1_g^s$	*G*-1 indicator of generator g in scenario s; 0 if the generator fails, 1 otherwise.
H_g	Available upper capacity of generator g.
L_g	Available lower capacity of generator g.
$K(\cdot)$	System-level general function.
$n(g)$	Bus location of generator g.
P_g^{max}	EcoMax of generator g.
P_g^{min}	EcoMin of generator g.
R_g	Ramping capability of generator g.
ψ_{nl}	Generation shift factor on transmission line l from bus n to the reference bus.

Variables:

i_n	Power net injection at bus n.
d_n	Load at bus n.
p_g	Generation level of generator g.
p_g^H	Upper capacity of generator g.
p_g^L	Lower capacity of generator g.
r_g^d	Ramping down reserves of generator g.
r_g^u	Ramping up reserves of generator g.
u_g	Commitment status of generator g.
δ_n	Dual variable with respect to node-balance constraint at bus n.
μ_l^+	Dual variable corresponding to the upper bound flow constraint for transmission line l.
μ_l^-	Dual variable corresponding to the upper bound flow constraint for transmission line l.
ϕ_g^+	Dual variable corresponding to the upper bound for production of generator g.
ϕ_g^-	Dual variable corresponding to the lower bound for production of generator g.
τ	Dual variable with respect to total injection constraint.

λ_n^{old} Shadow price of node-balance constraint at bus n.
λ_n^{new} Shadow price of load non-anticipativity constraint at bus n.
ξ_i^s Shadow price with respect to security constraint for extreme ray i in scenario s.

Remark: variables with ¯ are fixed inputs

1. Introduction

1.1 Research Premise

Electric power grids are one of the most complex engineered machines ever created. The National Academy of Engineering ranks the electrification as the greatest achievement of the 20th century [1]. Operating a power system involves many complex processes. Currently, two-thirds of the U.S. power system is served by regional transmission organizations (RTOs) and independent system operators (ISOs) [2]. RTO/ISOs operate power systems under market structures, with a goal to bring competition to achieve efficiency. Market models used by RTO/ISOs are approximation models to represent the complex power system, with a set of reasonable simplifications.

Power system security refers to the ability to survive potential disturbances (contingencies) without interruption to customer services [3]. The North American Electric Reliability Corporation (NERC) requires the *N*-1 reliability criterion for system operation, which states the system must be able to withstand any single bulk element failure (generator, transmission line, or transformer) [4]. In order to ensure system security, RTO/ISOs acquire reserves from generation resources. While most RTO/ISOs have market structures to procure reserves, their reserve requirements vary significantly. Reserve policies and reserve zone partitions to improve system security are studied by [5]-[10]. Since the reserve requirements are proxy policies to ensure system security, in day-ahead scheduling and real-time operation, the procured reserves may not be adequate or deliverable due to transmission limitations. RTO/ISOs also include different types of out-of-market, operator-initiated security requirements in their scheduling and operation [11]. These security requirements may result in committing more units or re-allocating the reserves. Out-of-market corrections are studied by [12]-[14]. However, the out-of-market, operator-initiated security requirements are not reflected in the market models and lack transparency. As a result, market prices may be distorted.

Recently, stochastic models have been studied to better hedge uncertainty in power systems, especially for unit commitment (UC) problems. The models can be categorized into scenario-based stochastic programming [15]-[24], robust optimization [25]-[31], and stochastic programs with chance-constrained formulations [32], [33], according to different modeling structures. The UC problem with *N*-1 criterion can be explicitly formulated as two-stage stochastic programming. Different decomposition algorithms are studied to solve the problem, including Benders' decomposition [19], [34], dual decomposition [22], [35], and progressive hedging [23], [24], [36], [37]. However, due to high computational complexity, stochastic programs have not been implemented by RTO/ISOs. In this report, the stochastic UC problem is transformed to an equivalent deterministic model with a set of security constraints, which matches the current industrial practice of using a deterministic model.

RTO/ISOs adopt locational marginal price (LMP) to represent energy prices [38]. The LMP captures three components, which include the marginal energy, marginal congestion, and marginal loss components [39]. In this report, a new component of LMP, marginal security component, is proposed to be added to better represent the energy prices. The marginal security components are the weighted shadow prices corresponding to the set of

security constraints to improve system security. With the marginal security component, the LMPs will capture the marginal cost from a secure system state to another secure system state; thus, capture the impacts of security requirements.

The main contributions of this report are listed as follows:

1) A set of security constraints to improve system security are explicitly represented; and their market implications are analyzed.

2) A new component of LMP, marginal security component, is proposed in order to capture the marginal cost from a secure system state to another secure system state.

1.2 Report Organization

The rest of the report is organized as follows: Section 2 describes the set of security constraints to withstand single-generator-failure (G-1) contingencies and analyzes their market implications. Section 3 gives a 3-bus system as illustrative example. Section 4 represents a case study for IEEE 73-bus system. Finally, Section 5 concludes this report.

2. Security Constraints and Market Implications

2.1 Market Model

Power flow problems are non-linear, non-convex problems [40]. RTO/ISOs adopt linearized power flow models to approximate the real power flow, as known as direct current optimal power flow (DCOPF) models [41]. In this report, a power transfer distribution factor (PTDF) based lossless DCOPF model is adopted. A generalized market model is represented as follows:

$$\min \quad C(\boldsymbol{p}) \tag{1}$$
$$s.t. \quad (\boldsymbol{p}^g, \boldsymbol{u}^g) \in \boldsymbol{X}^g \forall g \tag{2}$$
$$K(\boldsymbol{p}, \boldsymbol{D}) \leq 0 \tag{3}$$

Equation (1) represents an objective function to minimize total generation costs. Equation (2) is a set of resource-level constraints restricting each generator's commitment status, $\boldsymbol{u}$, and generation level output, $\boldsymbol{p}$, where $\boldsymbol{X}^g, \forall g$, are feasible commitment and dispatch subspaces of each generator. Equation (3) represents a set of system-level constraints where $K(\boldsymbol{p}, \boldsymbol{D})$ is a linear function of generation variables, $\boldsymbol{p}$, and forecasted load, $\boldsymbol{D}$. The system-level constraints usually include system-balance constraint (total generations equal to total loads) and network constraints (power flows are within transmission line limits). The network constraints may result in energy price separation (different marginal congestion components). In this report, the market model is improved by including more system-level constraints, i.e., the proposed security constraints.

2.2 Necessary and Sufficient Conditions for Feasible Dispatch

In order to derive the security constraints, first, consider a single-period dispatch model as follows:

$$\min \quad \textstyle\sum_{\forall g} C_g(p_g) \tag{4}$$
$$s.t. \quad L_g \leq p_g \leq H_g \quad \forall g \quad (\phi_g^-, \phi_g^+) \tag{5}$$
$$i_n = \textstyle\sum_{\forall g \in G(n)} p_g - D_n \quad \forall n \quad (\delta_n) \tag{6}$$
$$-F_l \leq \textstyle\sum_{\forall n} \psi_{nl}\, i_n \leq F_l \quad \forall l \quad (\mu_l^-, \mu_l^+) \tag{7}$$
$$\textstyle\sum_{\forall n} i_n = 0 \quad (\tau) \tag{8}$$

Equation (5) restricts generation level ranges. $[L_g, H_g], \forall g$, are the resulting available generation capacities, which are restricted by commitment status, minimum generation level (EcoMin), maximum generation level (EcoMax), ramping capabilities, and generator-failure contingencies. Equation (6) specifies the nodal net injection. Equation (7) gives the network constraints. $\psi_{n,l}, \forall n, l$, are the PTDFs, also referred as generation shift factors (GSFs). GSFs describe power flow distributions on each transmission line

when injecting one unit of power from one certain bus to a reference bus. GSFs are results of the Kirchhoff's laws. Finally, (8) requires total nodal net injections to be zero, i.e., the system-balance constraint. Corresponding dual variables of each constraint are listed on the right side of the constraints.

The following *Proposition 1* [42] gives a necessary and sufficient condition for a feasible dispatch in power systems.

Proposition 1: For any given system-state parameters, $L_g, H_g, D_n, F_l, \forall g, n, l$, a power system has a feasible dispatch if and only if, $\forall \boldsymbol{\gamma} = (\boldsymbol{\phi}^+, \boldsymbol{\phi}^-, \boldsymbol{\mu}^+, \boldsymbol{\mu}^-, \boldsymbol{\delta}, \tau) \in Q$,

$$\sum_{\forall g}(H_g \phi_g^+ - L_g \phi_g^-) + \sum_{\forall l} F_l(\mu_l^+ + \mu_l^-) - \sum_{\forall n} D_n \delta_n \geq 0 \tag{9}$$

where Q is feasible set of the following constraints and Q is a pointed cone, referred as *dual cone*.

$$\phi_g^+ - \phi_g^- - \delta_{n(g)} = 0 \qquad \forall g \tag{10}$$
$$\sum_{\forall l} \psi_{nl}\,(\mu_l^+ - \mu_l^-) + \delta_n + \tau = 0 \qquad \forall n \tag{11}$$
$$\phi_g^+, \phi_g^-, \mu_l^+, \mu_l^- \geq 0 \qquad \forall g, l \tag{12}$$

The results follow from Farkas' lemma [43]. Equation (9) gives a condition to ensure system security, i.e., the existence of a feasible dispatch after uncertain event happens. The condition (9) can be interpreted as the summation of weighted generation capacities, transmission line limits and loads has to be nonnegative, where the weights are obtained from the dual cone.

2.3 Extreme Rays of the Dual Cone

If every extreme ray in the dual cone satisfies (9), then $\forall \boldsymbol{\gamma} \in Q$ satisfies (9). Denote the extreme rays that may violate (9) as *crucial extreme rays*. The following *Proposition 2* [42] gives a handy guideline to characterize the crucial extreme rays of the dual cone.

Proposition 2: The crucial extreme rays of the dual cone can be characterized by combinatorial selections of transmission lines and buses in the power system.

The detailed proof can be found in [42]. The selection of the lines and buses can be obtained from engineering insights. Suppose enough reserves have been procured in the power system. When uncertainty happens, the power system is not secure because some reserves are unable to be delivered. There will be some congested transmission lines that reach their thermal limits; and there will be some buses have undelivered reserves, i.e., extra capacities. Line variables, μ_l^+/μ_l^-, corresponding to the non-congested lines have zero values. Bus variables, δ_n, corresponding to the buses with extra capacities have zero values. Then, all variables of the corresponding crucial extreme ray, $\overline{\boldsymbol{\gamma}} = \left(\overline{\boldsymbol{\phi}}^+, \overline{\boldsymbol{\phi}}^-, \overline{\boldsymbol{\mu}}^+, \overline{\boldsymbol{\mu}}^-, \overline{\boldsymbol{\delta}}, \overline{\tau}\right)$, can be determined.

2.4 Security Constraints for *G*-1 Contingencies

Based on *Proposition 1* and *Proposition 2*, a set of security constraints to withstand *G*-1 contingencies are given as follows:

$$\sum_{\forall g} G1_g^s\left(\bar{\phi}_{ig}^{+} p_{gt}^{H} - \bar{\phi}_{ig}^{-} p_{gt}^{L}\right) + \sum_{\forall l} F_l(\bar{\mu}_{il}^{+} + \bar{\mu}_{il}^{-}) - \sum_{\forall n} D_{nt}\bar{\delta}_{in} \geq 0 \qquad \forall i, s, t \qquad (13)$$

where, $\left(\bar{\boldsymbol{\phi}}^{+}, \bar{\boldsymbol{\phi}}^{-}, \bar{\boldsymbol{\mu}}^{+}, \bar{\boldsymbol{\mu}}^{-}, \bar{\boldsymbol{\delta}}\right), \forall i$, are given crucial extreme ray parameters of the dual cone that have been identified; index s is corresponding to *G*-1 contingency scenario; index t is corresponding to time period the contingency happens.

When a generator fails, the corresponding weighted capacity, $\bar{\phi}_{ig}^{+} p_{gt}^{H} - \bar{\phi}_{ig}^{-} p_{gt}^{L}$, is lost, which may result in the left side of (13) to be less than zero if (13) is not enforced. In (13), $p_{gt}^{L}/p_{gt}^{H}, \forall g, t$, are the post-contingency available generation capacities, that are described in the following constraints:

$$p_{gt}^{L} = p_{gt} - r_{gt}^{d} \qquad \forall g, t \qquad (14)$$
$$p_{gt}^{H} = p_{gt} + r_{gt}^{u} \qquad \forall g, t \qquad (15)$$
$$p_{gt} - r_{gt}^{d} \geq P_g^{min} u_{gt} \qquad \forall g, t \qquad (16)$$
$$p_{gt} + r_{gt}^{u} \leq P_g^{max} u_{gt} \qquad \forall g, t \qquad (17)$$
$$0 \leq r_{gt}^{d}, r_{gt}^{u} \leq R_g \qquad \forall g, t \qquad (18)$$

Equations (13)-(18) are included into market models in order to improve system security.

2.5 Market Implications

In current market designs, the LMPs are used to price the energy. The LMP is interpreted as the system total dispatch costs increment/decrement by increasing/decreasing one unit of power at the corresponding location.

If the security constraints (13) are to be included, the increment/decrement of load D_{nt} will also have impacts on these security constraints. Consider the reformulation as follows:

$$\sum_{\forall g \in G(n)} p_{gt} - d_{nt} - i_{nt} = 0 \qquad \forall n, t \qquad (\lambda_{nt}^{old}) \qquad (19)$$
$$\sum_{\forall g} G1_g^s\left(\bar{\phi}_{ig}^{+} p_{gt}^{H} - \bar{\phi}_{ig}^{-} p_{gt}^{L}\right) + \sum_{\forall l} F_l(\bar{\mu}_{il}^{+} + \bar{\mu}_{il}^{-}) - \sum_{\forall n} \bar{\delta}_{in} d_{nt} \geq 0$$
$$\forall i, s, t \qquad (\xi_{it}^{s}) \qquad (20)$$
$$d_{nt} = D_{nt} \qquad \forall n, t \qquad (\lambda_{nt}^{new}) \qquad (21)$$

The reformulation changes the original fixed loads, $D_{nt}, \forall n, t$, to variables, $d_{nt}, \forall n, t$; then enforces non-anticipativity constraints (21). When the load, D_{nt}, increases by one unit, it will not only affect the nodal net injection (19), but also affect the security constraints (20). Let $\lambda_{nt}^{old}, \xi_{it}^{s}, \lambda_{nt}^{new}$ represent the shadow prices of (19)-(21) respectively; their relations are specified by the following *Proposition 3*.

Proposition 3: The shadow prices of (19)-(21) satisfy,

$$\lambda_{nt}^{new} = \lambda_{nt}^{old} + \sum_{\forall i} \sum_{\forall s} \bar{\delta}_{in} \xi_{it}^{s} \qquad \forall n, t \qquad (22)$$

Proof: If deriving the dual of the reformulation, variables, $d_{nt}, \forall n, t$, only appear in (19)-(21), then the corresponding dual constraints are given as (22).

The shadow prices, $\lambda_{nt}^{new}, \forall n, t$, represent the change in the total system dispatch costs when the corresponding load, D_{nt}, increases by one unit. From (22), the price λ_{nt}^{new} is separated into two parts. The first part, λ_{nt}^{old}, is the current LMP that captures the marginal energy component and marginal congestion component in the lossless model. The additional part, $\sum_{\forall i} \sum_{\forall s} \bar{\delta}_{in} \xi_{it}^{s}$, is the marginal security component. The interpretation of this new component is that, if the security constraints are included in the model, when the load is increased by one unit, it may cost more in order to satisfy the security constraints. The extra costs are captured by the shadow prices of the security constraints.

3. Illustrative Example

In this section, an illustrative 3-bus system is used to explain the arguments in Section 2. Figure 1 gives the topology of the system and Tables 1-3 gives the system data.

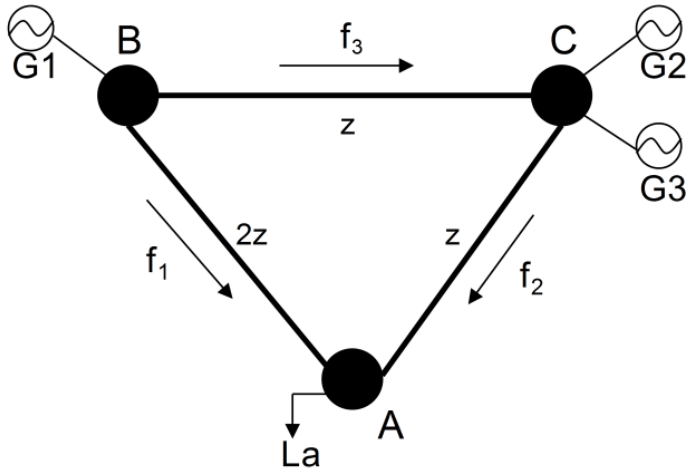

Figure 1. 3-bus system.

Table 1. Generator data.

	EcoMin (MW)	EcoMax (MW)	Ramp Rate (MW)	Variable Cost ($/MW)	No-load Cost ($)
Gen1	5	45	25	10	100
Gen2	20	45	25	20	100
Gen3	5	40	10	30	100

Table 2. Generation shift factors.

	Line 1	Line 2	Line 3
Bus A	0	0	0
Bus B	0.5	0.5	0.5
Bus C	0.25	0.75	-0.25

Table 3. Load and transmission line limits.

Load A	40 MW
Load B	0 MW
Load C	0 MW
Thermal Limit of Line 1	15 MW

The system reserve requirements, which ensure adequate reserves for *G*-1 contingency, are described as follows:

$$\sum_{\forall k \in G} r_k^u \geq p_g + r_g^u \qquad \forall g \qquad (23)$$

3.1 Base Case

First, consider the base case without the proposed security constraints. The full formulation to solve this single-period problem is explicitly given as follows:

$$\min \quad 10p_1 + 20p_2 + 30p_3 + 100(u_1 + u_2 + u_3) \qquad (24)$$
$$s.t. \quad p_1 \geq 5u_1 \qquad (25)$$
$$p_1 + r_1^u \leq 45u_1 \qquad (26)$$
$$0 \leq r_1^u \leq 25 \qquad (27)$$
$$p_2 \geq 20u_2 \qquad (28)$$
$$p_2 + r_2^u \leq 45u_2 \qquad (29)$$
$$0 \leq r_2^u \leq 25 \qquad (30)$$
$$p_3 \geq 5u_3 \qquad (31)$$
$$p_3 + r_3^u \leq 40u_3 \qquad (32)$$
$$0 \leq r_3^u \leq 10 \qquad (33)$$
$$p_1 + p_2 + p_3 = 40 \qquad (34)$$
$$r_1^u + r_2^u \geq p_3 \qquad (35)$$
$$r_1^u + r_3^u \geq p_2 \qquad (36)$$
$$r_2^u + r_3^u \geq p_1 \qquad (37)$$
$$0.5p_1 + 0.25(p_2 + p_3) \leq 15 \qquad (38)$$

Equation (24) is objective function to minimize the summation of generation costs and commitment costs. Equations (25)-(33) are the resource-level constraints. Equation (34) is the system energy-balance constraint. Equations (35)-(37) specify the system reserve requirements. Equation (38) is the network constraint.

Since Gen1 is the cheapest generation resource, it is preferred to supply the loads. However, Gen1 generating 40MW violates the thermal limit of transmission line 1 and the reserve requirements. Therefore, the optimal solution is committing Gen1 and the second cheapest generation resource, Gen2. Table 4 gives the commitment and dispatch solution for the base case.

LMPs are defined as the shadow prices by increasing or decreasing one unit of power at corresponding location. In the following, the LMPs are calculated as the shadow price by increasing one unit of power.

In this base case solution, transmission line 1 is congested; thus, price separation is expected. At bus A, if the load increases to 41MW, due to the transmission limit, Gen1 cannot dispatch one more unit of power. The solution will be Gen1 decreases 1MW output and Gen2 increases 2MW. Table 5 gives the commitment and dispatch solution for the base case when load at bus A increases by one unit.

When the load at bus A increases by 1MW, the total cost increment is \$30. Therefore, $LMP_A = 30$. Similarly, the load increment at Bus C can be only supplied by Gen2 due to transmission congestion, i.e., $LMP_C = 20$. Table 6 gives the LMPs for the base case.

Table 4. Base case solution.

	u	p	r
Gen1	1	20	25
Gen2	1	20	25
Gen3	0	0	0
Total Cost (\$)		800	

Table 5. Base case solution when Load A increases 1MW.

	u	p	r
Gen1	1	19	25
Gen2	1	22	23
Gen3	0	0	0
Total Cost (\$)		830	

Table 6. LMPs for base case.

LMP A	\$30/MWh
LMP B	\$10/MWh
LMP C	\$20/MWh

3.2 Security-Constrained Case

Although the base case solution meets the reserve requirement (23), it is not a secure solution with respect to *G*-1 contingency. Specifically, when Gen2 fails, even though Gen1 can dispatch up to 45MW, because of the network constraint, it can only dispatch 30MW instead. There is 10MW load shedding at bus A; thus, the system is not secure. Committing Gen3 is necessary.

Consider the proposed *G*-1 security constraints. First, characterize the extreme ray of the dual cone corresponding to the contingency. Equation (11) for this illustrative example is given as follows ($\tau = -1$ and $\boldsymbol{\mu} = \boldsymbol{\mu}^+ - \boldsymbol{\mu}^-$) [42]:

$$\delta_1 = 1 \tag{39}$$
$$0.5\mu_1 + 0.5\mu_2 + 0.5\mu_3 + \delta_2 = 1 \tag{40}$$
$$0.25\mu_1 + 0.75\mu_2 - 0.25\mu_3 + \delta_3 = 1 \tag{41}$$

When Gen2 fails, transmission line 1 is congested, and bus B has extra capacities that are unable to be delivered. Based on this engineering insight, follow *Proposition 2*, $\mu_2 = \mu_3 = 0$ and $\delta_2 = 0$. Then all variables in the dual cone can be calculated.

$$\bar{\gamma} = \begin{Bmatrix} \delta_1 = 1 & \mu_1^+ = 2 & \mu_1^- = 0 & \phi_1^+ = 1 & \phi_1^- = 0 \\ \delta_2 = 0 & \mu_2^+ = 0 & \mu_2^- = 0 & \phi_2^+ = 0 & \phi_2^- = 0 \\ \delta_3 = 0.5 & \mu_3^+ = 0 & \mu_3^- = 0 & \phi_3^+ = 0.5 & \phi_3^- = 0 \end{Bmatrix}$$

Plug in the extreme ray to the security constraint (13) with respect to the Gen2 failure scenario, the constraint is described as follows:

$$0.5(p_3 + r_3^u) + 30 - 40 \geq 0 \tag{42}$$

Combine (42) to (24)-(38), the security-constrained solution is given in Table 7. The security requirement changes the market settlement. One obvious change is to commit Gen3; thus, the total costs increase. In addition, price separation no longer exists since transmission line 1 is not congested. Table 8 gives the commitment and dispatch solution for the security-constrained case when load at bus A increases by one unit. Table 9 gives the LMPs for the security-constrained case without the marginal security component.

Table 7. Security-constrained case solution.

	u	p	r
Gen1	1	10	25
Gen2	1	20	25
Gen3	1	10	10
Total Cost ($)	1,100		

Table 8. Security-constrained case solution when Load A increases 1MW.

	u	p	r
Gen1	1	11	25
Gen2	1	20	25
Gen3	1	10	10
Total Cost ($)	1,110		

Table 9. LMPs for security-constrained case.

LMP A	\$10/MWh
LMP B	\$10/MWh
LMP C	\$10/MWh

3.3 Proposed Reformulation and Pricing Scheme

Consider the reformulation described in Section 3.5 applied to this illustrative example, the pricing model is described as follows.

$$\min \quad 10p_1 + 20p_2 + 30p_3 \tag{43}$$
$$s.t. \quad \text{Resource-level constraints (23)-(31) with fixed commitment solution} \tag{44}$$
$$\text{Reserve requirement (33)-(35)} \tag{45}$$
$$-d_1 - i_1 = 0 \tag{46}$$
$$p_1 - d_2 - i_2 = 0 \tag{47}$$
$$p_2 + p_3 - d_3 - i_3 = 0 \tag{48}$$
$$i_1 + i_2 + i_3 = 0 \tag{49}$$
$$0.5i_1 + 0.25i_2 \le 15 \tag{50}$$
$$0.5(p_3 + r_3^u) + 30 - d_1 - 0.5d_3 \ge 0 \tag{51}$$
$$d_1 = 40 \tag{52}$$
$$d_2 = 0 \tag{53}$$
$$d_3 = 0 \tag{54}$$

When the load at bus A increases by 1MW, it will not only affect the nodal net injection (46), but also the security constraint (51). The security constraint (51) then becomes $p_3 + r_3^u \ge 22$, which implies $p_3 \ge 12$ since $r_3^u \le 10$. If the re-formulated security constraint is not enforced, the solution will have Gen1 pick up the one more unit power, as shown in Table 8. This solution will not cause network violation in pre-contingency state; however, this solution is not secure when Gen2 fails. When Gen2 fails, Gen3 can only ramp to 20MW, which requires Gen1 to ramp to 21MW. In the post-contingency state, transmission line 1 is congested, load shedding occurs. Therefore, Gen3 has to increase its generation level in order to ensure the system security. The new dispatch solutions are given in Table 10.

The security constraint results in Gen3 increases 2MW and Gen1 decreases 1MW. The system costs increment is \$50, i.e., $LMP_A = 50$. This LMP is the summation of original LMP (\$10) and the weighted shadow prices of security constraints (\$40). When the load at bus A increases by one unit, it costs more than \$10 to supply the increment due to the security requirement. The model (43)-(54) captures the shadow prices from a secure state to a new secure state, instead of from a secure state to a feasible but not secure state.

Similarly, when the load at bus C increases by 1MW, the security constraint (51) requires $p_3 = 11$. Gen3 picks up the increased load. The total costs is increased by \$30, so $LMP_C = 10 + 0.5(40) = 30$. Table 11 gives the LMPs under the proposed pricing scheme.

The total load payment becomes $2,000. Gen2 makes profits. Gen1 and Gen3 are marginal units. The total uplift payment is reduced to $200. Prices separation still exists even no transmission line is congested. The prices separation is caused by the security constraints.

Table 10. Security-constrained case solution when Load A increases 1MW under the proposed scheme.

	u	p	r
Gen1	1	9	25
Gen2	1	20	25
Gen3	1	12	10
Total Cost ($)	1,150		

Table 11. LMPs for security-constrained case under the proposed scheme.

LMP A	$50/MWh
LMP B	$10/MWh
LMP C	$30/MWh

4. 73-Bus System Test Case

In this section, the proposed framework is tested on a modified IEEE 73-bus system (RTS 1996) [44]. The test system has 73 buses, 99 generators and 117 transmission lines. The total generation capacity is 10,215MW. The peak load is 8,550MW.

The discussions in this section focus on the day-ahead energy market. The problem is formulated as 24-period day-ahead model. The loads across all periods vary from 59%-100% of the peak load. The procedure of the day-ahead energy market clearing process is described in Figure 2.

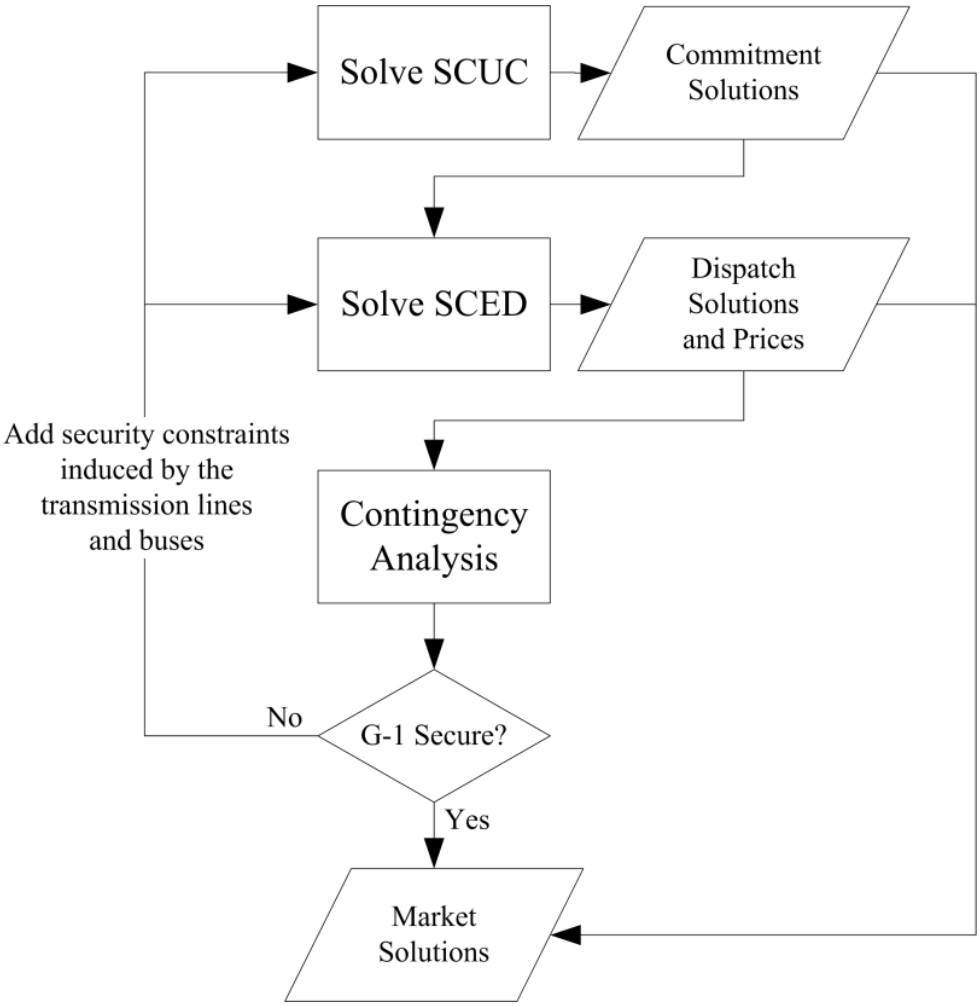

Figure 2. Market clearing process.

In the clearing process, a security-constrained unit commitment (SCUC) is solved to obtain binary commitment solutions. Then, a security-constrained economic dispatch (SCED) is solved. The dispatch solutions and LMPs are obtained. The dispatch solutions are tested for *G*-1 contingency analysis. If the system is insecure with respect to *G*-1

criterion, the proposed security constraints are added with respect to the violated scenario and period. The procedure is iterated until a secure solution is obtained. The market solution is posted with the secure commitment, dispatch solutions and the prices.

As described in Section 2, the proposed extreme ray security constraints are induced by the congested transmission lines and the buses with extra capacities in the post-contingency state. In this 73-bus system, 6 lines are identified to be congested in different post-contingency states; moreover, for each of the lines, there are certain buses with extra capacities that correspond to the congested line. The candidates of the congested lines and the buses with extra capacities are marked in Figure 3.

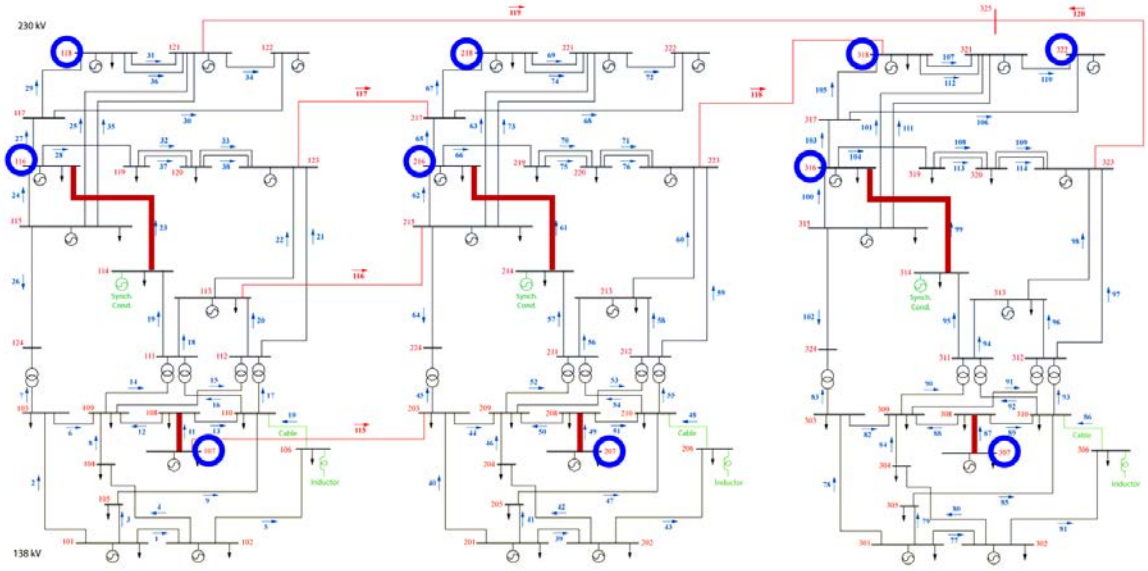

Figure 3. 73-bus system diagram.

Total 35 different line-bus induced extreme rays are identified. Some extreme rays appear in several *G*-1 scenarios and periods. Table 12 summarizes 15 out of 35 line-bus induced extreme rays that appear 8 times or more.

Table 12. Frequent line-bus induced extreme rays.

#	1	2	3	4	5
Frequency (times)	56	42	33	21	20
Lines	87	50,87	50	50,98	23,87
Buses	307	207,307	207	207,322	116,307
#	6	7	8	9	10
Frequency (times)	20	14	12	11	11
Lines	50,98	98	23,50	61	98
Buses	207,318	322	116,207	218	318
#	11	12	13	14	15
Frequency (times)	10	10	9	8	8
Lines	61	50,98	23	98	23,61
Buses	216	207,316	118	316	118,218

The added line-bus induced extreme ray security constraints in Figure 2 are the potential binding security constraints in SCED. If one constraint is not identified from the iterative process, then the constraint is not likely to be binding. The corresponding shadow price will be zero. Therefore, only the identified line-bus induced extreme ray security constraints are crucial to the marginal security component of LMPs. From the test results, even for the identified extreme ray security constraints, most of them are not binding in the SCED. There are 8 line-bus induced extreme ray security constraints identified to be binding in SCED and contribute to the marginal security components. The extreme rays are #1, #5, #7, #9, #11, #13, #14, and #15.

Two pricing schemes are compared: one is without the marginal security component (LMP1) and the other is with the marginal security component (LMP2). The two schemes have the same market commitment and dispatch solutions, but differ in LMPs.

First, the average price differences between the two schemes, i.e., the average marginal security components, are studied. The results are represented in Figure 4. The prices are increased significantly in high-load periods, as high as $47/MWh in peak-load periods. In addition, the price differences follow the pattern of total load percentage of the peak load. When the total system load increases and keeps at high level, the security constraints tend to be binding. The load increment cost more to keep the security constraints satisfied.

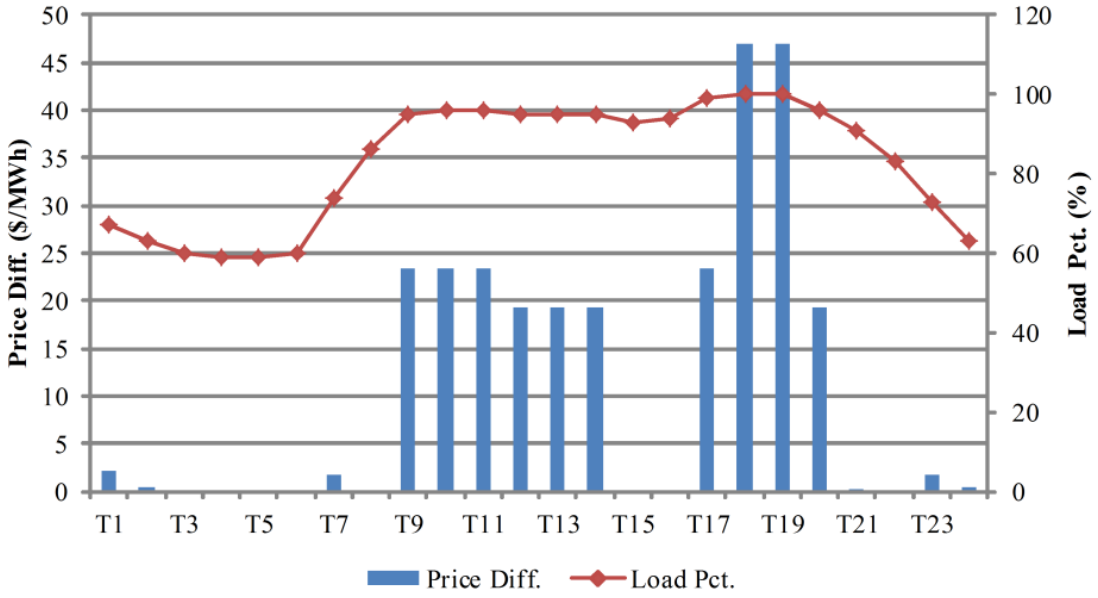

Figure 4. Average price difference across all periods.

Figure 5 and Figure 6 select two buses to compare the two pricings: bus 114, which has the largest accumulative price differences across all periods, and bus 16, which has the smallest accumulative price differences across all periods. At bus 114, the pattern is consistent with the average price difference pattern; during high-load periods, the proposed marginal security components are high. In periods 18 and 19, when at peak load, the marginal security component is as high as $213/MWh. The high price is an indication of network congestion. LMP1 represents the marginal cost from a secure system state to a feasible system state. In periods 18 and 19, LMP1 is as high as $156/MWh in order to move to a feasible system state. LMP2 represents the marginal cost from a secure system state to a new secure system state. It costs more to maintain a secure system state, the marginal costs in periods 18 and 19 are as high as $369/MWh. On the other hand, at bus 116, the price differences are not significant since the original LMPs are relatively low, which indicates the network congestion does not cost more to maintain system security at the location. The marginal security components are positively correlated to the original LMPs.

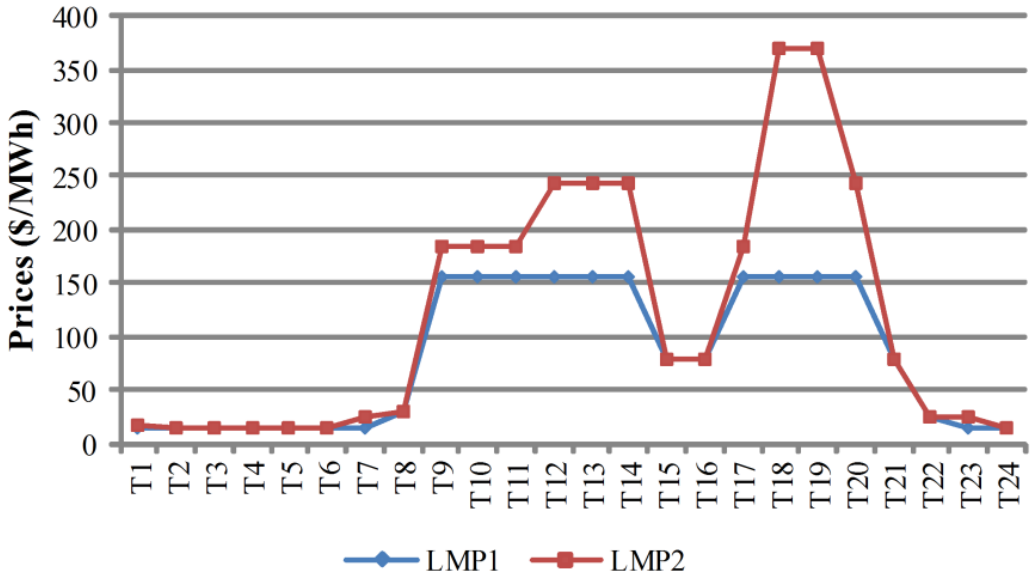

Figure 5. Price comparison at Bus 114.

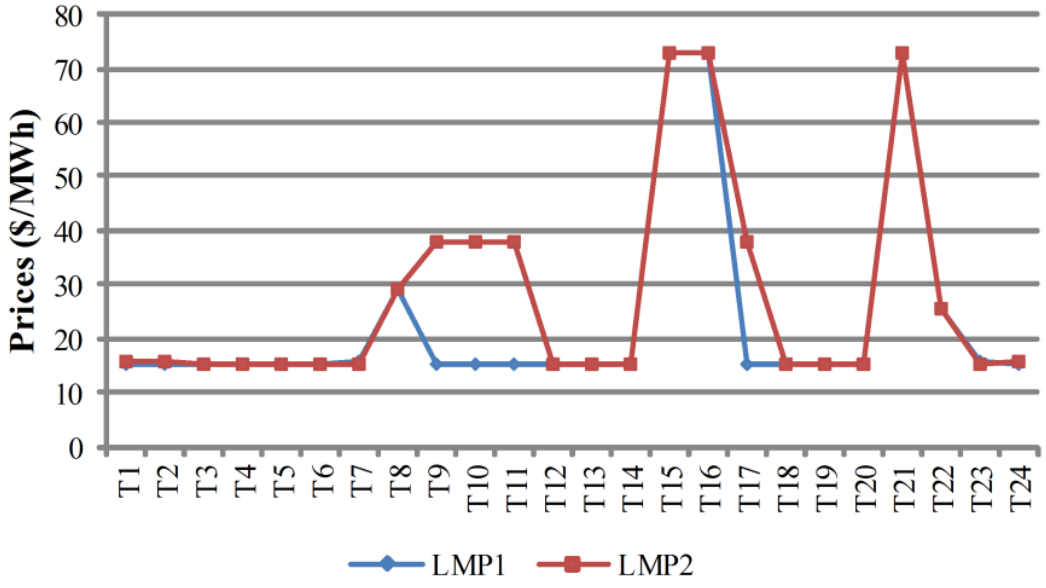

Figure 6. Price comparison at Bus 116.

The market surplus allocations under two pricing schemes are summarized in Table 13. Since energy prices are increased, the total load payment is increased 27.6% from LMP1 to LMP2. The total generation revenue is increased 43.9% from LMP1 to LMP2. The total uplift payment is reduced 49.1% from LMP1 to LMP2. Since RTO/ISOs do not prefer to implement uplift payments as they distort the market price signals, one benefit

from the proposed approach is that it reduces uplift payments. While this is not guaranteed to occur, the inclusion of security constraints further captures grid security requirements and reflects the value of service provided by generators to achieve grid security. This added value that is captured with the proposed method translates into prices that reflect that added value, which is expected to increase profits and, thus, decrease needed uplift payments.

Table 13. Market surplus allocation.

	LMP1	LMP2
Total Load Payment ($)	8,189,920	10,446,800
Total Generation Revenue ($)	3,773,714	5,429,060
Total Uplift Payment ($)	376,826	191,779

Finally, individual generator's market surplus is analyzed. Table 14 lists 5 representative generators' market surplus. Gen44 and Gen47 are slow-start coal units; Gen49 is fast-start gas-turbine unit; Gen57 is nuclear unit; and Gen58 is dis-patchable hydro unit. Under the proposed pricing scheme, the nuclear unit, which is with low variable cost and high capacity, has the highest profit improvement. The hydro unit also obtains significant profit increment due to the low costs. Gen44, Gen47, and Gen49 are likely to be the marginal units due to the high variable generation costs. Gen44 flips from the negative profit to the positive profit. Gen47, though still has negative profit, its revenue is increased significantly. The profits of fast-start units are relatively the same.

Table 14. Generator settlement.

	Gen44	Gen47	Gen49	Gen57	Gen58
Capacity (MW)	100	197	12	400	50
Generation Variable Cost ($/MWh)	75.6	74.8	94.7	5.5	0
Startup Cost ($)	4,754	6,510	571	2,400	0
No-load Cost ($)	839	1,160	73	215	0
Generation Cost ($)	121,989	165,079	1,771	57,578	0
Revenue under LMP1 ($)	104,643	115,242	482	321,022	39,827
Revenue under LMP2 ($)	132,260	159,933	776	432,359	53,627
Profit under LMP1 ($)	-17,346	-49,837	-1,289	263,444	39,827
Profit under LMP2 ($)	10,271	-5,146	-996	374,781	53,627
Profit Increment ($)	27,617	44,691	293	**111,337**	13,800

5. Conclusions

In this report, a new component of LMP, marginal security component, is proposed to be added on top of the current LMP components to better represent energy prices. The components are composed of weighted shadow prices of a set of single-generator-failure contingency security constraints to improve system security. With the proposed marginal security components, the LMPs capture the marginal cost from a secure system state to another secure system state.

The overall market design for electric power markets is a complex problem. This report focuses on the impacts of the security requirements on LMPs. The proposed pricing scheme will affect the design of other markets, such as ancillary services and financial transmission right markets. These topics are left for future study.

References

[1] National Academy of Engineering, "Greatest engineering achievements of the 20th century," March 2016. [Online]. Available: http://www.greatachievements.org/.

[2] California Independent System Operator, "Company information and facts," March 2016. [Online]. Available: http://www.caiso.com/Documents/CompanyInformation_Facts.pdf.

[3] P. Kundur, J. Paserba, V. Ajjarapu, *et al*, "Definition and classification of power system stability: IEEE/CIGRE joint task force on stability terms and definitions," *IEEE Transactions on Power Systems*, vol. 19, no. 2, pp. 1387-1401, 2014.

[4] North American Electric Reliability Corporation, "Reliability concepts," March 2016. [Online]. Available: http://www.nerc.com/files/concepts_v1.0.2.pdf.

[5] R. Doherty and M. O'Malley, "A new approach to quantify reserve demand in systems with significant installed wind capacity," *IEEE Transactions on Power Systems*, vol. 20, no. 2, pp. 587–595, 2005.

[6] T. Zheng and E. Litvinov, "Contingency-based zonal reserve modeling and pricing in a co-optimized energy and reserve market," *IEEE Transactions on Power Systems*, vol. 23, no. 2, pp. 277–286, 2008.

[7] M. Ortega-Vazquez and D. Kirschen, "Estimating the spinning reserve requirements in systems with significant wind power generation penetration," *IEEE Transactions on Power Systems*, vol. 24, no. 1, pp. 114–123, 2009.

[8] E. Cotilla-Sanchez, P. D. Hines, C. Barrows, *et al*, "Multi-attribute partitioning of power networks based on electrical distance," *IEEE Transactions on Power Systems*, vol. 28, no. 4, pp. 4979-4987, 2013.

[9] J. D. Lyon, M. Zhang, and K. W. Hedman, "Locational reserve disqualification for distinct scenarios," *IEEE Transactions on Power Systems*, vol. 30, no. 1, pp. 357-364, 2015.

[10] F. Wang and K. W. Hedman, "Dynamic reserve zones for day-ahead unit commitment with renewable resources," *IEEE Transactions on Power Systems*, vol. 30, no. 2, pp. 612-620, 2015.

[11] Federal Energy Regulatory Commission, "Operator-initiated commitments in RTO and ISO markets," 2014. [Online]. Available: http://www.ferc.gov/legal/staff-reports/2014/AD14-14-operator-actions.pdf.

[12] Y. Al-Abdullah, M. Abdi-Khorsand, and K. W. Hedman, "Analyzing the impacts of out of market corrections," *Proc. IREP Symposium*, Rethymno, Greece, August 2013.

[13] G. L. LaBove, R. B. Hytowitz, and K. W. Hedman, "Market implications of reliability unit commitment formulations for day-ahead scheduling," *Proc. IEEE PES General Meeting*, National Harbor, MD, July 2014.

[14] Y. Al-Abdullah, M. Abdi-Khorsand, and K. W. Hedman, "The role of out-of-market corrections in day-ahead scheduling," *IEEE Transactions on Power Systems*, vol. 30, no. 4, pp. 1937-1946, 2015.

[15] S. Takriti, J. R. Birge, and E. Long, "A stochastic model for the unit commitment problem," *IEEE Transactions on Power Systems*, vol. 11, no. 3, pp. 1497–1508, 1996.
[16] T. Shiina and J. R. Birge, "Stochastic unit commitment problem," *International Transactions in Operational Research*, vol. 11, pp. 19–32, 2004, 2004.
[17] F. Bouffard, F. D. Galiana, and A. J. Conejo, "Market-clearing with stochastic security-part I: formulation," *IEEE Transactions on Power Systems*, vol. 20, no. 4, pp. 1818-1826, 2005.
[18] M. Shahidehpour, W. F. Tinney, and Y. Fu, "Impact of security on power systems operation," *Proc. IEEE*, vol. 93, no. 11, pp. 2013-2025, 2005.
[19] J. Wang, M. Shahidehpour, and Z. Li, "Security-constrained unit commitment with volatile wind power generation," *IEEE Transactions on Power Systems*, vol. 23, no. 3, pp. 1319-1327, 2008.
[20] L. Wu, M. Shahidehpour, and T. Li, "Cost of reliability analysis based on stochastic unit commitment," *IEEE Transactions on Power Systems*, vol. 23, no. 3, pp. 1364-1374, 2008.
[21] K. W. Hedman, M. C. Ferris, R. P. O'Neill, *et al*, "Co-optimization of generation unit commitment and transmission switching with *N*-1 reliability," *IEEE Transactions on Power Systems*, vol. 25, no. 2, pp. 1052–1063, 2010.
[22] A. Papavasiliou and S. S. Oren, "Multiarea stochastic unit commitment for high wind penetration in a transmission constrained network," *Operations Research*, vol. 61, no. 3, pp. 578-592, 2013.
[23] S. M. Ryan, C. Silva-Monroy, J. P. Watson, *et al*, "Toward scalable, parallel progressive hedging for stochastic unit commitment," *Proc. IEEE PES General Meeting*, Vancouver, Canada, July 2013.
[24] C. Li, M. Zhang, and K. W. Hedman, "*N*-1 reliable unit commitment via progressive hedging," *Journal of Energy Engineering*, vol. 141, no. 1, 2015.
[25] A. Street, F. Oliveira, and J. M. Arroyo, "Contingency-constrained unit commitment with n-k security criterion: A robust optimization approach," *IEEE Transactions on Power Systems*, vol. 26, no. 3, pp. 1581-1590, 2011.
[26] L. Zhao and B. Zeng, "Robust unit commitment problem with demand response and wind energy," *Proc. IEEE PES General Meeting*, San Diego, CA, July 2012.
[27] R. Jiang, J. Wang, and Y. Guan, "Robust unit commitment with wind power and pumped storage hydro," *IEEE Transactions on Power Systems*, vol. 27, no. 2, pp. 800-810, 2012.
[28] D. Bertsimas, E. Litvinov, X. A. Sun, *et al*, "Adaptive robust optimization for the security constrained unit commitment problem," *IEEE Transactions on Power Systems*, vol. 28, no. 1, pp. 52- 63, 2013.
[29] Q. Wang, J. P. Watson, and Y. Guan, "Two-stage robust optimization for N-k contingency-constrained unit commitment," *IEEE Transactions on Power Systems*, vol. 28, no. 3, pp. 2366-2375, 2013.
[30] R. Jiang, M. Zhang, G. Li, *et al*, "Two-stage network con-strained robust unit commitment problem," *European Journal of Operational Research*, vol. 234, no. 2, pp. 751-762, 2014.

[31] C. Zhao, J. Wang, J. P. Watson, *et al*, "Multi-stage robust unit commitment considering wind and demand response uncertainties," *IEEE Transactions on Power Systems*, vol. 28, no. 3, pp. 2708-2717, 2013.

[32] U. A. Ozturk, M. Mazumdar, and B. A. Norman, "A solution to the stochastic unit commitment problem using chance constrained programming," *IEEE Transactions on Power Systems*, vol. 19, no. 3, pp. 1589–1598, 2004.

[33] Q. Wang, Y. Guan, and J. Wang, "A chance-constrained two-stage stochastic program for unit commitment with uncertain wind power output," *IEEE Transactions on Power Systems*, vol. 21, no. 1, pp. 206-215, 2012.

[34] J. Benders, "Partitioning procedures for solving mixed-variables programming problems," *Numerische Mathematik*, vol. 4, pp. 238-252, 1962.

[35] C. C. Carøe and R. Schultz, "Dual decomposition in stochastic integer programming," *Operations Research Letter*, vol. 24, no. 1, pp. 37–45, 1999.

[36] R. T. Rockafellar, and R. J. B. Wets, "Scenarios and policy aggregation in optimization under uncertainty," *Mathematics of Operations Research*, vol. 16, no. 1, pp. 119-147, 1991.

[37] J. P. Watson and D. L. Woodruff, "Progressive hedging innovations for a class of stochastic mixed-integer resource allocation problems," *Computational Management Science*, vol. 8, no. 4, pp. 355–370, 2011.

[38] S. L. Pope, "Price formation in ISOs and RTOs: Principles and improvements," *FTI Consulting*, Oct. 2014. [Online]. Available: https://www.epsa.org/forms/uploadFiles/2CC210000016F.filename.EPSA_Price_Formation_Oct_29_2014_FINAL.pdf.

[39] Independent System Operator of New England, "Locational marginal prices," March 2016. [Online]. Available: http://www.iso-ne.com/static-assets/documents/support/training/courses/wem301/wem301_lmp.pdf.

[40] A. J. Wood and B. F. Wollenberg, *Power Generation, Operation, and Control*, 2nd Ed. Wiley and Sons, Inc., 1996.

[41] FERC, "Recent ISO software enhancements and future software and modeling plans," 2011. [Online]. Available: http://www.ferc.gov/industries/electric/indus-act/rto/rto-iso-soft-2011.pdf.

[42] C. Li, M. Zhang, and K. W. Hedman, "Extreme ray feasibility cuts for unit commitment with uncertainty," *European Journal of Operational Research*, under review.

[43] M. S. Bazaraa, H. D. Sherali, and C. M. Shetty, *Nonlinear Programming: Theory and Algorithm*, 3rd Ed. Wiley and Sons, Inc., 2006.

[44] University of Washington, "Power systems test case archive," March 2016. [Online]. Available: https://www.ee.washington.edu/research/pstca/.

Part IV

Day-Ahead Stochastic Co-optimization of Energy and Locational Contingency Reserves

Jose Fernando Prada
Marija D. Ilić

Carnegie Mellon University

For information about this project, contact

Marija D. Ilić
Carnegie Mellon University
Electrical and Computer Engineering Department
5000 Forbes Ave, Hamerschlag Hall.
Pittsburgh, PA 15213-3890
Phone: 412-268-9520
Fax: 412-268-3890
Email: milic@ece.cmu.edu

Power Systems Engineering Research Center

The Power Systems Engineering Research Center (PSERC) is a multi-university Center conducting research on challenges facing the electric power industry and educating the next generation of power engineers. More information about PSERC can be found at the Center's website: http://www.pserc.org.

For additional information, contact:

Power Systems Engineering Research Center
Arizona State University
527 Engineering Research Center
Tempe, Arizona 85287-5706
Phone: 480-965-1643
Fax: 480-965-0745

Notice Concerning Copyright Material

Table of Contents

List of Figures

List of Tables

Nomenclature

Indices and Sets:

i	index of available generating units.
j	index of generating units able to provide reserves.
k	index of single generation contingencies.
l	index of single transmission line contingencies.
m, n	index of electrical nodes of transmission network.
t	index of time periods (hours).
$I^{(k)}$	set of available generation units under contingency k.
I_n	set of available generating units connected to node n.
$J^{(k)}$	set of generation units available to provide reserves under contingency k (subset of $I^{(k)}$).
K	set of selected single generation contingencies, running from 0 (no contingency) to K.
L	set of selected transmission line contingencies, running from 0 (no contingency) to L.
M_n	set of electrical nodes directly connected to node n.
N	set of electrical nodes of the transmission network, running from 1 to N.
T	set of (hourly) time periods, running from 1 to T.

Variables and Parameters:

$g_{it}^{(k)}$	generation of unit i in period t under contingency k (MW).
r_{it}^{sp}	spinning reserve of unit i in period t (MW).
r_{it}^{ns}	nonspinning reserve of unit i in period t (MW).
$\theta_{nt}^{(k)}$	voltage phase angle at node n in period t under contingency k (rad).
$u_{it}^{(k)}$	binary variable {0,1}, 1 when unit i is committed in period t under contingency k and 0 otherwise.
$x_{it}^{(k)}$	binary variable {0,1}, 1 when unit i is started up in period t under contingency k and 0 otherwise.
$y_{it}^{(k)}$	binary variable {0,1}, 1 when unit i is shut down in period t under contingency k and 0 otherwise.
$w_t^{(k)}$	probability of contingency k occurring in period t given that no contingency has occurred before.
$g_i^{\min}$	minimum power output of unit i (MW).
$g_i^{\max}$	maximum power output of unit i (MW).
$\Delta\theta^{\max}$	maximum voltage phase angle difference (rad).
$R_{it}^{sp\_\max}$	maximum spinning reserve limit of unit i (MW).
$R_{it}^{ns\_\max}$	maximum nonspinning reserve limit of unit i (MW).
RD_i	maximum inter-period ramp-down limit of unit i (MW).
RU_i	maximum inter-period ramp-up limit of unit i (MW).
$RD^{10}{}_j$	maximum 10-minute ramp-down limit of unit j (MW).

RU^{10}_j	maximum 10-minute ramp-up limit of unit j (MW).
DT_i	minimum down time of unit i (hours).
UT_i	minimum up time of unit i (hours).
D_{nt}	electrical demand at node n in period t (MW).
$B_{nm}^{(l)}$	electrical susceptance of transmission line between nodes n and m under contingency l (S).
$FN_{nm}^{\max}$	continuous power rating of transmission line between nodes n and m (MW).
$FE_{nm}^{\max}$	1-hour emergency power rating of transmission line between nodes n and m (MW).

Functions:

$SC_{it}( )$	generation startup cost of unit i in period t ($/h).
$GC_{it}( )$	no load and variable generation dispatch cost of unit i in period t ($/h).
$RC^{sp}_{it}( )$	spinning reserve cost of generation unit i in period t ($/h).
$RC^{ns}_{it}( )$	nonspinning reserve cost of generation unit i in period t ($/h).

When not specified, variables and parameters (e.g. u_{it}) correspond to a system condition without contingencies ($k= 0$).

1 Introduction

Providing a reliable and efficient electricity service to customers is the fundamental objective of a power system's planning and operation. In particular, a critical aspect of the bulk power system reliability is the security of real-time operations, which refers to the ability of the system to withstand sudden disturbances. A typical disturbance is the unplanned loss of a major component –a contingency–, normally a generation unit or transmission line [1]. The analysis of power systems security has two dimensions. First, the system must settle into a post contingency feasible operating condition. Second, the system must be able to reach that new condition. In the first part, a steady-state analysis verifies that no physical constraints are violated during the post contingency operating condition, whereas the second part involves the dynamic analysis of system stability [2]. This report is concerned with the static security analysis after the occurrence of generation contingencies.

1.1 Background

In general, system security (operational reliability) is preserved by examining the effect of a set of more likely or "credible" contingencies, usually the loss of single major elements in the system. Accordingly, the widely used N-1 reliability criterion requires that the bulk power system stay within its operating limits after the occurrence of a single contingency event [3]. To ensure N-1 compliance, adequate generation capacity should be available throughout the system, in order to prevent load shedding when a single generation unit or transmission line is unexpectedly disconnected from the grid. In practice, a security-constrained generation dispatch is able to cope with transmission outages. However, in order to restore the power balance after a generation outage, sufficient backup capacity should be kept standing by as a contingency reserve. Contingency reserves are the main component of system operating reserves.

The preferred approach to assign and price contingency reserves in US electricity markets is the co-optimization during the resource scheduling process [4]. Co-optimization refers to the simultaneous determination of energy and reserves within the scheduling optimization problem. Scheduling system resources is actually a complex task comprising several stages and details. There are important differences in the way scheduling is implemented in each regional electricity market, but also common aspects that allow a generalization of the process as described in [5] and outlined below. With some simplifications, this procedure is similarly used by operators of vertically integrated systems.

To ensure the reliability and efficiency of operations, the core of the scheduling process is a security-constrained unit commitment (SCUC) market model. The SCUC is a mixed-integer optimization problem, which is run a day ahead to establish the optimal daily generation commitment and dispatch program, including reserves, as well as related market transactions, for each market period of the operation day. The day-ahead program is subsequently adjusted for reliability reasons and to accommodate changes in network conditions. Finally, a security-constrained economic dispatch (SCED) is used to determine real-time operations, according to the actual load and grid conditions. The co-optimization of

energy and reserves takes into account the cost of providing both products, considering the technical constraints resulting from transmission and generation operational limits and from additional security requirements. Formulations of the traditional deterministic SCUC problem, as well as proposed stochastic SCUC models can be found in [6]–[12].

1.2 Reserves Requirements

In the SCUC model, the N-1 security criterion is enforced for single line outages through additional power balance constraints, ensuring the system is able to reach a new feasible generation dispatch after losing a single transmission line. In the case of generation outages, N-1 is met by imposing a deterministic and global reserve requirement that needs to be kept during normal operation. A fixed reserve requirement is often adopted, based on some heuristics such as the largest expected generation outage or a percentage of the expected demand. In this case the required reserve stems more from judgement and accumulated operating experience, rather than being actually based on reliability calculations. This global reserve requirement should be met with spare capacity of fast generation units already online –spinning reserve–, but it can also be fulfilled with available capacity of offline but fast-starting units, or nonspinning reserve. Upon request, the contingency reserve should be delivered typically in a maximum of 10 minutes. However, the division between spinning and nonspinning reserve is rather arbitrary. PJM, for instance, requires that 100% of the contingency reserve be spinning, and it schedules an additional 50% as non-spinning reserve. Its neighbor, NYISO, on the contrary requires that at least 50% of the reserve should be spinning but the rest can be nonspinning. Same applies in CAISO.

A number of problems have been identified with the use of a fixed reserve requirement in the solution of the day-ahead SCUC. A central and well-known criticism is that this method does not guarantee N-1 security against generation outages, since transmission congestion may prevent the effective use of reserves when a contingency occurs [13]. The reason is that the global reserve method does not verify the feasibility of reserve delivery during a post contingency state, therefore failing to define appropriate locational reserves in the system. As a consequence, system operators need to run offline contingency analyses, and frequently resort to manually adjusting the generation dispatch to comply with security criteria using out-of-market corrections, a procedure that is economically inefficient [14]. A common partial fix is to divide the system into reserve zones, based on known transmission bottlenecks. Then, reserve requirements are defined for each zone in the SCUC, resulting in the allocation of zonal reserves. Using zones mitigates the problem of reserve delivery, but it is still based on ad-hoc definitions of zones and reserve requirements, and it does not guarantee N-1 compliance under all generation outages [15].

In addition, the procedure to schedule generation reserves is purely deterministic, not taking into account the probability of failure of generating units. Therefore, it treats all outages as having equal risk and impact, unnecessarily increasing system costs. The allocation of contingency reserves based on a global requirement does not provide an operation program to dispatch reserves either. That is, what reserves to use after a generation outage has occurred, which should vary according to the specific contingency realized. Lastly, the division between spinning and non-spinning reserve lacks technical bases as indicated before. On the other hand, the current approach to reserve pricing in competitive

markets is based on the marginal purchase cost of the global requirement. This method is inefficient in the sense that it does not remunerate the actual reserves required in the system, in terms of location and quantity. Therefore current reserve prices do not provide efficient economic signals for operation and investment.

Setting a global reserve requirement equal to the loss of the largest generation unit online would be adequate for a system without transmission constraints, but it has serious shortcomings for real networks where transmission congestion is a permanent rather that transitory condition. Zonal reserve requirements mitigate the congestion effects, but they are still loosely related to the set of credible contingencies that need to be addressed under the N-1 criterion. A better approach needs to be based on a spatial distribution of the reserves that allows the system to respond to the actual conditions present after a contingency has occurred (post contingency state). These reserves are necessarily locational, ensuring deliverability of energy under any of the different possible contingencies. The purpose of this paper is to formulate methods to allocate and price locational contingency reserves, under a set of credible single generation outages. These methods consider the stochastic nature of the problem by modeling the probability of failure of generation units and associated post-contingency scenarios.

1.3 Related Work

The idea of using generation rescheduling as a corrective action to find an optimal security-constrained solution for economic dispatch problems has long been discussed, of which references [16] and [17] are illustrative. In both cases a deterministic optimal power flow (OPF) with pre contingency operating constraints is complemented with post contingency constraints to ensure system security. The authors present different solution methodologies but do not consider reserve costs or allocation. The main difficulty of implementing this approach has been computational complexity, since the inclusion of multiple contingencies greatly increases the size of the OPF problem. A more recent example is found in [18], where the authors implement transmission switching techniques using a unit commitment model that is N-1 compliant using post contingency security constraints, but do not address reserve allocation nor pricing.

In recent years there has also been an increasing interest in stochastic formulations for the unit commitment problem or SUC, as illustrated in [8]–[11]. SUC models are mainly focused on the uncertainty introduced by load forecast deviations and by intermittent energy production from renewable generation (both having continuous probability distributions), instead of the uncertainty due to the random occurrence of generation and line outages (with discrete probability distributions). Composite probabilistic scenarios are usually synthetized and reduced to ensure computational tractability. Load shedding is also often accepted to ensure problem feasibility. Importantly, SUC models enforce security constraints but do not have explicit representation of reserves, in both quantity and prices. Computational complexity is still a big challenge for SUC, so applications with detailed uncertainty representation in large systems require advanced decomposition techniques and parallelization or are just unsolvable in practice with current computational capabilities. In a related but alternative perspective [12] proposed a robust adaptive optimization solution for the SCUC problem, but still with fixed reserve requirements.

In terms of reserve allocation, [19]-[20] proposed improvements to the use of zonal reserves, but the methods still rely on ad-hoc zonal requirements. Reference [21] presented a joint energy/reserve market model with network and contingency constraints, introducing upward and downward spinning reserves. The model is deterministic and only examines short-term generation dispatch, without multi-period constraints nor unit commitment. Stochastic models use scenario-weighted co-optimization of energy and reserves, which effectively recognizes the probability of generation outages. Thus, [22] proposed a joint energy-reserve market with locational scheduling and pricing of reserves. This formulation uses a particular definition of reserves and deals with short-term generation dispatch, without considering the commitment of generation units, which is the essential scheduling problem, nor nonspinning reserves. A more complete stochastic market clearing model is proposed in [23]-[24], based on a SCUC with post contingency constraints, including energy plus spinning and nonspinning reserves (upwards and downwards). Generation reserves are defined as the difference between pre and post contingency dispatch values. This model departs from the N-1 security standard and use a probabilistic security criterion, allowing load shedding and minimizing the expected value of operating costs plus non-served energy (monetized at an assumed value of lost load VOLL). The solution is based on stochastic programming with replication of scenario variables, assuming that reserves are continuously used from the occurrence of a contingency until the end of the operation day. Consequently, the model is computationally costly and it is solved under several simplifying assumptions for tractability. A similar formulation is used in [25, Ch. 10], but with a different definition of reserves and without considering reserve pricing.

References [26]–[27] includes upward and downward spinning reserves, within a bigger framework of an optimal power flow (OPF) encompassing multiple resources and scheduling functions, with co-optimization through multiple scenarios. As with other stochastic models, they include uncertainty from other sources besides generation outages and use a probabilistic security criterion that minimizes non served energy. The basic model is a single period security-constrained OPF, considering coupling constraints among scenarios but not the unit commitment problem with intertemporal constraints.

1.4 Report Organization

This first section has provided background information on the scheduling of contingency reserves, described problems with current reserve allocation methods and discussed relevant literature. The rest of the report is organized as follows: section 2 presents the general approach and proposed methods to allocate locational contingency reserves, section 3 presents numerical results of simulations on the IEEE Reliability Test System 96 and section 4 summarizes findings and discusses policy implications for power system reliability.

2 General Approach and Proposed Methods

The overall purpose of this work is to formulate practical alternatives to determine the contingency reserves necessary to fully comply with mandatory N-1 operational reliability criteria. The required reserves –in type, location and quantity– are allocated and priced within the framework of the scheduling process followed by system operators in US competitive electricity markets, in a manner compatible with the operation of reserve markets.

2.1 Locational Contingency Reserves

To identify the contingency reserves actually required in the bulk power system, it is necessary to differentiate the role that preventive and corrective actions play to guarantee operational security. Firstly, transmission line outages are subject to preventive control, since the feasibility of the SCUC solution under different line contingencies ensures that the system will remain within its operational limits after the failure of a single transmission line. This is accomplished by redistributing power flows and without any immediate operator intervention. There is no explicit allocation of reserves, but they are implicit in the "security-constrained" dispatch of generation. This preventive control is effective to handle line outages, although it inherently increases operating costs. Secondly, contingency reserves are kept as a preventive control against generation outages, but a corrective control will always be required to restore the power unbalance created by an outage [28]. The corrective control action requires manually ramping up generators with reserved available capacity, to physically rebalance the system until a new secure economic dispatch can be found. Although not strictly required, the system may also benefit from ramping down other generation units to reduce overall costs or even for feasibility of the post contingency redispatch.

Accordingly, to meet N-1 operational reliability, the contingency reserves to be kept during normal operation are those necessary for the system to quickly respond to any credible single generation outage, and operate in a post-contingency state without load shedding. The spare capacity needed from a particular generation unit is the difference between its network-constrained post and pre-contingency dispatches. As there are several credible generation contingencies considered, the actual reserve required from a unit is the maximum difference across all those contingencies. In principle, contingency reserves should be kept online, as spinning reserve. However, because frequency-responsive reserves start responding immediately to power mismatches, there is some acceptable time within which all the contingency reserves should act, usually ten minutes. This also allows fast-start units to provide contingency reserves, even if they are offline, as nonspinning reserve. Additionally, besides starting up offline units, at least theoretically there may be an economic benefit from shutting down a unit after a contingency occurs.

Hence, locational contingency reserves can be "upward" spinning and non-spinning reserves (r^{sp+}, r^{ns+}), which is consistent with the conventional definition. But it is also

possible to define "downward" spinning and non-spinning reserves (r^{sp-}, r^{ns-}), as explained above. The different types of locational reserves are illustrated in Figure 1.

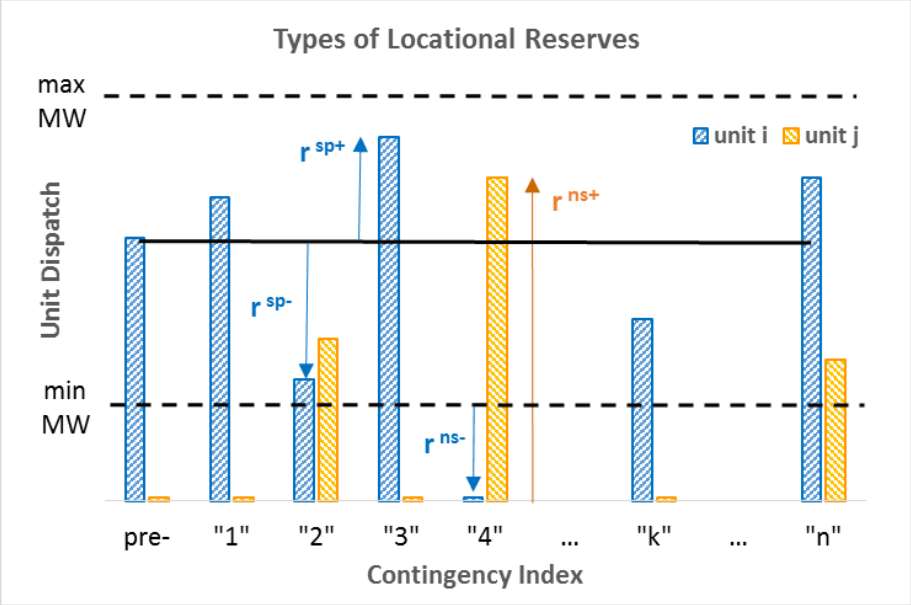

Figure 1. Four types of locational contingency reserves.

2.2 Stochastic Allocation of Reserves

Contingency reserves need to be assigned for every market period during the day-ahead scheduling process, so they should be co-optimized and allocated using a unit commitment market model. In addition, the occurrence of a particular contingency (a single generator outage at a particular time) is a random event. The allocation of contingency reserves should therefore consider a stochastic model of the uncertain generation outages, based on specific contingency scenarios with associated probabilities. Accordingly, we use a stochastic security-constrained UC model to co-optimize energy and locational reserves. The objective is to minimize the expected total operating cost, considering generation costs under normal conditions (no outages) and the cost of redispatching the system after a generation outage (post contingency). An important factor to consider is that the post contingency state reached after using the contingency reserve is stable but insecure, in the sense that the system would not be able to survive a new contingency. Therefore, this condition is allowed to persist until system operators can redispatch all available resources again (including slow online and offline units), restore the reserves, and reestablish a secure operation. The practical implications are that the reserves are only used during a rather short post contingency period and that operators can use the short term emergency ratings of transmission lines during that period [29].

Under the N-1 security standard, the contingencies of interest are single generation outages, that is, the events where only one generation unit is lost. Given the time horizon

and resolution of the day-ahead unit commitment problem, the different contingency scenarios correspond to single generation outages that can occur in any hourly period of the day. Importantly, there is no need to consider the occurrence of successive contingencies, since as we explained above, in a relatively short period of time after a contingency occurs, the system is dispatched again with security constraints and the reserve is restored. Therefore, the scenario to consider is one where a single contingency occurs at a specific hourly period given that there has not been any contingency before, together with its associated conditional probability.

For simplicity and without loss of generality, we assume that the contingency occurs after the beginning of each hourly period, so the system transitions from the normal pre contingency state to a post-contingency state during the same time period. Moreover, we only need to consider a network-constrained post contingency redispatch for one time period, which is the maximum time assumed before the system can be dispatched again and the reserve reestablished. To assume that the reserves are going to be used beyond that point and for the rest of the day would result in a non-secure operation, precludes the use of short-time line emergency ratings, and unnecessarily constrains the feasible solution space. The proposed approach is therefore consistent with standard system operation practices and allows a simpler and compact formulation of the stochastic SCUC, which is fundamental to ensure computational tractability.

Consequently, the available generation uncertainty is completely described by maximum K.T scenarios, where K is the number of generation units available for day-ahead scheduling, and T the number of time periods covered by the UC analysis horizon (assumed here to be 24 hourly periods). Each scenario includes the commitment and dispatch of units under normal conditions until a period $t = \tau$ where a single unit $k = \kappa$ fails. A corrective redispatch is carried out in that period, finding new commitment and dispatch values for the available generation units. Each scenario is defined by the pair (t, k), as illustrated in Figure 2.

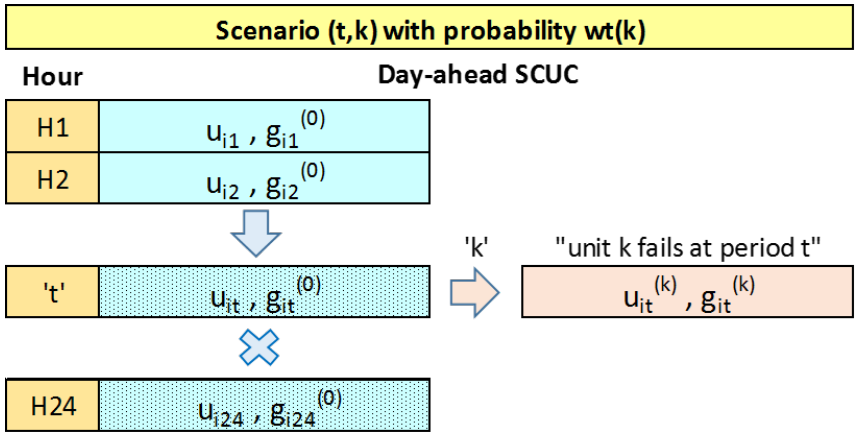

Figure. 2. Contingency scenarios for the stochastic SCUC

The calculation of scenario probabilities is based on reliability models of generation failure, which are well established as described in [30]. Assuming a constant failure rate λ and exponentially distributed times of unit failures, the probability of a unit *i* failing at time *t* (after being put in service), is approximately $p_{it}=1–exp(-\lambda_i t)$. Otherwise, the long term probability of failure, equivalent to the unit forced outage rate, can be used. Accordingly, $\overline{p_{it}}$ is the probability that unit *i* has not failed at period *t* or before. Given the single failure probabilities for each unit and time period, and assuming generation units fail independently, we can find the probability $w_t^{(k)}$ of the scenario (*t*, *k*), that is, of the event of having a single contingency of unit *k* at period *t* and none before, as follows:

$$w_t{}^{(k)} = \overline{p_{1t}}.\,\overline{p_{2t}} \ldots p_{kt} \ldots \overline{p_{Kt}} \qquad (1)$$

It is also easy to show that the probability of finding the system in a normal state (that is, with no single generation contingencies) in a time period t is equal to:

$$w_t{}^{(0)} = 1 - \sum_{q=1}^{t} \left(\sum\nolimits_k w_q{}^{(k)} \right) \qquad (2)$$

Based on the general approach and stochastic model described in this section, next we formulate two stochastic SCUC models to co-optimize energy and contingency reserves as part of the day-ahead scheduling process. In general the models minimize total expected daily operation costs, considering generation startup, dispatch, reserve and redispatch costs across the no-contingency condition and the contingency scenarios. For simplicity a demand benefit function and generation shutdown costs are not explicitly represented, but they can be easily added to the models.

The optimization models are mixed integer programs (MIP) and the representation is compact by using a stochastic programming node-variable formulation instead of a scenario-variable formulation [25, Ch. 2]. This avoids the replication of variables and constraints per scenario and the use of non-anticipativity constraints, which is computationally very costly for the unit commitment problem. The SCUC models include static security constraints, network constraints, generation power limits and ramping limits. We use a dc-power-flow network linear approximation for computational tractability. All problem constraints of the SCUC models are linear, so the characteristics of the cost functions define the type of optimization problem. Thus, a quadratic generation cost function determines a quadratic MIP problem, whereas a piecewise linear approximation or a stepwise supply offer function define a linear MIP problem (MILP).

2.3 Co-optimization of Energy and Spinning Reserves

The first model co-optimizes energy and spinning reserves. The problem minimizes expected generation cost in order to supply forecast demand meeting the N-1 security standard over the 24 hours of the operation day. Generation costs included startup, dispatch and spinning reserve costs without contingencies plus post contingency redispatch costs. The objective function to minimize is:

$$\sum_{t \in T} {w_t}^{(0)} \left\{ \sum_{i \in I^{(0)}} \left[SC_{it}(x_{it}) + GC_{it}\left(u_{it}, {g_{it}}^{(0)}\right) + RC_{it}({r_{it}}^{sp}) \right] \right\}$$

$$+ \sum_{t \in T} \left\{ \sum_{\substack{k \in K \\ k \neq 0}} {w_t}^{(k)} \left(\sum_{i \in I^{(k)}} GC_{it}\left(u_{it}, {g_{it}}^{(k)}\right) \right) \right\} \quad (3)$$

The decision variables are u_{it}, x_{it}, y_{it} and ${g_{it}}^{(k)}$. The spinning reserves variables (r^{sp+}, r^{sp-}) are explicitly represented but they are function of other decision variables instead of independent optimization variables. Also notice that since only spinning reserve is considered, only online units are redispatched in the post-contingency condition.

1) Problem constraints

The different constraints of the co-optimization problem (3) are described below. Some are characteristic of SCUC problems and others are specific to the present formulation.

- Nodal power balances

$$\sum_{i \in I_n} g_{it}^{(k)} - \sum_{m \in Mn} {B_{nm}}^{(0)} . \left(\theta_{nt}^{(k)} - \theta_{mt}^{(k)} \right) = D_{nt} \; ; \; \forall \, n \in N, k \in K, t \in T \quad (4)$$

$$\sum_{i \in I_n} {g_{it}}^{(0)} - \sum_{m \in Mn} {B_{nm}}^{(l)} . \left(\theta_{nt}^{(l)} - \theta_{mt}^{(l)} \right) = D_{nt} \; ; \; \forall \, n \in N, l \in L, t \in T \quad (5)$$

Equations (4) are dc power flows for normal conditions and single generation outages, whereas (5) are dc power flow equations with single transmission outages, in particular ${B_{nm}}^{(l)}$ is 0 when the line *nm* is out.

- Static security limits

$$-\Delta\theta^{\max} \leq \left(\theta_{nt}^{(k)} - \theta_{mt}^{(k)} \right) \leq +\Delta\theta^{\max} \; ; \; \forall \, n \in N, m \in M_n, k \in K, t \in T \quad (6)$$

$$-{FN_{nm}}^{\max} \leq {B_{nm}}^{(0)} . \left(\theta_{nt}^{(0)} - \theta_{mt}^{(0)} \right) \leq +{FN_{nm}}^{\max} \; ; \; \forall \, n \in N, m \in M_n, t \in T \quad (7)$$

$$-{FE_{nm}}^{\max} \leq {B_{nm}}^{(0)} . \left(\theta_{nt}^{(k)} - \theta_{mt}^{(k)} \right) \leq +{FE_{nm}}^{\max} \; ; \; k \neq 0, \forall \, n \in N, m \in M_n, k \in K, t \in T \quad (8)$$

$$-{FE_{nm}}^{\max} \leq {B_{nm}}^{(l)} . \left(\theta_{nt}^{(l)} - \theta_{mt}^{(l)} \right) \leq +{FE_{nm}}^{\max} \; ; \; l \neq 0, \forall \, n \in N, m \in M_n, l \in L, t \in T \quad (9)$$

Equations (6) limit the maximum voltage angle difference between connected nodes, whereas (7)–(9) set maximum power flow limits on transmission lines for normal conditions and contingencies.

- Generation operating limits

$$g_{it}{}^{(0)} - r_{it}{}^{sp-} \geq g_i^{\min}.u_{it}\ ;\ \forall\, i \in I^{(0)}, t \in T \qquad (10)$$

$$g_{it}{}^{(0)} + r_{it}{}^{sp+} \leq g_i^{\max}.u_{it}\ ;\ \forall\, i \in I^{(0)}, t \in T \qquad (11)$$

$$-RD_i \leq g_{i,t}{}^{(0)} - g_{i,t-1}{}^{(0)} \leq RU_i\ ;\ \forall\, i \in I^{(0)}, t \in T \qquad (12)$$

Equations (10)–(12) set generation power and ramp limits for normal conditions.

$$g_{\kappa t}^{(k)} = 0 \quad ;\ \kappa\text{: unit out in } k, k \neq 0, \forall\, k \in K, t \in T \qquad (13)$$

$$g_{it}^{(k)} = g_{it}{}^{(0)}\ ;\ i \neq \kappa, i \neq j, \forall\, i \in I^{(k)}, j \in J^{(k)}, t \in T \qquad (14)$$

$$g_j^{\min}.u_{jt} \leq g_{jt}{}^{(k)} \leq g_j^{\max}.u_{jt}\ ;\ j \neq \kappa, k \neq 0, \forall\, j \in j^{(k)}, k \in K, t \in T \qquad (15)$$

$$-RD^{10}{}_j \leq g_{jt}^{(k)} - g_{jt}^{(0)} \leq +RU^{10}{}_j\ ;\ j \neq \kappa, k \neq 0, \forall\, j \in J^{(k)}, k \in K, t \in T \qquad (16)$$

Equations (13)–(16) set generation power and ramp limits for post contingency states.

- Generation startup and shutdown constraints

$$x_{it} - y_{it} = u_{i,t} - u_{i,t-1}\ ;\ \forall\, i \in I^{(0)}, t \in T \qquad (17)$$

$$x_{it} + y_{it} \leq 1\ ;\ \forall\, i \in I^{(0)}, t \in T \qquad (18)$$

$$x_{it} \leq u_{i,t+q}\ ;\ q = 1, \ldots, \min[(UT_i - 1), T], \forall\, i \in I^{(0)}, t \in T \qquad (19)$$

$$y_{it} \leq 1 - u_{i,t+q}\ ;\ q = 1, \ldots, \min[(DT_i - 1), T], \forall\, i \in I^{(0)}, t \in T \qquad (20)$$

Equations (17)–(18) define the unit startup and shutdown sequence, and (19)–(20) set minimum unit up and down time restrictions for normal conditions.

2) Spinning reserves allocation and pricing

Spinning reserves required from each generating unit are defined as follows:

$$r_{it}{}^{sp+} = \max_k \left[\left(g_{it}^{(k)} - g_{it}^{(0)}\right), 0\right]\ ;\ \forall\, i \in I^{(0)}, t \in T \qquad (21)$$

$$r_{it}{}^{sp-} = \max_k \left[\left(g_{it}^{(0)} - g_{it}^{(k)}\right), 0\right]\ ;\ \forall\, i \in I^{(0)}, t \in T \qquad (22)$$

$$r_{it}{}^{sp} = r_{it}{}^{sp+} + r_{it}{}^{sp-} \leq R_{it}{}^{sp\_\max}\ ;\ \forall\, i \in I^{(0)}, t \in T \qquad (23)$$

The total spinning reserve provided by a unit is the sum of allocated upward and downward reserve. Also in (23), $R_{it}{}^{sp\_\max}$ is a physical limit or the maximum amount of spinning reserve that a generator is willing to provide. The interpretation of these reserves is that the unit *i* should be available to be dispatched at period *t* in the range [$g_{it}{}^{(0)} - r_{it}{}^{sp-}$, $g_{it}{}^{(0)} + r_{it}{}^{sp+}$]. Total system reserves are the sum of the reserves assigned to each unit. We

assume that any actual energy opportunity cost arising from providing spinning reserves is recovered as a separate make-whole payment. Therefore, reserve costs only reflect the cost of making the capacity available to the system and, from the point of view of generators, there is no difference between providing reserves up or down. Accordingly, in (3) both types of spinning reserves have the same cost (i.e. no separate offers are required for up and down reserves). Pricing of locational spinning reserves is based on the previous reserve allocation: the marginal reserve cost on each node sets the nodal contingency reserve price. Therefore, if ρ_{nt}^{sp} is the locational price of spinning reserves at node *n* in period *t*, we have:

$$\rho_{nt}{}^{sp} = \max_i [RC_{it}(r_{it}{}^{sp})]\ ;\ \{i \in I_n : r_{it}{}^{sp} > 0\}, \forall\, n \in N, t \in T \qquad (24)$$

2.4 Co-optimization of Spinning and Nonspinning Reserves

To include nonspinning reserves in the scheduling problem, we need to allow able generation units to start and ramp up to provide energy to rebalance the system after a contingency occurs, as upward nonspinning reserve. We can also allow units to shut down if it reduces costs, and we consider that they provide downward nonspinning reserve. In this case we need to include the cost of starting up nonspinning reserves (but we do not explicitly represent shut-down costs as before). The objective function to minimize is:

$$\sum_{t \in T} w_t{}^{(0)} \left\{ \sum_{i \in I^{(0)}} \left[SC_{it}\left(x_{it}{}^{(0)}\right) + GC_{it}\left(u_{it}{}^{(0)}, g_{it}{}^{(0)}\right) + RC_{it}^{sp}\left(r_{it}^{sp+}, r_{it}^{sp-}\right) + RC_{it}^{ns}(r_{it}^{ns+}, r_{it}^{ns-}) \right] \right\}$$

$$+ \sum_{t \in T} \sum_{\substack{k \in K \\ k \neq 0}} w_t{}^{(k)} \left(\sum_{i \in I^{(k)}} \left[SC_{it}\left(x_{it}{}^{(k)}\right) + GC_{it}\left(u_{it}{}^{(k)}, g_{it}{}^{(k)}\right) \right] \right) \qquad (25)$$

The decision variables are $u_{it}^{(k)}$, $x_{it}^{(k)}$, $y_{it}^{(k)}$ and $g_{it}^{(k)}$. The spinning and nonspinning reserve variables (r^{sp+}, r^{sp-}, r^{ns+}, r^{ns-}) are explicitly represented but they are function of other variables. In (25) we have assumed that units providing upward nonspinning reserves will not fail to start, so we can use the same scenario probabilities that we used in the previous case where only spinning reserves where considered (in fact failure to start a reserve could be considered a second contingency). In general, assigning upward nonspinning reserves is a tradeoff between incurring an additional low probability startup cost or expected lower reserve costs.

1) Problem constraints

The nodal power balance and static security constraints are identical to the previous problem. Below we list the generation-related constraints that are different or specific to the co-optimization of energy, spinning and nonspinning reserves.

- Generation operating limits

$$g_j^{\min}.u_{jt}{}^{(k)} \le g_{jt}{}^{(k)} \le g_j^{\max}.u_{jt}{}^{(k)}\ ;\ j \ne \kappa, k \ne 0, \forall\, j \in J^{(k)}, k \in K, t \in T \quad (26)$$

Equations (26) modifies (15) to set generation power limits for post contingency states.

- Generation startup and shutdown constraints

$$u_{\kappa t}{}^{(k)} = 0 \quad ;\ \kappa\text{: unit out in } k, k \ne 0, \forall\, k \in K, t \in T \quad (27)$$

$$u_{it}{}^{(k)} = u_{it}{}^{(0)}\ ;\ \ i \ne \kappa, i \ne j, \forall\, i \in I^{(k)}, j \in J^{(k)}, t \in T \quad (28)$$

$$x_{it}{}^{(k)} - y_{it}{}^{(k)} = u_{it}{}^{(k)} - u_{it}{}^{(0)}\ ;\ k \ne 0, \forall\, i \in I^{(k)}, k \in K, t \in T \quad (29)$$

$$x_{it}{}^{(k)} + y_{it}{}^{(k)} \le 1\ ;\ k \ne 0, \forall\, i \in I^{(k)}, k \in K, t \in T \quad (30)$$

$$x_{it} \le u_{i,t+q}{}^{(k)}\ ;\ \ q = 1, \dots, \min[(UT_i - 1), T - t], k \ne 0, \forall\, i \in I^{(k)}, k \in K, t \in T \quad (31)$$

$$y_{it} \le 1 - u_{i,t+q}{}^{(k)};\ q = 1, \dots, \min[(DT_i - 1), T - t], k \ne 0, \forall\, i \in I^{(k)}, k \in K, t \in T \quad (32)$$

Equations (27)–(30) define the unit startup and shutdown sequence for post contingency states and (31)–(32) set minimum unit up and down time restrictions including post contingency states.

2) Spinning reserves allocation and pricing

Spinning and nonspinning reserves required from each generating unit are defined as follows:

$$r_{it}{}^{sp+} = \max_k \left[\left(g_{it}^{(k)} - g_{it}^{(0)}\right).u_{it}{}^{(0)}.u_{it}{}^{(k)}, 0\right]\ ;\ \forall\, i \in I^{(0)}, t \in T \quad (33)$$

$$r_{it}{}^{sp-} = \max_k \left[\left(g_{it}^{(0)} - g_{it}^{(k)}\right).u_{it}{}^{(0)}.u_{it}{}^{(k)}, 0\right]\ ;\ \forall\, i \in I^{(0)}, t \in T \quad (34)$$

$$r_{it}{}^{sp} = r_{it}{}^{sp+} + r_{it}{}^{sp-} \le R_{it}{}^{sp\_\max}\ ;\ \forall\, i \in I^{(0)}, t \in T \quad (35)$$

$$r_{it}{}^{ns+} = \max_k \left[\left(g_{it}^{(k)}\right).\left(1 - u_{it}{}^{(0)}\right).u_{it}{}^{(k)}, 0\right];\ \forall\, i \in I^{(0)}, t \in T \quad (36)$$

$$r_{it}{}^{ns-} = \max_k \left[\left(g_i{}^{\min}\right).u_{it}{}^{(0)}.\left(1 - u_{it}{}^{(k)}\right), 0\right];\ \forall\, i \in I^{(0)}, t \in T \quad (37)$$

$$r_{it}{}^{ns+} \le R_i{}^{ns\_\max}\ ;\ \forall\, i \in I^{(0)}, t \in T \quad (38)$$

As before, the spinning reserve provided by a unit is the sum of the assigned upward and downward reserve, and this reserve is subject to a physical or offer limit $R_{it}{}^{sp\_\max}$ (35). The conventional upward nonspinning reserve is also subject to a limit $R_{it}{}^{ns\_\max}$ (38), whereas the downward nonspinning reserve can only be 0 or the minimum generation limit of the unit (see Figure 1). The interpretation is that a unit providing

nonspinning reserves should be available to be either started up or shut down at period *t*, depending on the case. We assume that any start-up or shut-down cost actually incurred by using nonspinning reserves is remunerated as a separate make-whole payment. Therefore, nonspinning reserve costs only reflect availability of the unit and consequently we assume in (25) that both types of nonspinning reserves have the same cost (i.e. no separate offers are required for up and down reserves). As before, the pricing of locational reserves is based on the marginal cost of the reserves assigned in each node. Besides the spinning reserve prices ρ_{nt}^{sp} established in (24), we define nodal nonspinning reserve prices ρ_{nt}^{ns} as follows:

$$\rho_{nt}^{ns} = \max_i [RC_{it}^{ns}(r_{it}^{ns+}, r_{it}^{ns-})] \; ; \{i \in In : r_{it}^{ns+} + r_{it}^{ns-} > 0\}, \forall\, n \in N, t \in T \quad (39)$$

Finally, the stochastic SCUC models presented in this section can be adapted to co-optimize energy and any specific types of reserves, for instance only upward spinning reserve or only upward spinning and nonspinning reserves.

3 Numerical Simulations

In order to test the validity of the proposed methods and evaluate their computational tractability, we carried out numerical simulations to co-optimize energy and locational contingency reserves over a 24-hour horizon period, using the IEEE one-area Reliability Test System 96 [31]. The one-area RTS96 system has 24 buses, 32 generation units and 38 transmission lines, with two voltage levels of 230 and 138 kV. The topology of the system is shown in Figure 3.

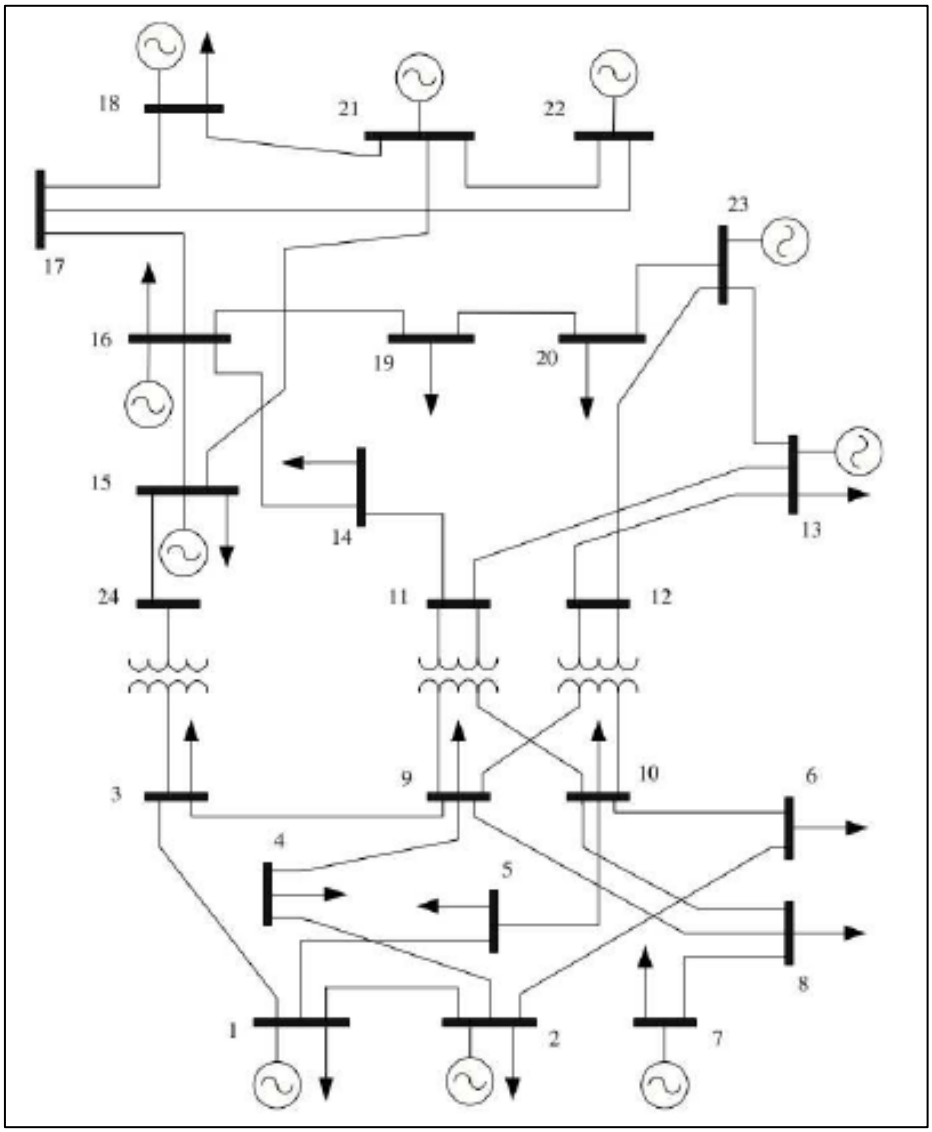

Fig. 3. IEEE one-area Reliability Test System 96

3.1 Characteristics and Data of the Test System

The RTS96 has a total installed capacity of 3,405 MW and the annual peak load is 2,850 MW. Bus data, branch data and system load profile are provided in [31, Table 1, Table 12 and Tables 2–5]. For the simulations, we chose the hourly load profile corresponding to the day of higher consumption in the year (2^{nd} day of calendar week 51 for a winter peaking system). Generator data, including size, type, fuel, forced outage rate, heat rate, startup heat, cycling and ramping data are provided in [31, Table 6 and Tables 8–10]. On the original data we corrected a jump in the load profile at hour 01 and added the initial conditions of generation units. The RTS96 lacks generation flexibility, since besides some nuclear and hydro units, it is mostly composed of conventional steam plants burning coal or fuel oil. In order to add fast-response and peaking capacity, necessary to deploy spinning and non-spinning reserves, we replaced the original 3x100 MW steam units at node 7 with a group of gas turbines of the same size. On the other hand, the RTS96 system has ample transmission capacity. An examination of load flows indicated that even at maximum peak load there was not a single congested transmission line. As our goal was to evaluate the allocation of reserves under transmission congestion, we reduced the continuous and long-term emergency ratings of the transmission line between nodes 16 and 17 to 250/300MW respectively.

The RTS96 data provide the incremental heat rate of thermal units at four output levels. The lower level was considered as the minimum power output of each unit and the rated capacity as its maximum power output. The ramp rate (MW/min) of each unit was used to compute 60-min inter-period and 10-min contingency ramp up and ramp down limits. The physical limits of each unit were used to compute its reserve limits. The incremental heat rate data was combined with average fuel costs for year 2015 [32], to build a piecewise linear generation cost function *GC*. Likewise, the fuel cost data was used to calculate the startup cost *SC* of the units assuming hot starting. Finally spinning and nonspinning reserve costs, RC^{sp} and RC^{ns} were assumed to be equivalent to 20% and 10% of the highest marginal energy costs of each unit, respectively. Under these cost assumptions, the stochastic SCUC models used in the simulations were all mixed-integer linear problems. In principle, the contingency scenarios to be considered correspond to the outage of any single unit at any of the 24 hourly periods of the UC horizon. For the purpose of the simulations and without loss of completeness, the contingency scenarios selected were those corresponding to distinct outages. That is, those of different units or of units located in different nodes of the system. Thus, 14 unit outages and 336 contingency scenarios were simulated. Actually, a more reduced set of credible contingencies could have been selected by disregarding outages of smaller units that are dominated by outages of bigger units. In effect, the simulation results confirmed that only outages above 100 MW were relevant. Generation units type, size and fuel cost are shown in Table I.

With the above conditions, we simulated the day-ahead co-optimization of energy and locational contingency reserves using the stochastic SCUC models described in section II. To focus on the effect of generation outages on reserves, the security constraints (5) and (9) related to transmission outages were not enforced. The objective

of the simulations were to (i) compare the results of allocating contingency reserves using a conventional method vs the proposed locational method; (ii) evaluate the effect of including "downward" reserves in addition to the traditional "upward" reserves, and (iii) to investigate the feasibility and impact of co-optimizing spinning and nonspinning reserves. The results of the simulations are described next. The optimization models were implemented using OPL and solved with CPLEX v12.6.1 [33], with pre-specified solution gap of 0.1%, using a laptop computer with 2.10 GHz CPU and 4GB of RAM.

Table 1. Test System Generation Units Data

No. x Size (MW)	Type	Fuel	Total MW
2 x 400	Nuclear	Nuclear	800
1 x 350	Steam	Coal	350
3 x 197	Steam	Fuel Oil #6	591
4 x 155	Steam	Coal	465
3 x100	Gas Turbine	Fuel Oil #2	300
4 x 76	Steam	Coal	304
6 x 50	Hydro	---	300
4 x 20	Combustion Turbine	Fuel Oil #2	80
5 x 12	Steam	Fuel Oil #6	60

Fuel cost ($/MMBTU): Fuel oil #2 $13.90, Fuel oil #6 $10.20, Coal $2.20, Uranium $0.80.

3.2 Case 1 – Global Reserves vs Locational Reserves

In Case 1 we wanted to compare the results of co-optimizing energy and contingency reserves using a conventional method vis-à-vis the proposed locational method. To do this we first simulated the results of a deterministic SCUC with a spinning reserve requirement. The initial option was to apply a traditional fixed requirement based on the heuristic of a reserve equal to the "largest unit online" [30, Ch. 5]. An exogenous spinning reserve requirement SR_t is then imposed as an additional constraint of the optimization problem (40). For the RTS96 system the required hourly reserve is equal to 400 MW (see Table 1).

$$\sum_i r_{it}{}^{sp} \geq SR_t \; ; \; \forall \; i \in I, t \in T \qquad (40)$$

This ad-hoc assignment can lead to overscheduling (reliable but uneconomic) or underscheduling (not secure but less costly) reserves. A better approach as described in [34] is to define a reserve requirement equal to the maximum generation online but not necessarily the largest unit, as in (41). In this case the total reserve is not an exogenous value but another decision variable of the optimization problem.

$$\sum_i r_{it}^{sp} \geq g_{it} \; ; \; \forall \, i \in I, t \in T \qquad (41)$$

We found that the direct application of (41) results in a naïve allocation of reserves, since the unit with the largest generation can also carry a reserve itself, so losing the unit also reduces the reserve available and creates a capacity deficit. The correct reserve requirement is then provided by (42), which we call the global reserve requirement corresponding to the global reserve method.

$$\sum_i r_{it}^{sp} \geq g_{it} + r_{it} \; ; \; \forall \, i \in I, t \in T \qquad (42)$$

We used the global and locational reserve methods to allocate upward spinning reserves in the test system; the main characteristics of both problems are compared in Table 2 and the total reserve assigned each hour is shown in Table 3.

Table 2. Case 1 – Problem Size and Solution Time

Parameter	Global Reserves	Locational Reserves
No. of variables	6,001	34,753
Binary	2,304	2,304
Other	3,697	32,449
No. of constraints	11,917	87,037
No. of nonzero elements	29,221	212,893
Solution time (s)	22.8	360.7

Table 3. Case 1 – Total Hourly Contingency Reserves

H	Load (MW)	Global (MW)	Locat. (MW)	H	Load (MW)	Global (MW)	Locat. (MW)
01	1795.5	400.0	370.0	13	2707.5	400.0	400.0
02	1795.5	400.0	370.0	14	2707.5	400.0	400.0
03	1710.0	400.0	352.8	15	2650.5	400.0	400.0
04	1681.5	400.0	355.6	16	2679.0	400.0	400.0
05	1681.5	400.0	355.6	17	2821.5	400.0	400.0
06	1710.0	400.0	352.8	18	2850.0	400.0	400.0
07	2109.0	400.0	400.0	19	2850.0	400.0	400.0
08	2451.0	400.0	400.0	20	2736.0	400.0	400.0
09	2707.5	400.0	400.0	21	2593.5	400.0	400.0
10	2736.0	400.0	400.0	22	2365.5	400.0	400.0
11	2736.0	400.0	400.0	23	2080.5	400.0	400.0
12	2707.5	400.0	400.0	24	1909.5	400.0	400.0

The stochastic model is a much bigger problem in terms of variables and constraints, but notice that it has the same number of integer variables as the deterministic problem, which favors tractability. The global method solved in seconds and the locational method in a few minutes. Also notice that the locational method was able to adjust the required reserves according to the demand in off-peak hours. Figures 4 and 5 compare the spatial distribution of reserves and prices at a specific time period (hour 22). The concentration on the global reserve distribution is evident.

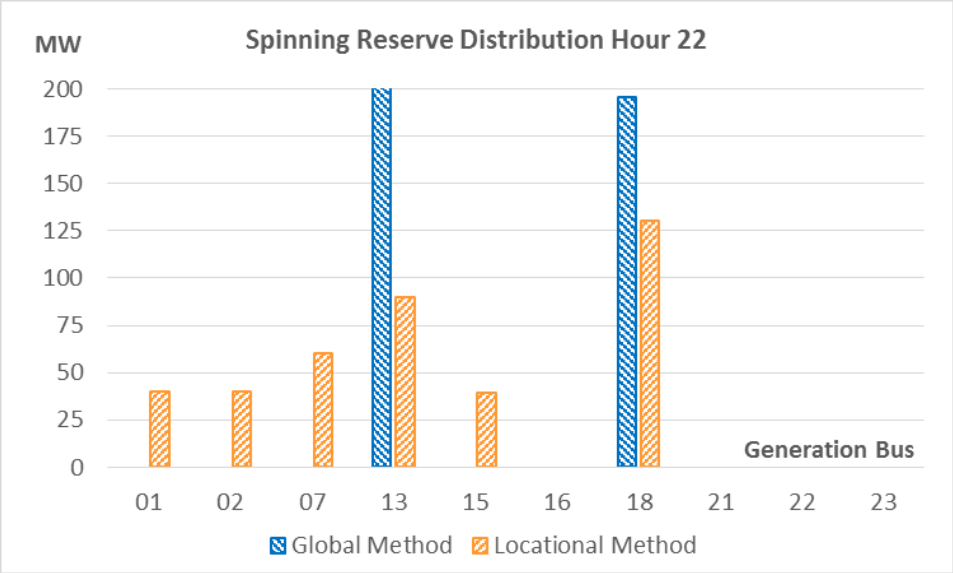

Figure 4. Distribution of spinning reserves over the system buses, hour 22.

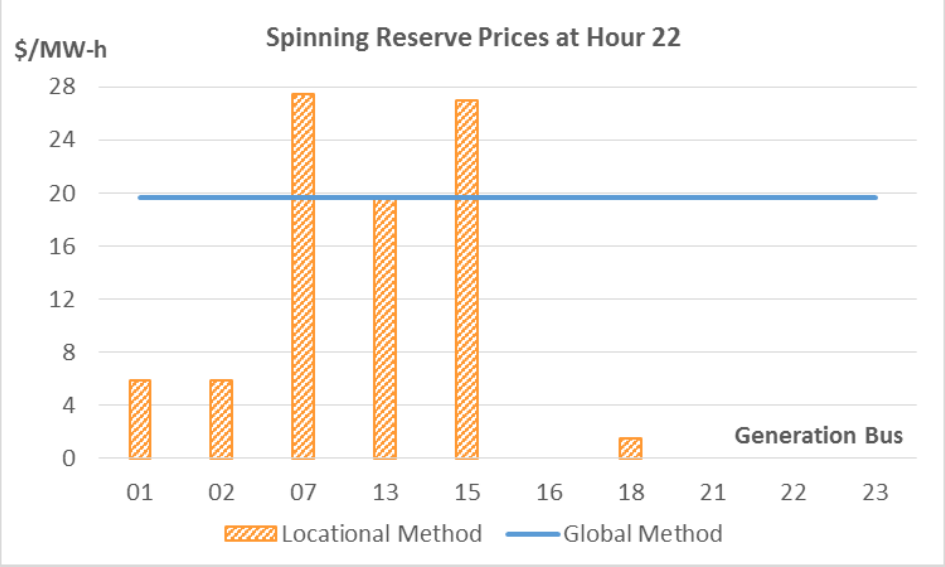

Figure 5. Distribution of spinning reserves prices over the system buses, hour 22

To compare the cost of both solutions we divided total operation cost into dispatch cost (normal condition), startup cost, reserve cost and redispatch cost (post contingency). Dispatch and startup cost are the "energy" costs whereas reserves plus redispatch are "security" costs. The costs of both methods are not directly comparable, because the global reserve method is deterministic, whereas the locational method is stochastic. To make a fair comparison we used the stochastic model of the locational method to compute the equivalent expected costs of the global method, and also calculated its redispatch costs, including the value of the ENS for a VoLL equal to $5,000 per MWh. Table 4 compares the costs of both methods. In general, total operation costs are dominated by dispatch costs (approximately 90%) followed by reserve costs (around 7%). Startup and redispatch costs are around the same order of magnitude. Security costs are 8% to 9% of total costs. Total costs (energy and security) of the global method are lower, as expected, because it is a less constrained problem, although redispatch costs are higher because of the ENS. In summary, the global method resulted in a more economic but unreliable operation, whereas the locational method was able to find a 24-hour secure dispatch at a reasonable additional cost of around 4%.

Table 4. Case 1 – Cost Comparison

Cost ($)	**Global Method**	**Locational Method**
Dispatch	1,156,667	1,197,631
Startup	20,959	23,523
Energy	*1,177,626*	*1,221,155*
Reserve	87,050	102,499
Redispatch	22,269	13,230
Security	*109,319*	*115,728*
Total	**1,286,944**	**1,336,883**

3.3 Case 2 – The Value of Downward Spinning Reserve

A generation outage causes a capacity deficit in the system that must be covered by ramping up standby reserves. That is the reason why, conventionally, all contingency reserves are "upwards" (contrary to regulation reserves that act up and down). However, the definition of locational reserves allows assigning contingency reserves "downwards", by reducing generation or shutting down units (see Figure 1), if that lowers total operation costs. In Case 2 we wanted to evaluate the convenience of allocating downward reserves in addition to upward reserves, using the test system. First, to probe the concept, we simulated the addition of downward spinning reserves at no cost. As a result, effectively the locational method assigned hourly downward spinning reserves in the range of 90 MW to 130 MW, in order to find a lower cost solution. However, it took much more computational effort (solution time was 1 hour, that is 10 times higher), and

the reduction in cost was only 0.03% in total, which is lower than our solution tolerance. The reduction was essentially due to lower redispatch costs (-2.3%).

In effect, when we included the cost of the downward spinning reserves in the simulation, the result is that no downward reserves were allocated, since the additional reserve cost is not compensated by the reduction in redispatch costs. In consequence, we found no value in defining and adding a downward spinning reserve product to the tested system. Even if some cost reduction were achievable, this should be marginal anyway given the lower weight of redispatch costs on the total, and it probably would not justify the increase in computational complexity. Given this result, we are even more skeptical about the value of adding downward nonspinning reserves. This especially because shutting down a unit as a response to a generation contingency has implications beyond the single redispatch period considered in our model (for instance if the unit cannot be restarted shortly), that we cannot capture in the simulations. Intuitively, shutting down units in a post contingency state would be a risky operational practice.

3.4 Case 3 – Co-optimization of Spinning and Nonspinning Reserves

Allocating nonspinning reserves as part of the contingency reserve is a common practice in power systems operation. The concept is that fast-starting units can also respond in a post contingency situation without sacrificing reliability. The risk is that a nonspinning reserve could fail to start when required, which would be a sort of N-1-1 event. The benefit is that, since generation outages are infrequent, keeping reserves offline is less expensive because it lowers dispatch and reserve costs. This trade-off is reflected in heuristic rules, fixing the nonspinning reserve as a percentage of the spinning reserve, without further technical basis to decide the optimal allocation between spinning and nonspinning reserves. In Case 3, we aimed at testing the validity of the locational method to co-optimize spinning and nonspinning reserves and wanted to investigate the efficiency of the result. Therefore, we simulated the co-optimization of energy, spinning and nonspinning reserves in the test system using the locational method and compared results with Case 1, where only energy and spinning reserves were co-optimized. According to the analysis of Case 2, we only considered upward reserves.

The main characteristics of both problems are compared in Table 5. Including nonspinning reserves notably increases problem size, especially in terms of the number of integer variables, since it considers starting up units in every contingency scenario. The solution time almost doubled when compared with Case 1, but it was still within an acceptable range (10 minutes). Table 6 shows the total amount of spinning and nonspinning reserves assigned each hour. The locational method assigned an appreciable amount of nonspinning reserves during the intermediate and peak load periods and none for valley periods, where reserve requirements are lower and there is more head room in dispatched units. Notice that the optimal amount of nonspinning reserves as percentage of total contingency reserves varies hour by hour. Compared with Table 3, the total amount of hourly contingency reserves is very similar, with small differences due to the minimum power limits of the units. In both cases solutions are fully N-1 compliant.

Table 7 compares the solutions in terms of costs. As expected, there are appreciable cost savings in reserve and startup costs, but even more in dispatch costs because the model is able to find a less constrained dispatch solution. The effect on redispatch costs is negligible. Overall, security but especially energy costs are reduced by including nonspinning reserves, and total savings in operation costs is 8.4%. In summary, the application of the locational method resulted in an efficient allocation of spinning and nonspinning reserves in the test system, and their co-optimization created sizable cost savings.

Table 5. Case 3 – Problem Size and Solution Time

Parameter	Only Spinning Reserves	With Nonspinning Reserves
No. of variables	34,753	56,873
Binary	2,304	23,656
Other	32,449	33,217
No. of constraints	87,037	153,661
No. of nonzero elements	212,893	406,645
Solution time (s)	360.7	615.1

Table 6. Case 3 – Spinning and Nonspinning Hourly Contingency Reserves

H	Load (MW)	Spin. (MW)	Nonsp. (MW)	H	Load (MW)	Spin (MW)	Nonsp. (MW)
01	1795.5	370.0	0.0	13	2707.5	155.0	252.8
02	1795.5	70.0	0.0	14	2707.5	126.2	273.8
03	1710.0	352.8	0.0	15	2650.5	126.2	273.8
04	1681.5	355.6	0.0	16	2679.0	126.2	273.8
05	1681.5	355.6	0.0	17	2821.5	121.4	278.6
06	1710.0	352.8	0.0	18	2850.0	117.5	283.5
07	2109.0	155.0	245.8	19	2850.0	117.5	282.5
08	2451.0	126.2	273.8	20	2736.0	155.0	252.8
09	2707.5	126.2	273.8	21	2593.5	126.2	273.8
10	2736.0	126.2	273.8	22	2365.5	130.4	269.6
11	2736.0	126.2	273.8	23	2080.5	178.7	221.3
12	2707.5	155.0	252.8	24	1909.5	326.0	74.0

Table 7. Case 3 – Cost Comparison

Cost ($)	Only Spin. Reserves	With Nonsp. Reserves
Dispatch	1,197,631	1,131,690
Startup	23,523	12,683
Energy	*1,221,155*	*1,144,373*
Reserve	102,499	66,516
Redispatch	13,230	13,623
Security	*115,728*	*80,139*
Total	**1,336,883**	**1,224,512**

4 Conclusions

The optimal calculation and distribution of contingency reserves in power systems have long been discussed, both from the point of view of operational reliability (security) and efficiency. However, current practices to allocate spinning and nonspinning reserves produce workable solutions but still have serious shortcomings as discussed in the introduction. There is a general consensus on the main problems and requirements (deliverability, uncertainty modeling, etc.), but up to now the computational complexity of the proposed solutions has been a limitation to its development. Recently, advances in computational power and algorithms to solve large optimization problems have brought new opportunities to improve the methods to determine optimal contingency reserves for secure real-time operations. This paper contributes to this field by developing new formulations for the day-ahead stochastic co-optimization of energy and locational contingency reserves. These formulations model the uncertainty of generation outages and enforce full compliance with the widely used N–1 reliability standard under transmission congestion. The proposed methods exploit the structure and characteristics of the problem, according to actual operational practices, to improve the computational tractability of the solution. The proposed stochastic SCUC models were used to simulate different cases of contingency reserve allocation in the IEEE one-area RTS96 system.

The simulations confirmed that the traditional method cannot account for congestion on post contingency states, so it does not guarantee the security of operations or require cumbersome and costly offline corrections. On the contrary, the proposed locational method is able to find an N–1 secure dispatch at a reasonable extra cost. Optimal locational reserves, both spinning and nonspinning, vary according to the demand and conditions of the system, indicating that the use of fixed reserve requirements is inefficient. Additionally, the simulations indicated little value of assigning “downward” contingency reserves, but they confirmed sizable cost savings from the co-optimization of spinning and nonspinning reserves. Overall, the proposed formulations showed to be computationally tractable for the tested system.

We believe that the compact stochastic SCUC models presented in this paper can be scaled up to be used in larger systems and still be tractable, but further simulations are needed to confirm it. In any case, several decomposition methods [35–37] and more efficient SCUC models [38] can also be applied to solve problems of larger size, for implementation in real-world systems. Additional research in this direction is required. Finally, one limitation of the proposed methods is that they rely on a linear approximation of the network model, which introduces simplifications that may result on suboptimal solutions or require additional corrections. The integration of full ac network models with stochastic UC formulations is an area where future research is fundamental.

References

[1] NERC Reliability Criteria Subcommittee, “Reliability Concepts in Power Systems”, North American Electric Reliability Council (NERC), Feb. 1985.

[2] P. Kundur et al., IEEE/CIGRE Joint Task Force on Stability Terms and Definitions, “Definition and Classification of Power System Stability”, IEEE Trans. Power Syst., vol. 19, no. 2, pp. 1387–1401, May 2004.

[3] NERC Planning Committee, “Reliability Assessment Guidebook”, North American Electric Reliability Corporation (NERC), Atlanta, GA, v. 3.1, Aug. 2012.

[4] J. F. Ellison, L. S. Tesfatsion, V. W. Loose and R.H. Byrne, “A Survey of Operating Reserve Markets in US ISO/RTO-managed Electric Energy Regions”, Sandia National Laboratories, Albuquerque, NM, Proj. Rep. SAND2012-1000, Sep. 2012.

[5] U. Helman, B. F. Hobbs and R. P. O’Neill, “The Design of US Wholesale Energy and Ancillary Service Auction Markets”, in Competitive Electricity Markets: Design, Implementation, Performance, F. P. Sioshansi, Ed. Oxford, UK: Elsevier, 2008, ch. 5, pp. 179–243.

[6] M. Shahidehpour, H. Yamin and Z. Li, “Security-Constrained Unit Commitment”, in Market Operations in Electric Power Systems. New York, NY, USA: Wiley, 2002, ch. 8, pp. 275–310.

[7] X. Ma, H. Song, M. Hong, J. Wan, Y. Chen and E. Zak, “The Security-Constrained Commitment and Dispatch for Midwest ISO Day-Ahead Co-Optimized Energy and Ancillary Service Market”, in Proc. IEEE PES General Meeting, Calgary, July 2009, 8 p.

[8] S. Takriti, J. R. Birge and E. Long, “A Stochastic Model for the Unit Commitment Problem”, IEEE Trans. Power Syst., vol. 11, no. 3, pp. 1497–1508, Aug. 1996.

[9] L. Wu, M. Shahidehpour and T. Li, “Stochastic Security-Constrained Unit Commitment”, IEEE Trans. Power Syst., vol. 22, no. 2, pp. 800–811, May 2007.

[10] P. A. Ruiz, R. C. Philbrick, E. Zack, K. W. Cheung, and P. Sauer, “Uncertainty Management in the Unit Commitment Problem”, IEEE Trans. Power Syst., vol. 24, no. 2, pp. 642–651, May 2009.

[11] A. Papavasiliou and S. S. Oren, “A Comparative Study of Stochastic Unit Commitment and Security-Constrained Unit Commitment Using High Performance Computing”, in ECC European Control Conference, Zurich, July 2013, pp. 2507-2512.

[12] D. Bertsimas, E. Litvinov, X. A. Sun, J. Zhao, and T. Zheng, “Adaptive Robust Optimization for the Security Constrained Unit Commitment Problem”, IEEE Trans. Power Syst., vol. 28, no. 1, pp. 52-63, Feb. 2013.

[13] R. P. O'Neill, U. Helman, P. M. Sotkiewicz, M. H. Rothhkopf and W. R. Stewart Jr., "Regulatory Evolution, Market Design and Unit Commitment", in Next Generation of Electric Power Unit Commitment Models, B. F. Hobbs, M. H. Rothkopf, R. P. O'Neill and H-P. Chao, Eds. New York, NY, USA: Kluwer A.P., 2001, ch. 2, pp. 15–37.

[14] Y. M. Al-Abdullah, M. Abdi-Khorsand and K. W. Hedman, "The Role of Out-of-Market Corrections in Day-Ahead Scheduling", IEEE Trans. Power Syst., vol. 30, no. 4

[15] J. D. Lyon, K. W. Hedman and M. Zhang, "Reserve Requirements to Efficiently Manage Intra-Zonal Congestion", IEEE Tran. Power Syst., vol. 29, no. 1, pp. 251–258, Jan. 2014.

[16] O. Alsac and B. Stott, "Optimal Load Flow with Steady-State Security", IEEE Trans. Power App. Syst., vol. 93, issue 3, pp. 745–751, May 1974.

[17] A. Monticelli, M. V. F. Pereira, and S. Granville, "Security-Constrained Optimal Power Flow with Post-Contingency Corrective Rescheduling", IEEE Trans. Power Syst., vol. PWRS-2, no. 1, pp. 175-180, Feb. 1987.

[18] K. W. Hedman, M. C. Ferris, R. P. O'Neill, E. B. Fisher and S. Oren, "Co-Optimization of Generation Unit Commitment and Transmission Switching with N-1 Reliability", IEEE Trans. Power Syst., vol. 25, no. 2, pp. 1052–1063, May 2010.

[19] T. Zheng and E. Litvinov, "Contingency-Based Zonal Reserve Modeling and Pricing in a Co-optimized Energy and Reserve Market", IEEE Trans. Power Syst., vol. 23, no. 2, pp. 277–286, May 2008.

[20] F. Wand and K. W. Hedman, "Reserve Zone Determination Based on Statistical Clustering Methods", in North American Power Symposium (NAPS), Chicago, IL, Sep. 2012.

[21] J. M. Arroyo and F. D. Galiana, "Energy and Reserve Pricing in Security and Network-Constrained Electricity Markets", IEEE Trans. Power Syst., vol. 20, no. 2, pp. 634–643, May 2005.

[22] J. Chen, J. S. Thorp, R. J. Thomas and T. D. Mount, "Locational Pricing and Scheduling for an Integrated Energy-Reserve Market", in Proc. 36th Annual Hawaii International Conference on System Sciences, Jan. 2003.

[23] F. Bouffard, F. D. Galiana and A. J. Conejo, "Market-Clearing with Stochastic Security - Part I: Formulation", IEEE Trans. Power Syst., vol. 20, no. 4, pp. 1818–1826, Nov. 2005.

[24] F. Bouffard, F. D. Galiana and A. J. Conejo, "Market-Clearing with Stochastic Security - Part II: Case Studies", IEEE Trans. Power Syst., vol. 20, no. 4, pp. 1827–1835, Nov. 2005.

[25] A. J. Conejo, M. Carrión and J. M. Morales, "Market Clearing Considering Equipment Failures", in Decision Making Under Uncertainty in Electricity Markets. New York, NY, USA: Springer, 2010.

[26] A. Lamadrid, S. Maneevitjit, T. D. Mount, C. Murillo-Sanchez, R. J. Thomas, R. D. Zimmerman, “A ‘SuperOPF’ Framework”, CERTS, Berkeley, CA, USA, Report, Dec. 2008.

[27] C. E. Murillo-Sánchez, R. D. Zimmerman, C. L. Anderson and R. J. Thomas, “A Stochastic, Contingency-Based Security-Constrained Optimal Power Flow for the Procurement of Energy and Distributed Reserve”, Elsevier Decision Support Systems, vol. 56, pp. 1–10, Dec. 2013.

[28] L Wehenkel, “Emergency Control and its Strategies’, in Proc. 13th Power Systems Computation Conference (PSCC), Trondheim, Norway, July 1999.

[29] S. D. Kim, S. R. Kim and M. M. Morcos, “Application and Evaluation of Short-Term Emergency Ratings for Double-Circuit Transmission Lines”, Electric Power Components and Systems, vol. 40, issue 7, pp. 729-740, 2012.

[30] R. Billinton and R. Allan, Reliability Evaluation of Power Systems, 2nd ed. New York, NY, USA: Springer, 1996.

[31] C. Grigg et al., “The IEEE Reliability Test System – 1996, A report prepared by the Reliability Test System Task Force of the Application of Probability Methods Subcommittee”, IEEE Trans. Power Syst., vol. 14, no. 3, pp. 1010–1020, Aug. 1999.

[32] US Energy Information Administration, Short-Term Energy Outlook, Table 2 “Energy Prices”, Washington, DC, Mar. 2016.

[33] IBM ILOG CPLEX Optimization Studio / OPL Language Reference Manual, version 12 release 6, IBM, USA, 2015, 152 p.

[34] D. Chattopadhyay and R. Baldick, “Unit Commitment with Probabilistic Reserve”, in Proc. IEEE PES Winter Meeting, New York, NY, Jan. 2002, vol.1, pp. 280–285.

[35] Z. Li and M. Shahidehpour, “Security-Constrained Unit Commitment for Simultaneous Clearing of Energy and Ancillary Services Markets”, IEEE Trans. Power Syst., vol. 20, no. 2, pp. 1079–1088, May 2005.

[36] A. Nasri, S. J. Kazampour, A. J. Conejo and M. Ghandhari, “Network-Constrained AC Unit Commitment Under Uncertainty: A Bender’s Decomposition Approach”, IEEE Trans. Power Syst., vol. 31, no. 1, pp. 412–421, May 2005.

[37] A. Kargarian, Y. Fu and Z. Li, “Distributed Security-Constrained Unit Commitment for Large-Scale Power Systems”, IEEE Trans. Power Syst., vol. 30, no. 4, pp. 1925–1936, July 2015.

[38] G. Morales-España, J. M. Latorre and A. Ramos, “Tight and Compact MILP Formulation for the Thermal Unit Commitment Problem”, IEEE Trans. Power Syst., vol. 20, no. 2, pp. 4897–4908, Nov. 2013.